

Direct Decomposition of Nitric Oxide By Copper Containing ZSM-5

Peter R. Seidel

*Research Report Submitted
In Partial Fulfillment of the Requirements
for the Degree of
Masters of Science*

California Institute of Technology
Pasadena, California
1996

Acknowledgments

I would like to thank Professor Mark E. Davis for his guidance and support in the completion of this project. I would also like to thank Dr. Jay Labinger for his interest and many suggestions.

I want to thank all the members of the Davis research group, both past and present for being excellent labmates and friends. Dr. Clemens Freyhardt spent a lot of time with me discussing my project and future options. Dr. Chris Dartt, Dr. John Lewis and John Nagel helped me during my first year in lab. Dr. Larry Beck would always take the time to discuss my project and advise me on NMR. Alex Katz, Dave Foss, Wayez Ahmad, Shervin Khodabandeh, and the rest of my ChE class have made the past two years very entertaining.

Tara Weiscarger deserves special credit for putting up with me through some very stressful times. She never lost faith in me and was always there when I needed someone to lean on.

Finally, I want to thank my mom, dad, and brother for all their help and support. My student career has been long and expensive, and I thank you for everything you have done to make it possible.

Abstract

Currently there is an enormous demand for nitric oxide decomposition catalysts and hydrocarbon-based selective catalytic reduction catalysts to eliminate NO. The incorporation of copper atoms into the pores of ZSM-5 has endowed this solid with the catalytic ability for the direct decomposition of NO to N₂ and O₂. This report describes the synthesis, characterization, ion-exchange, and reactivity of several ZSM-5 samples prepared by various methods. ZSM-5 is prepared using TPA and also by template-free synthesis methods. Ion-exchange was performed using copper acetate and a copper ethylene complex. Reaction studies include determining rates and turnover frequencies for certain ZSM-5 samples. It was found that ion-exchange with copper ethylene almost doubled the copper weight percent and the reaction rate compared to samples exchanged with copper acetate, however, the turnover frequencies were similar.

Table of Contents

Acknowledgments	ii
Abstract.....	iii
Table of Contents	iv
List of Tables	vi
List of Figures	vii
1. Introduction.....	1
1.1 Zeolites	2
1.2 NO _x Catalysis	4
1.2.1 Direct NO Decomposition	4
1.2.2 Selective Catalytic Reduction of NO _x with CH ₄	5
1.3 Objectives.....	5
2. Experimental	7
2.1 Samples Preparation	7
2.2 Characterization	8
2.3 Ion Exchange.....	10
2.4 Catalytic Reactions.....	11
3. Results and Discussion	13
3.1 ZSM-5 Samples.....	13
3.2 Ion-Exchange Isotherms.....	17
3.2.1 Copper Acetate Exchange.....	17
3.2.2 Copper Ethylene Complex Exchange	21
3.3 Catalytic Studies on Cu-ZSM-5	22
3.3.1 Sample Reactivity	22
3.3.2 Differential Reactor Regime	23
4. Conclusions and Future Directions.....	29
4.1 Conclusions	29
4.2 Future Directions.....	29
4.2.1 Exchange on Different Si/Al Samples	29
4.2.2 Temperature Programmed Desorption of Isopropylamine (IPA)	30
4.2.3 Activity of Other Copper Ion-Exchanged Zeolites	31
5. References.....	32

Appendices.....	33
Appendix I. List of Chemicals Used	33
Appendix II. List of Samples	34
Appendix III. Characterization of Samples.....	35
Appendix IV. X-ray Powder Diffraction Patterns.....	36
Appendix V. Thermogravimetric Analyses	57
Appendix VI. NMR Spectra.....	73
Appendix VII. Conversion versus W/F Plots for VAW sample 1.....	99

List of Tables

Table 1	Synthesis conditions for ZSM-5 zeolites with varying Si/Al and Defects.	8
Table 2	Characterization Data for ZSM-5 Zeolites.	15
Table 3	Elemental Analysis on Copper Exchanged Samples	22
Table 4	Reaction conversions	23
Table 5	Reaction Rates and Turnover Frequencies	25
Table 6	Activation Energies	27

List of Figures

Figure 1	Tetrahedral building units in zeolites (adapted from ref.[5])	2
Figure 2	Structure of ZSM-5.	3
Figure 3	Setup for copper ethylene complex exchange.	11
Figure 4	Setup of catalytic reactor. Can monitor all exit gases with a mass spectrometer.....	12
Figure 5	^{29}Si MAS NMR spectra of ZSM-5 sample 2 (top) and 4 (bottom) with deconvolution peaks.	16
Figure 6	Copper acetate ion-exchange data for VAW NH_4^+ ZSM-5.....	17
Figure 7	Copper acetate ion-exchange data for VAW H^+ ZSM-5.....	18
Figure 8	Copper acetate ion-exchange data for VAW Na^+ ZSM-5	18
Figure 9	Copper acetate ion-exchange data for sample 2 from the Na^+ form.....	20
Figure 10	Copper acetate ion-exchange data for sample 4 from the Na^+ form.....	20
Figure 11	Reaction run for sample 1, ion-exchanged with the copper ethylene complex.....	23
Figure 12	Conversion versus W/F for VAW sample 1. Temperature was 502°C.....	24
Figure 13	Turnover frequency versus temperature for VAW sample 1 exchanged with copper acetate.	26
Figure 14	Turnover frequency versus temperature for VAW sample 1 exchanged with copper ethylene.	26
Figure 15	Arrhenius plot for VAW sample 1 exchanged with copper acetate.	28
Figure 16	Arrhenius plot for VAW sample 1 exchanged with copper ethylene.....	28

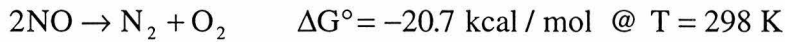
Appendices

Figure VII-1 Sample 1 ion-exchanged with copper acetate, T=526 °C.....	99
Figure VII-2 Sample 1 ion-exchanged with copper acetate, T=500 °C.....	99
Figure VII-3 Sample 1 ion-exchanged with copper acetate, T=473 °C.....	100
Figure VII-4 Sample 1 ion-exchanged with copper acetate, T=447 °C.....	100
Figure VII-5 Sample 1 ion-exchanged with copper acetate, T=422 °C.....	101
Figure VII-6 Sample 1 ion-exchanged with copper ethylene complex, T=525 °C.....	101
Figure VII-7 Sample 1 ion-exchanged with copper ethylene complex, T=500 °C.....	102
Figure VII-8 Sample 1 ion-exchanged with copper ethylene complex, T=477 °C.....	102
Figure VII-9 Sample 1 ion-exchanged with copper ethylene complex, T=450 °C.....	103
Figure VII-10 Sample 1 ion-exchanged with copper ethylene complex, T=425 °C.....	103

1. Introduction

The removal of nitric oxide from combustion exhaust streams has become increasingly important as NO has been linked to smog formation, acid rain, ozone effects and other harmful consequences.¹ In the future, stricter federal and state emissions regulations will dramatically increase gas equipment operating costs. The outlay of ammonia-based selective catalytic reduction (SCR) is currently very high, and non-catalytic processes perform inefficiently at relevant operating temperatures. As automobile manufactures move toward more efficient "lean burn" engines, an additional catalytic converter will be required to handle the increased levels of NO production. There is clearly a growing need for NO_x decomposition or hydrocarbon-based SCR catalysts to eliminate nitric oxides.

Thermodynamically, nitric oxide is unstable to its molecular elements O₂ and N₂, except at very high temperatures.²



Therefore, NO decomposition is thermodynamically favorable. The equilibrium for this reaction lies far to the right up to high temperatures, as characterized by the following expression.³

$$K = \frac{[\text{N}_2][\text{O}_2]}{[\text{NO}]^2} \quad \text{with} \quad \log K = -1.63 + 9452 / T$$

This reaction, however, is very slow from a kinetic standpoint. In the absence of a catalyst, several days are required to establish equilibrium even at 1000°C.⁴ This data supports the need for NO_x decomposition catalysts.

1.1 Zeolites

Zeolites are microporous crystalline aluminosilicates that are constructed from TO_4 tetrahedra (T represents a tetrahedral atom such as Si or Al.) These tetrahedral atoms are the primary building blocks in the formation of zeolites.⁵ Each oxygen atom bridges two neighboring T-atoms and shares its two negative charges equally. This causes each SiO_4 unit to become electronically neutral as a result of the +4 charge of Si and the four -1 charges from the oxygen atoms (see Figure 1). An AlO_4 unit will therefore have a -1 charge. A framework made up entirely of SiO_4 units will contain no charge, and a material containing Si and Al atoms will be negatively charged.

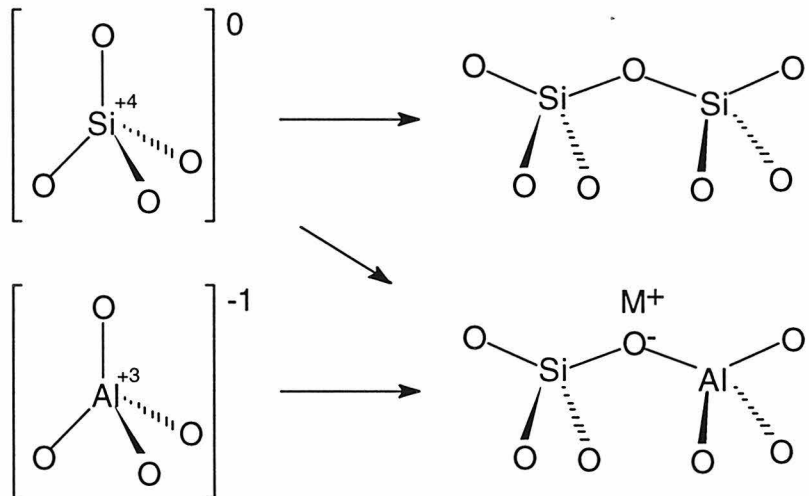


Figure 1 Tetrahedral building units in zeolites (adapted from ref.[5])

Since zeolites are crystalline, all the pores, cages, and channels have exactly the same dimensions. Some zeolite frameworks form independently of a structure directing agent (an organic molecule which creates a cage or channel by crystallizing TO_4 units around itself.) Other zeolites cannot form without a structure directing agent. Some

zeolites can be synthesized both ways, such as ZSM-5. Most ZSM-5 produced today is made by a template-free method⁶. It can also be made using tetrapropylammonium ions (TPA^+) as a structure-directing agent. Both preparation methods lead to the same framework structure, but the ordering of aluminum in the zeolite and the number of defects sites (silanol groups SiO_3OH and siloxy groups SiO_3O^-) will differ. Figure 2 shows the structure of ZSM-5. It has 10 membered rings with intersecting channels. The channels which lie in the plane of the paper are sinusoidal.

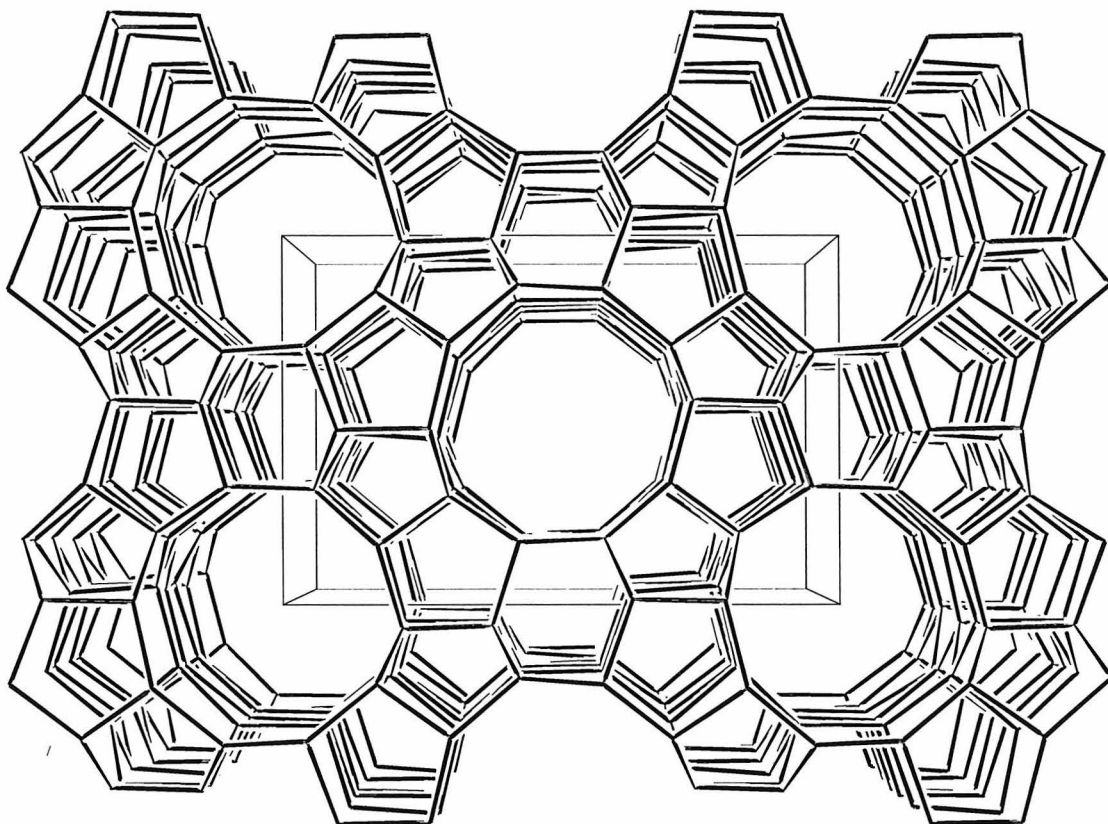


Figure 2 Structure of ZSM-5.

During synthesis of an aluminosilicate there must be a cation present to balance the negative charge of the AlO_4 unit. After synthesis this cation can be replaced by

performing an ion-exchange. ZSM-5 prepared by a template-free method will have Na^+ balancing the negatively charged aluminum in the framework, but the Na^+ can then be replaced with copper by ion-exchanging with a copper acetate solution. As previously mentioned, the ordering of the aluminum in a zeolite, and thus the cation balancing this charge, is dependent upon the synthesis method.

1.2 NO_x Catalysis

Currently, the most active catalyst reported for the direct decomposition of NO to O_2 and N_2 is ZSM-5 which has been excessively copper ion-exchanged.⁷ It is also well known that in the presence of additional species (H_2O , SO_2 , O_2), the ability of Cu-ZSM-5 to catalyze this reaction greatly decreases.^{8,9} Selective catalytic reduction of NO_x with hydrocarbons is becoming a popular option as a possible replacement to current ammonia-based SCR processes. Cobalt ion-exchanged ferrierite (FER) catalysts show the greatest activity for SCR of NO with methane, especially in the presence of water.¹⁰

1.2.1 Direct NO Decomposition

Most studies on NO decomposition have investigated Cu-ZSM-5 synthesized by the template-free method with Si/Al around 15-20.^{7,9,10,11,12} The number of aluminum per intersection in ZSM-5 prepared by this method is unknown. Other studies report ZSM-5 preparations with no mention of the synthesis method. The literature reports ion-exchange levels of 100% and more, termed "over exchanged." For a divalent ion, 100% exchange would give $\text{M}^{+2}/\text{Al} = 0.5$. However, the exchange of M^{+2} implies a paired Al center (Al-O-Si-O-Al), unlikely for high Si/Al ZSM-5 unless there is very strong Al zoning within

the crystal. Transition-metal ions can hydrolyze water to lower their effective charge. Copper could then ion-exchange as $[\text{Cu}^{2+}(\text{H}_2\text{O})_5\text{OH}]^+$. The definition of over exchange hinges upon what copper species ion-exchanges into ZSM-5.

Another possible explanation for reaching overexchange is that for exchange levels up to 70% (100% = Cu/Al = 0.5) $[\text{Cu}^{2+}\text{OH}]^+$ exchanges for Na^+ .⁷ At higher levels of exchange Larsen *et al.* speculate that Cu^{2+} or H^+ exchange as well. Valyon and Hall showed that ion-exchanging copper into ZSM-5 at pH ~6 yields higher copper loadings than at pH ~4.¹² This is also consistent with Larsen *et al.* in that $[\text{Cu}^{2+}\text{OH}]^+$ forms more readily as the pH is raised. One certain observation is that high levels of copper exchange in ZSM-5 are necessary for maximum activity.

1.2.2 Selective Catalytic Reduction of NO_x with CH_4

Li and Armor have shown that Cu-ZSM-5 is a very poor catalyst for NO reduction in the presence of O_2 .^{9,10,13,14} They found that Co-ZSM-5 performed better than Cu-ZSM-5 for SCR of NO with CH_4 in the presence of O_2 and occasionally H_2O . However, Co-ZSM-5 is a very poor catalyst for the direct decomposition of NO to N_2 and O_2 . The best catalyst for SCR of NO with CH_4 , in the presence or absence of H_2O , is Co-FER. Similar to Cu-ZSM-5, Co-FER and Co-ZSM-5 are highly ion-exchanged with cobalt to achieve maximum activity. Although these trends have been verified by other studies, it is not understood why they exist.

1.3 Objectives

Currently, little is known about the features of metal-loaded zeolites which endow them with their catalytic properties for NO_x reactions. Our first objective is to synthesize a

broad spectrum of zeolite samples. This includes the synthesis of ZSM-5 by three different procedures, with Si/Al ratios ranging from 15 to 40. Next, these samples will be characterized by several techniques. Some of the characterization techniques to be used are powder x-ray diffraction (XRD), nuclear magnetic resonance (NMR), temperature program desorption (TPD), thermogravimetric analysis (TGA), ultraviolet spectroscopy (UV), infrared spectroscopy (IR), and Far IR spectroscopy. Full ion-exchange isotherms will be generated for some samples to give insight into how copper ion-exchanges into ZSM-5. The catalytic activity of certain samples will be tested in a packed bed reactor for direct decomposition of NO. Rates and turnover frequencies will be calculated for these samples.

2. Experimental

2.1 Samples Preparation

ZSM-5 was prepared by three different methods. The synthesis of all ZSM-5 samples were conducted in Teflon-lined, stainless steel reactors. Fumed SiO_2 from Cab-O-Sil, Grade M5 was used as the silicon source. The fluid gel was heated statically and at autogenous pressure for 6 to 14 days, depending on the synthesis method used. The three synthesis methods used are summarized in Table 1. In addition to the samples prepared in our lab, experiments were performed using a ZSM-5 sample produced by VAW.⁶ This sample had a $\text{Si}/\text{Al} = 11$ and was made using a continuous template-free method.

The Na^+ method corresponds to samples 2 and 3 in Table 1. TPABr was used as a structure directing agent and hydroxide from NaOH as a mineralizing agent. The F method corresponds to samples 4-6 in Table 1. TPABr was again used as a structure directing agent, but the fluoride ion from NH_4F was the mineralizing agent. The template-free method corresponds to sample 7 in Table 1. No template was used in this synthesis, though a few crystals of ZSM-5 were added as seeds for nucleation.⁷ NaOH was used for mineralizing.

All of the above samples were calcined in a muffle furnace. The samples were first dehydrated by being heated to 250°C and held for an hour. The temperature was then raised to 580°C, and held steady for 8 hours. During the first two heating steps, nitrogen was flowed over the samples. For the last 7 hours at 580°C, air was passed over the samples.

Table 1 Synthesis conditions for ZSM-5 zeolites with varying Si/Al and Defects.

No	gel composition	gel Si/Al	mineralizing agent	T (°C)
1	VAW unknown, but has NH_4^+ balancing Al^- , no template	-----	-----	-----
2	0.1 TPABr : SiO_2 : 36 H_2O : 0.25 NaOH : 0.05 $\text{Al}(\text{NO}_3)_3$	20	OH^-	150
3	0.1 TPABr : SiO_2 : 36 H_2O : 0.25 NaOH : 0.025 $\text{Al}(\text{NO}_3)_3$	40	OH^-	150
4	0.1 TPABr : SiO_2 : 25 H_2O : 0.5 NH_4F : 0.067 $\text{Al}(\text{NO}_3)_3$	14.9	F^-	175
5	0.1 TPABr : SiO_2 : 25 H_2O : 0.5 NH_4F : 0.042 $\text{Al}(\text{NO}_3)_3$	23.8	F^-	175
6	0.1 TPABr : SiO_2 : 25 H_2O : 0.5 NH_4F : 0.025 $\text{Al}(\text{NO}_3)_3$	40	F^-	175
7	SiO_2 : 19.5 H_2O : 0.21 NaOH : 0.054 $\text{Al}(\text{OH})_3$: seeds	18	OH^-	175

2.2 Characterization

X-ray powder diffraction (XRD) patterns were collected for all samples on a Scintag XDS-2000 diffractometer equipped with a liquid-nitrogen-cooled germanium solid state detector using Cu-K α radiation. Data were acquired using a Digital Instruments MicroVax 3100 system.

Thermogravimetric analyses (TGA) were performed in air at a constant heating rate of 10 K/min from 298 K to 1173 K on a DuPont 951 TGA.

All NMR spectra were collected at room temperature on a Bruker AM 300 spectrometer equipped with a high-power assembly for solids. Sample holders were 7 mm ZrO_2 rotors. The magic angle spinning (MAS) technique was used for ^{29}Si , ^{27}Al and ^{13}C

NMR spectra with recycle delays between 10 and 60 s to avoid relaxation effects in the signal intensities. The chemical shift for ^{29}Si and ^{13}C were referred to tetramethylsilane and adamantane respectively. For ^{27}Al NMR spectra, a 1M solution of $\text{Al}(\text{NO}_3)_3$ was used as reference.

Elemental analysis was performed by Galbraith Laboratories Inc., Knoxville, TN, and on campus using a single amu resolution quadropole Elan 5000 Inductively Coupled Plasma Mass Spectrometer (ICP-MS). ICP standards from VWR and Aldrich were used for calibration, and scandium was used as an internal standard to correct for drift during sampling.

To prepare a sample for ICP analysis, the zeolite must be dissolved into an aqueous solution. One way to do this is to digest the zeolite with HF/HNO_3 in Teflon-lined, Parr autoclaves.^{15,16} The difficulty with this method is that silicon tetraflouride forms as a gas, and one can not accurately determine silicon values. Another method is to mix 20 mg of zeolite with 2 g of lithium metaborate and heat in a platinum crucible until a clear melt forms.¹⁷ A pinch of cesium iodide is then added, and the melt is poured into a beaker of water containing 15% concentrated nitric acid and a teaspoon of tartaric acid. The melt dissolves and is ready for ICP analysis. This technique enables one to measure silicon and therefore calculate Si/Al. However, this technique deposits significant amounts of lithium into the ICP-MS, so a variation of this procedure was implemented. The zeolite was mixed with 2 g of potassium carbonate and heated in a platinum crucible until a clear melt formed. The crucible was cooled and then placed in water with stirring. 10 ml of

concentrated nitric acid and additional water were added to reach 100 ml total volume. The solution was diluted and elements measured with an ICP-MS.

2.3 Ion Exchange

All samples were ion exchanged two times with 0.1M NaCl for 24 hours at 80°C, unless otherwise stated. Copper acetate exchange was carried out at room temperature in 0.0013M solutions. The maximum copper exchange of a zeolite was controlled by varying the volume of the exchange solution, holding the copper concentration constant. The extent of exchange was determined by measuring the amount of NH_4^+ or Na^+ that came out of the sample during exchange and the amount of copper that was removed from the solution. NH_4^+ and Na^+ were measured by an ion chromatograph and copper by a UV spectrometer.

A copper(I) ethylene complex $[\text{Cu}(\text{C}_2\text{H}_4)(\text{H}_2\text{O})_x]^+$ was generated and exchanged into samples 1, 2, and 4 by a multi-step process. The ethylene complex was generated by flowing ethylene through a reaction vessel containing copper(II) perchlorate hexahydrate and copper powder¹⁸ (see Figure 3). Methanol was then added through a serum cup to avoid exposure to air. The solution turned clear within an hour indicating that the copper(I) complex had formed. The reaction vessel was tilted, enabling the solution to filter through a frit and mix with the already dehydrated zeolite. The exchange and drying of the zeolite were performed under an ethylene atmosphere.

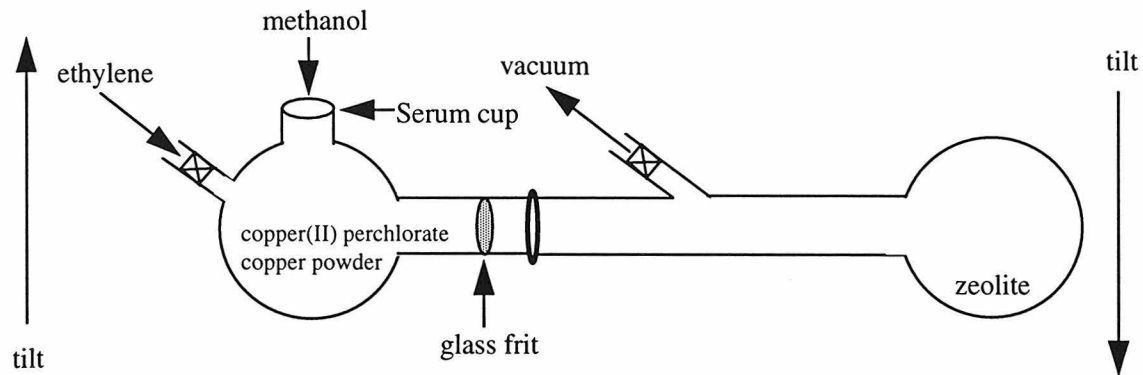


Figure 3 Setup for copper ethylene complex exchange.

2.4 Catalytic Reactions

Figure 4 shows the setup of the packed bed reactor that was constructed for catalytic testing. Mass flow controllers regulated the inlet gas flow rate, and an Aero Vac 2900 mass spectrometer system equipped with an electron multiplier was used to monitor the exit gases. Standard gas mixtures from Matheson were used to calibrate the mass spectrometer. The zeolite catalysts were compacted without binder into pellets which were subsequently crushed and size separated. The resulting particle size was -60/+80 mesh. Sample weights ranged from 20 to 150 mg. Catalyst pretreatment consisted of activation at 500°C under flowing helium for 3 hours. Reactions were run at 425°C to 525°C with flow rates from 25 to 120 ml/min, all containing 4% NO in helium.

In order to eliminate the effects of mass diffusion in the reactor bed, reaction rates and turn over frequencies were measured for sample 1, ion-exchanged with copper acetate and copper ethylene. The reactor was operated as a differential bed, and the rate of NO decomposition was assumed to be independent of conversion. By using 20 mg of catalyst

(W) and varying the total flow rate (F), the conversion was decreased into the differential regime. NO, N₂, and O₂ concentrations were monitored and used to calculate conversion.

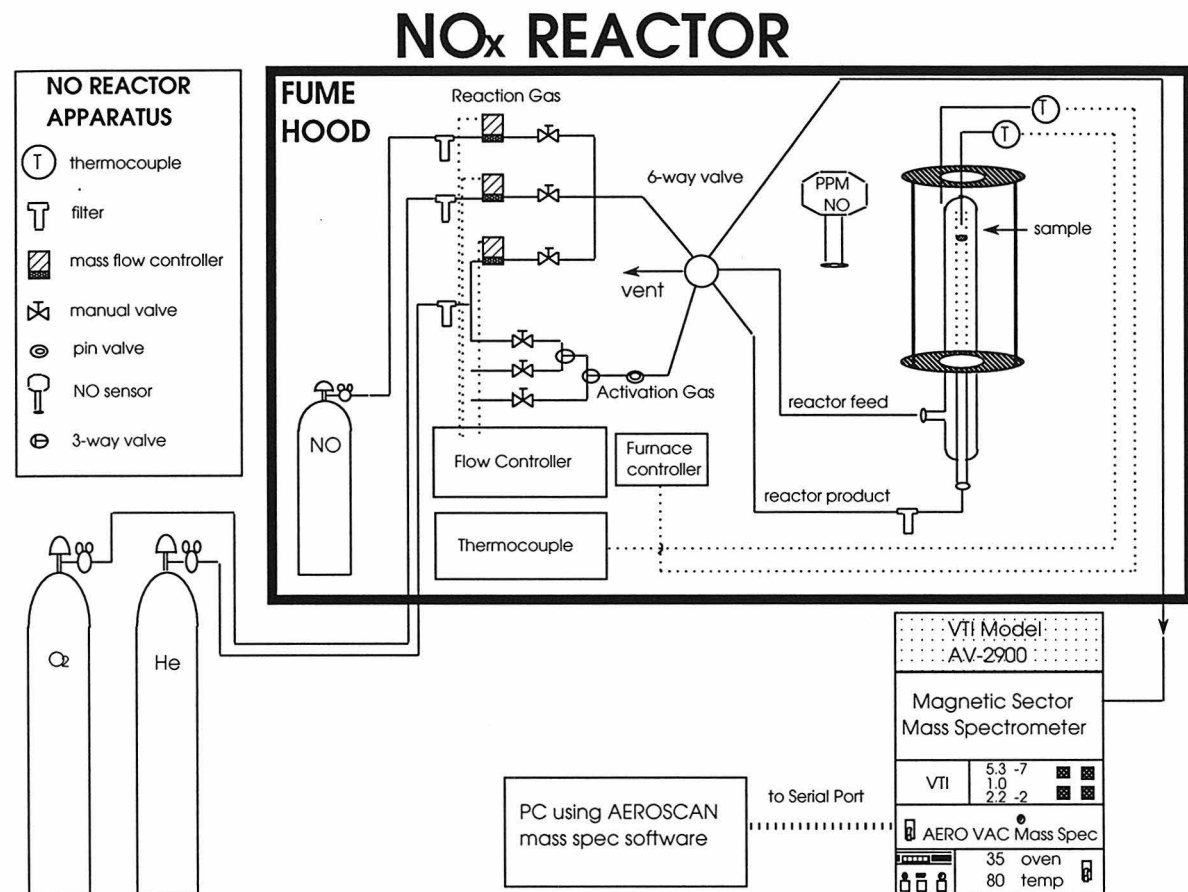


Figure 4 Setup of catalytic reactor. Can monitor all exit gases with a mass spectrometer.

3. Results and Discussion

3.1 ZSM-5 Samples

For the Na^+ method, TPA^+ and Na^+ balance the negative charge from the AlO_4 units. The aluminum therefore need not be evenly distributed throughout the framework, because the Na^+ ions are not confined to the pore intersections, like the TPA^+ ions. Thus it is possible for several Na^+ ions to balance aluminum atoms in one unit cell, while another unit cell may not contain any aluminum. For the F^- method only TPA^+ balance the AlO_4 units, because NH_4^+ is the only other cation present and it has never been found to balance charges inside a zeolite during synthesis. In this situation, the aluminum must be evenly distributed throughout the framework, because the TPA^+ ions are only located in pore intersections of the zeolite. This method also produces nearly defect free crystals. For the template-free method Na^+ balance the negative charge from the AlO_4 units, so again, uniform distribution of the aluminum throughout the framework may not occur.

The multi-step calcination procedure reduced the extent of dealumination during calcination. Two steps are involved in the removal of an organic template. First, the organic turns to coke, and then, in the presence of oxygen, it oxidizes and burns out of the pores. The oxidation process is very exothermic, and although the oven is at 580°C , the temperature inside a pore of the zeolite may be much higher. This high temperature tends to drive aluminum out of the framework and create defect sites. So by first heating the samples in a nitrogen rich environment, the oxidation process is slowed down, keeping the pore temperature lower. Yet even with this multi-step calcination process, some dealumination still occurs.

XRD data show that all the samples are very crystalline before and after calcination and have the MFI structure. The high peak intensities for the F⁻ method samples are caused by the preferred orientation of the extra large crystals that this method produces.

The weight loss in the TGA plots show removal of water and bulk removal of TPA, followed by removal of occluded organic species. The water content for most samples was 3% to 4% of the initial sample weight. The amount of TPA⁺ per unit cell was determined from the weight loss above 300°C (see Table 2). The samples containing TPA had between 2.7 and 4.1 TPA⁺ per unit cell, which is reasonable, as there are four channel intersections per unit cell. TGA was also run after calcination to determine the dehydrated weight of the calcined zeolites. All the samples, regardless of the synthesis method, had a dehydrated weight of 88% to 91%.

From the ²⁹Si MAS NMR spectrum the framework Si/Al was determined. The NMR data shown were taken by Hubert Koller.¹⁹ Figure 5 shows the deconvolution of the NMR spectrum for samples 2 and 4. There are two Q⁴ peaks which represent silicon tetrahedra with no aluminum. The next Q⁴ peak corresponds to silicon tetrahedra with an aluminum [(Si-O)₃-Si-O-Al]. Finally, there is a Q³ peak which represents a silicon with a silanol or siloxy group [(Si-O)₃-Si-OH or -O⁻]. This peak denotes the number of defect sites in the framework. From the figure it is evident that the fluoride sample has little or no Q³ peak, which corresponds to very few defect sites.

The data for elemental analysis are shown in Table 2. The values with an asterisk were measured on campus and those without an asterisk were measured by Galbraith Laboratories Inc. Elemental analysis is another way to determine the Si/Al. However, this

technique does not differentiate between aluminum in the framework versus in the channels. The Si/Al values for elemental analysis are usually lower than those determined by NMR. Sample 4 and 6 after calcination is an exception with Si/Al = 36 and 69 determined by elemental analysis verses 32.5 and 56.3 determined by NMR. The reason for this exception is that these samples were calcined and ion-exchanged before elemental analysis. So any aluminum which came out of the framework during calcination was washed out of the zeolite during ion-exchange.

Table 2 Characterization Data for ZSM-5 Zeolites.

No	29 Si MAS NMR				elemental analysis				TGA TPA ^{+/} u.c.
	Si / Al (as made)	Q ³ / %	Si / Al (calcined)	Q ³ / %	Si / Al (calcined)	Si / Al (calcined)	Al / u.c.	TPA ⁺ / u.c.	
1	11.5	~3	16.5		12.1*		7.4*	-----	-----
2	22	11	29	6	21	22*	4.4	3.1	2.7
3			29	4.6		19*	4.8*		3.22
4	~23-30	< 0.5	32.5	< 0.5	25	36*	3.7	3.9	3.5-3.9
5			40.8	< 0.5		37*	2.5*		3.6-4.0
6	~35-45	< 0.5	56.3	< 0.5	41	69*	2.3	3.9	3.7-4.1
7					25*		1.4*	3.7*	-----

*Elemental analysis performed on campus using ICP-MS.

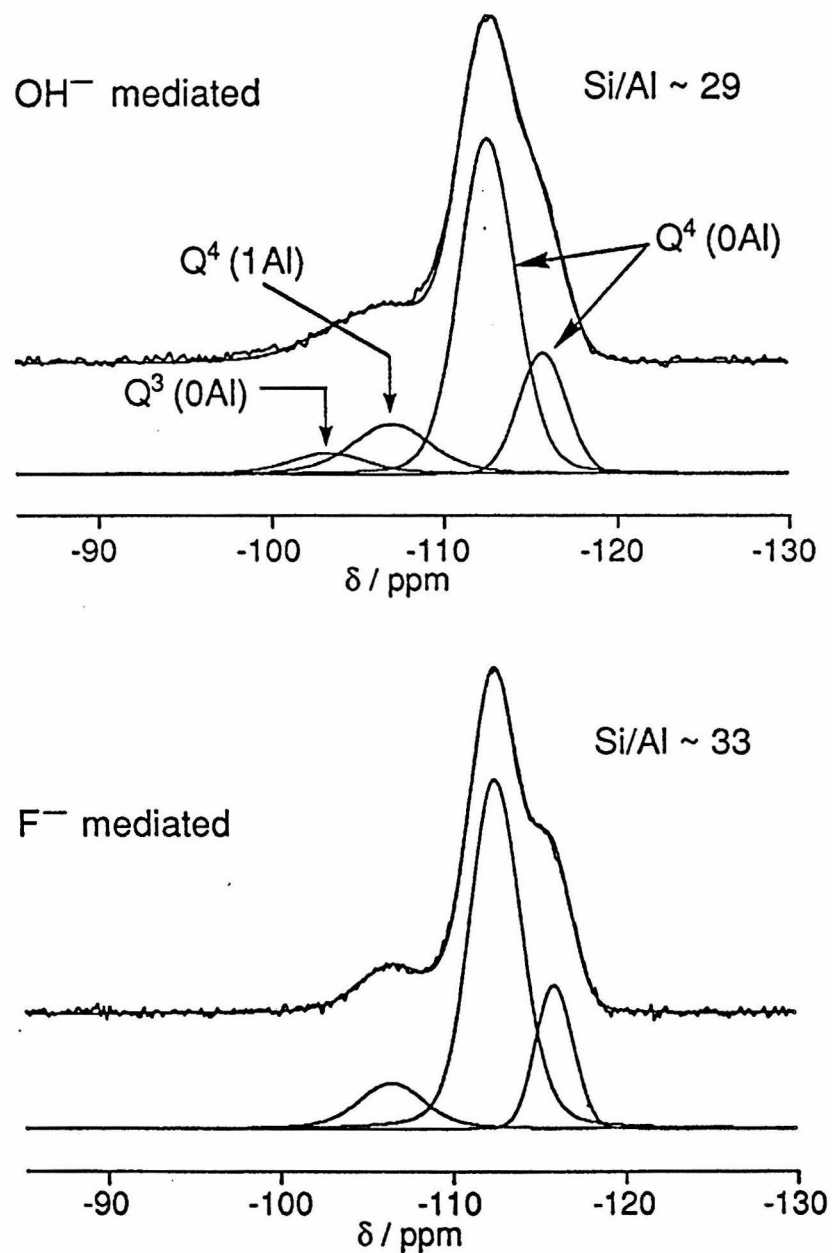


Figure 5 ^{29}Si MAS NMR spectra of ZSM-5 sample 2 (top) and 4 (bottom) with deconvolution peaks.

3.2 Ion-Exchange Isotherms

3.2.1 Copper Acetate Exchange

The VAW sample was ion-exchanged with copper acetate from three forms: NH_4^+ , H^+ (calcined), and Na^+ (see Figures 6-8). This first test was performed to see if ion-exchange depends on the cation being replaced. As shown in Figure 8, the maximum loading of copper is the point at which 0.85 of the aluminum sites have copper exchanged. The figures also imply that one copper atom exchanges for two NH_4^+ , H^+ , or Na^+ ions, since the maximum Cu/Al is 0.41. We suspect that a copper complex of the form $[\text{Cu}^{2+}(\text{H}_2\text{O})_5\text{OH}^-]^+---\text{H}^+$ is actually what ion-exchanged into the zeolite. In the VAW sample there are on average two aluminum atoms per intersection. So a copper complex of the above form could bridge two aluminum sites in a single intersection.

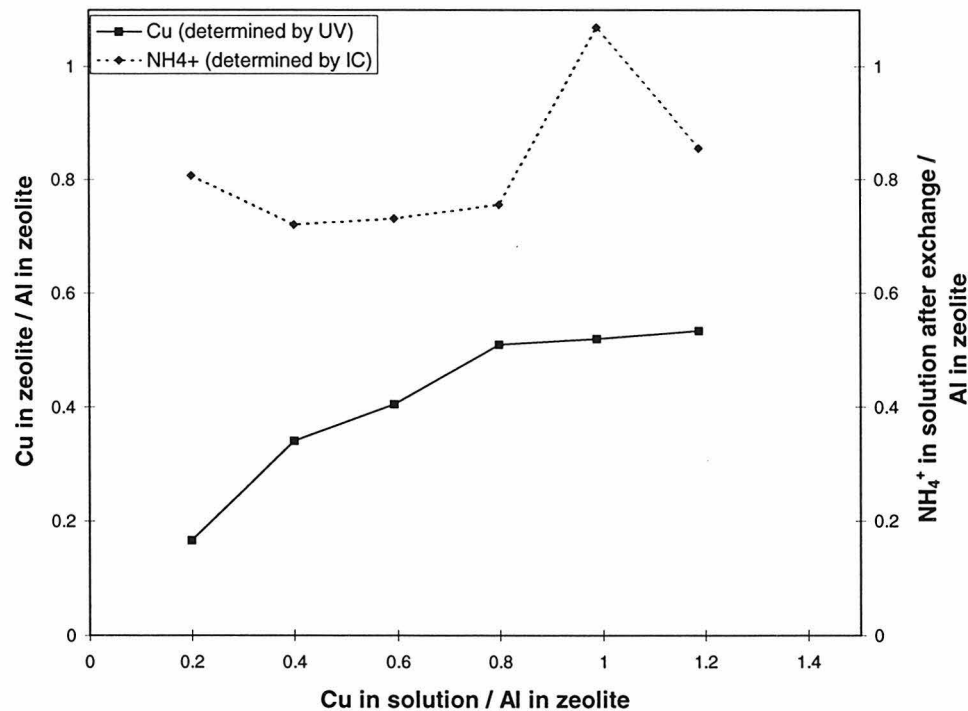


Figure 6 Copper acetate ion-exchange data for VAW NH_4^+ ZSM-5

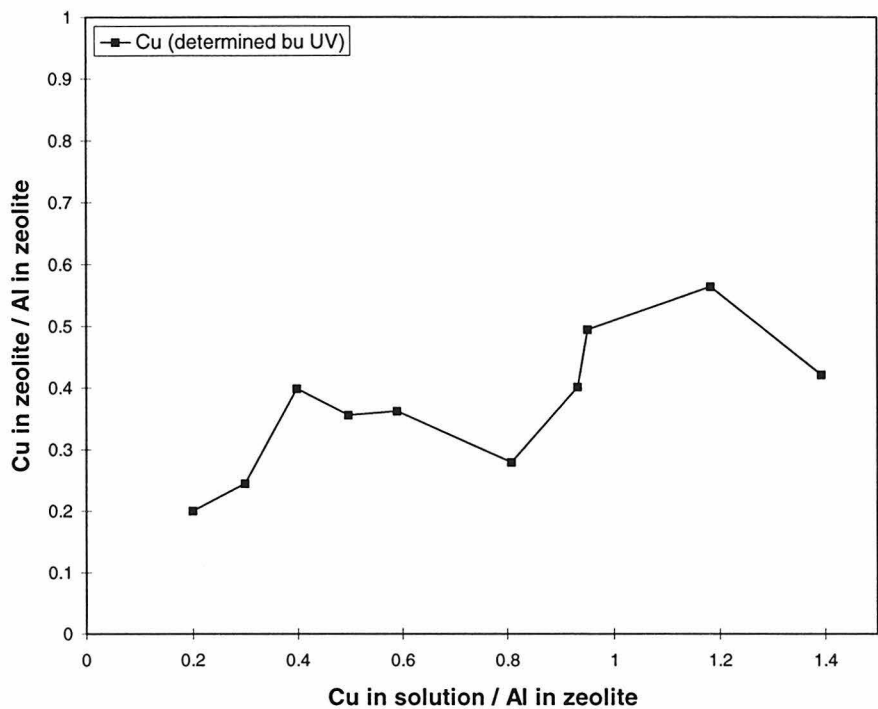


Figure 7 Copper acetate ion-exchange data for VAW H⁺ ZSM-5

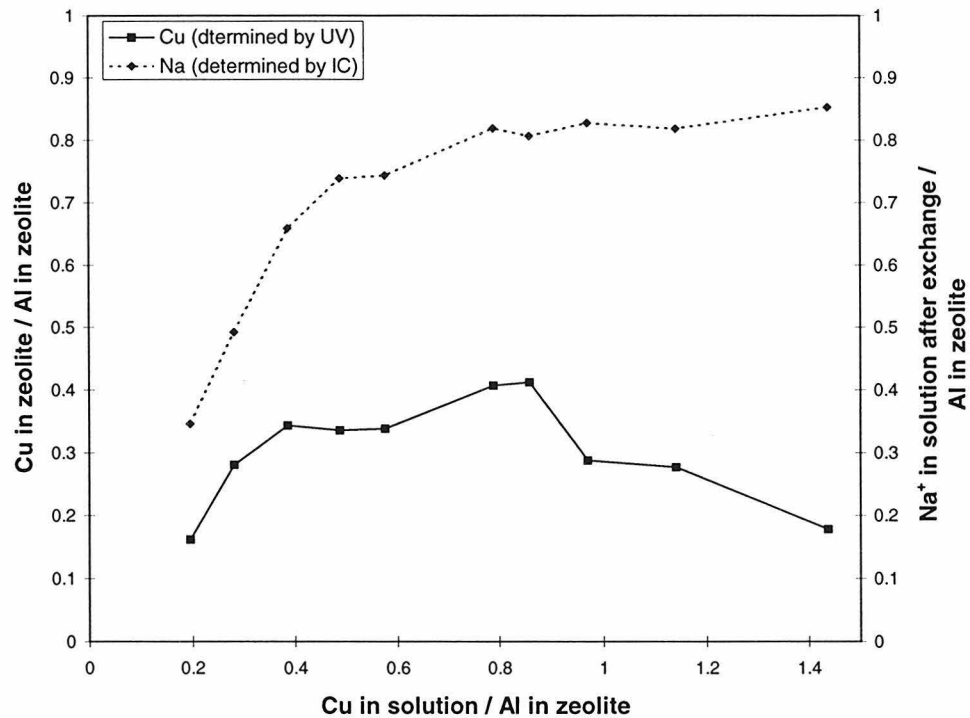


Figure 8 Copper acetate ion-exchange data for VAW Na⁺ ZSM-5

In the next step, copper acetate exchange isotherms were generated for samples 2 and 4 starting from the Na^+ form. The Na^+ form was chosen as the standard exchange state, because after calcination the samples made with TPA have Na^+ and H^+ balancing the Al^+ sites. Figures 9 and 10 show the isotherms for samples 2 and 4 respectively. It is clear that very little copper exchanges into the samples made with TPA, especially the fluoride method sample. The maximum loading of copper for samples 2 and 4 is the point at which Cu/Al was 0.18 and 0.12, respectively. In these samples, it appears that one copper atom exchanges for one Na^+ ion. As mentioned in the introduction, transition-metals can hydrolyze water. So we suspect that a copper complex of the form $[\text{Cu}^{2+}(\text{H}_2\text{O})_5\text{OH}^-]^+$ is what ion-exchanged into these zeolites. A zeolite with $\text{Si}/\text{Al} \geq 24$ has one or less aluminum atoms per intersection. So a copper complex of the form $[\text{Cu}^{2+}(\text{H}_2\text{O})_5\text{OH}^-]^+$ --- H^+ could not bridge two aluminum sites because the aluminum atoms are too far apart.

One problem with comparing these samples is that their Si/Al are not exactly the same. These particular samples were chosen because they have the closest Si/Al of the samples synthesized. However, in the calcined material, the VAW sample 1 has $\text{Si}/\text{Al} \sim 16$, the Na^+ method sample 2 has $\text{Si}/\text{Al} \sim 22$, and the F^- method sample 4 has $\text{Si}/\text{Al} \sim 33$. Unfortunately it is not possible to synthesize samples by templated methods with Si/Al below 20 or so. For the F^- method it is difficult to make samples with Si/Al below 30.

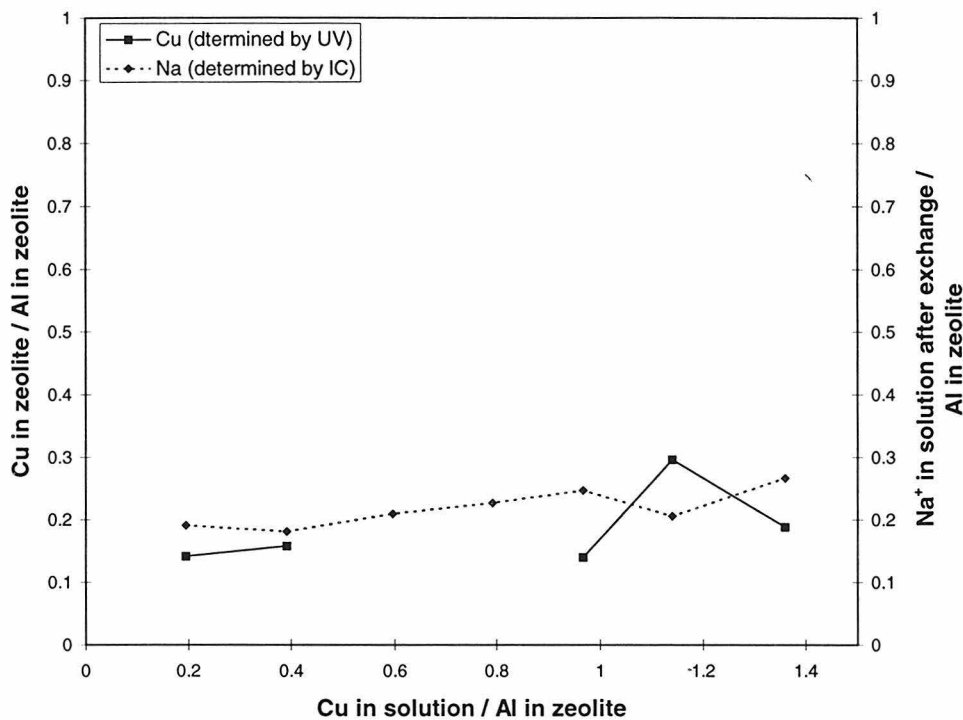


Figure 9 Copper acetate ion-exchange data for sample 2 from the Na^+ form.

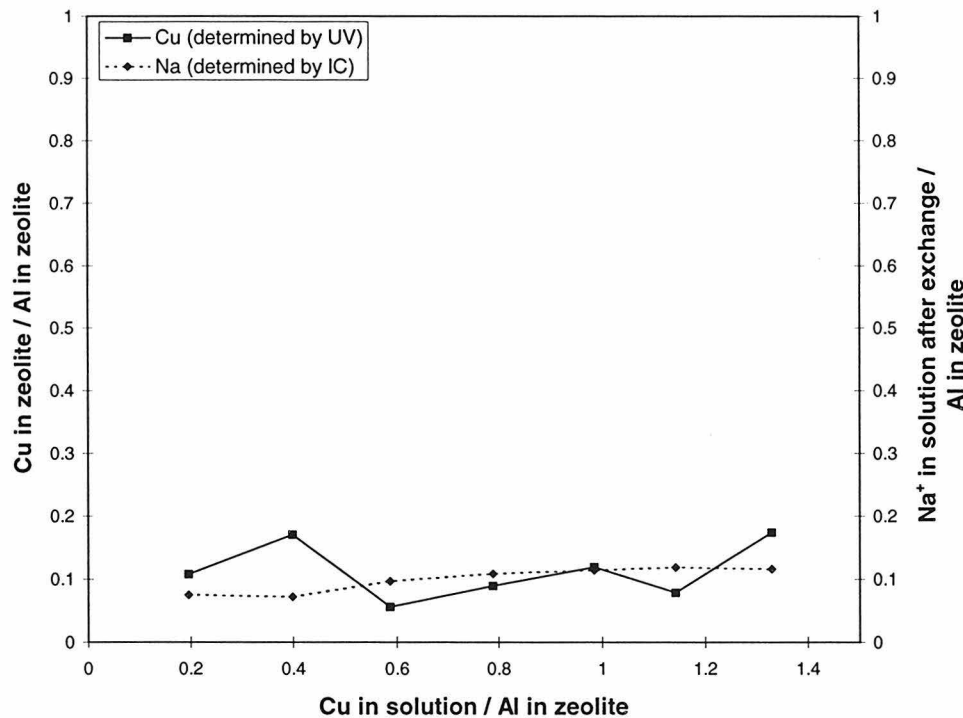


Figure 10 Copper acetate ion-exchange data for sample 4 from the Na^+ form.

3.2.2 Copper Ethylene Complex Exchange

One observation worth noting about sample 1 after copper ethylene exchange is that when the dried zeolite was removed from the flask, its color was white, and a few hours after contact with air, it turned yellowish-green. This probably has to do with the removal of ethylene from the copper complex. ^{13}C NMR did not indicate the presence of ethylene inside the zeolite after exchange and exposure to air. A sample was also prepared for NMR in a glove box directly after ion-exchange. This spectrum, which was taken under a nitrogen spinning environment, showed the presence of methanol, but no significant amount of ethylene. Ethylene desorption was also checked for during activation by mass spectrometry, but no increase in ion current for masses 28, 27, 26, and 14 were observed up to 500 °C.

Elemental analysis was performed on samples, exchanged with the copper ethylene complex and with copper acetate, to determine the extent of exchange (Table 3). A Cu/Al of 0.74 for the VAW sample 1 exchanged with the copper ethylene complex is almost twice the Cu/Al value of 0.41 obtained by ion-exchange with copper acetate. The same is true for sample 2. Thus higher copper loadings are attainable by exchanging with the ethylene complex because copper is in an oxidation state of one. To balance the charge from the same number of aluminum atoms, it takes twice as many copper ethylene molecules as copper acetate molecules.

The very low values for Na/Al led us to believe that total sodium exchange was not taking place. For high silicon content zeolites, it is very difficult to ion-exchange certain cations. However, elemental analysis before copper exchange showed that the Na/Al was

0.75 or higher. Sodium exchange with 0.1M NaOH (pH=13) was also tried, but gave Na/Al values much greater than one, indicating that NaOH had been occluded in the zeolite pores. Copper acetate exchange data from elemental analysis is consistent with the results found from the ion-exchange isotherms shown previously.

Table 3 Elemental Analysis on Copper Exchanged Samples

Sample	exchange method	Si/Al	Cu/Al	Na/Al
1 (VAW)	ethylene complex	12.3	0.74	0.0
1 (VAW)	copper acetate	11.8	0.41	0.05
2 (Na ⁺ method)	ethylene complex	22.1	0.38	0.0
2 (Na ⁺ method)	copper acetate	23.4	0.16	0.33
4 (F ⁻ method)	ethylene complex	35.8	0.0	0.07
4 (F ⁻ method)	copper acetate	32.8	0.0	0.93

3.3 Catalytic Studies on Cu-ZSM-5

3.3.1 Sample Reactivity

Samples 1, 2, and 4 were tested for catalytic activity in the packed bed reactor. Figure 11 shows the reaction run for sample 1 after exchange with the copper ethylene complex. The conversion was calculated from the decrease in NO concentration during the reaction. Table 4 lists the conversion, the copper weight percent, and the conversion per mole of copper in the zeolite. The conversion per mole of copper is on the same order of magnitude for all the samples that were reactive. It is clear that samples 2 and 4 take in little or no copper during exchange and therefore have very low conversions.

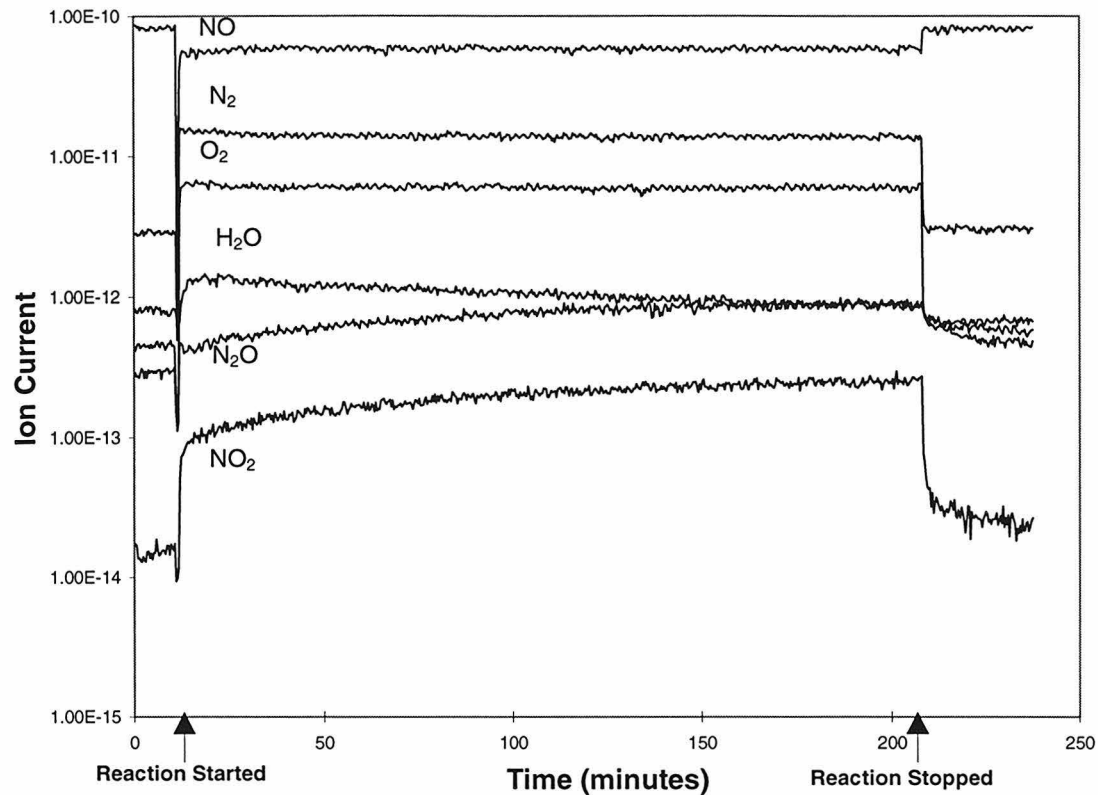


Figure 11 Reaction run for sample 1, ion-exchanged with the copper ethylene complex.

Table 4 Reaction conversions

Sample	Ion-Exchange Method	Conversion	Cu wt%	Conversion/ mole Cu $\times 10^{-5}$
1 (VAW)	copper acetate	24	3.3	3.1
1 (VAW)	ethylene complex	29	5.5	2.2
2 (Na ⁺ method)	copper acetate	2	0.7	1.2
4 (F ⁻ method)	copper acetate	0	0	-----

3.3.2 Differential Reactor Regime

Figure 12 plots conversion versus W/F for three different weights of sample 1 ion-exchanged with copper acetate. It was necessary to decrease the sample weight because even with a catalyst weight of 20 mg and a flow rate of 125 ml/min, a conversion of 4%

was obtained. Samples weighing 20 mg were used to determine rates and turnover frequencies for sample 1 exchanged with copper acetate and copper ethylene, see Table 5. Reaction rates were determined from the decrease in NO concentration and also from the increase in N_2 and O_2 concentration. The rates were calculated by finding the slope of the best fit line through the origin and the three lowest W/F data points ($F = 80, 100$, and 120 ml/min), see Appendix VII. Turnover frequencies were calculated from the rate data using the Cu/Al values from elemental analysis. The turnover frequencies are plotted versus temperature in Figures 13 and 14. The TOF passes through a maximum as a function of reaction temperature, which is in agreement with plots reported in the literature.¹²

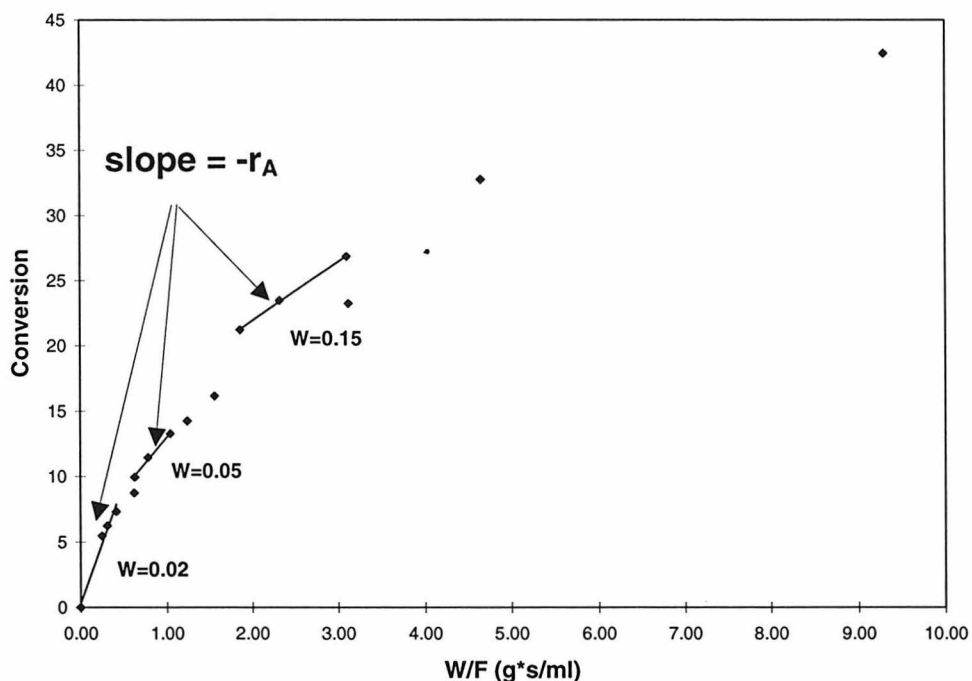


Figure 12 Conversion versus W/F for VAW sample 1. Temperature was 502°C

It is clear from Table 5 that the rate for the copper ethylene exchanged sample is almost double that of the copper acetate exchanged sample. However, the turnover frequencies are very similar. This shows that although the copper ethylene exchange method greatly increases the copper weight percent in the sample, the activity of each copper atom toward the decomposition of nitric oxide is the same.

Table 5 Reaction Rates and Turnover Frequencies

Temperature (°C)	Rate x 10 ⁶ (moles NO / g cat * s)		TOF x 10 ² (s ⁻¹)	
	Copper Acetate	Copper Ethylene	Copper Acetate	Copper Ethylene
Decrease in NO Concentration		Decrease in NO Concentration		
525	5.98	12.4	1.21	1.39
500	5.98	13.1	1.22	1.48
475	5.72	10.6	1.16	1.19
450	4.12	8.98	0.837	1.01
425	3.98	6.63	0.809	0.747
Increase in N₂ Concentration		Increase in N₂ Concentration		
525	5.13	8.30	1.04	0.934
500	4.48	7.98	0.910	0.899
475	3.83	6.39	0.778	0.720
450	3.42	4.69	0.696	0.528
425	3.04	3.78	0.618	0.425
Increase in O₂ Concentration		Increase in O₂ Concentration		
525	1.93	4.94	0.392	0.557
500	1.29	4.25	0.262	0.479
475	0.775	2.56	0.157	0.288
450	0.445	1.18	0.0904	0.133
425	0.341	0.557	0.0693	0.0627

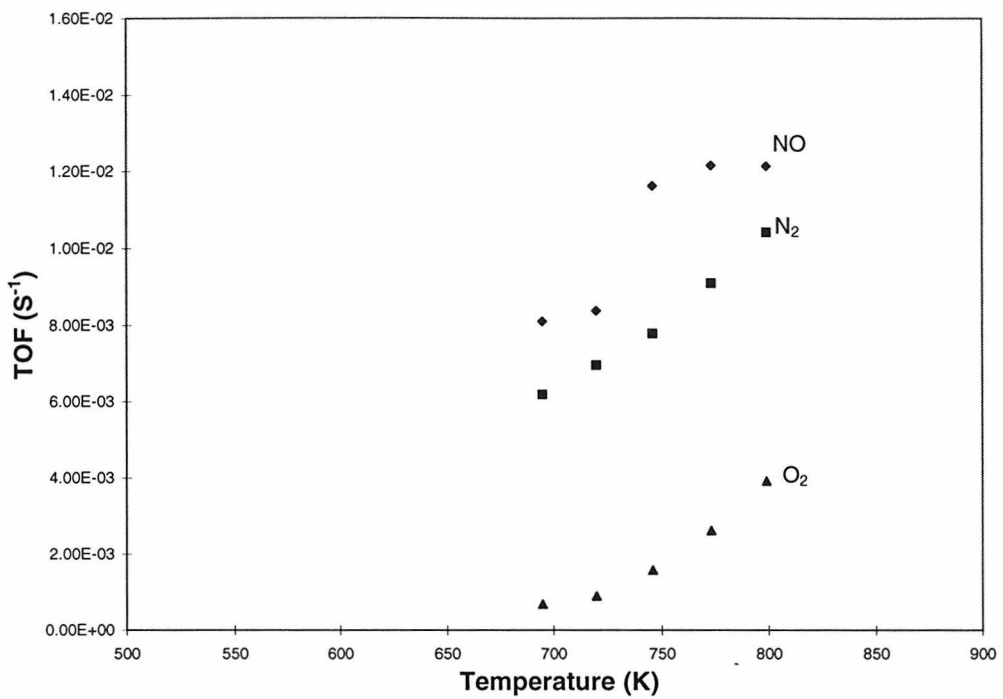


Figure 13 Turnover frequency versus temperature for VAW sample 1 exchanged with copper acetate.

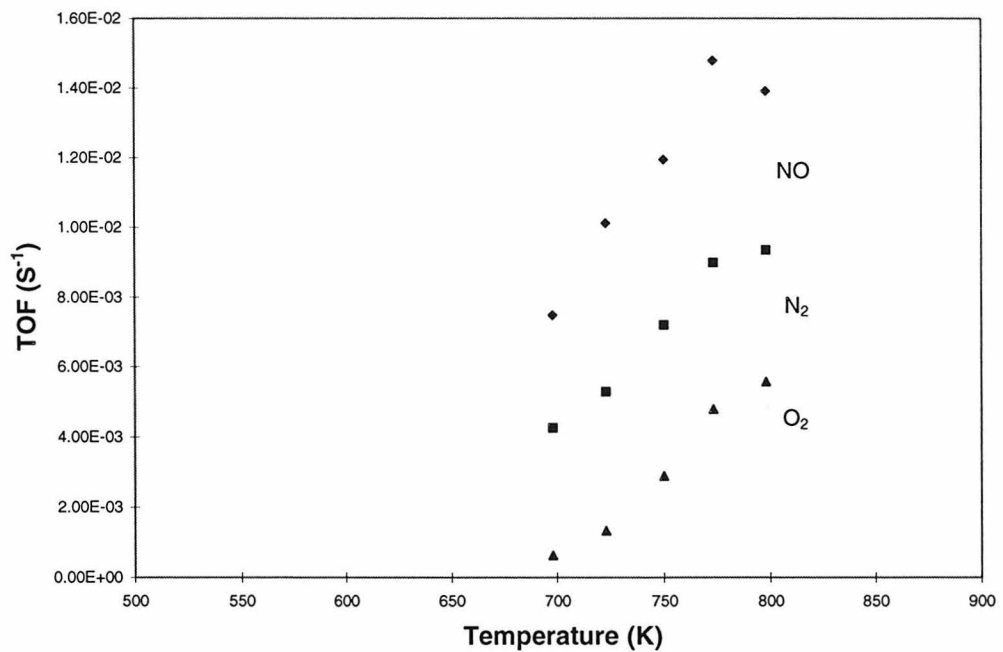


Figure 14 Turnover frequency versus temperature for VAW sample 1 exchanged with copper ethylene.

The temperature dependence of the activities was determined by generating arrhenius plots ($\ln(\text{rate})$ versus $1/T$), see Figures 15 and 16. The activation energy of the reaction can be calculated from the slope of the best fit line.²⁰ The data point at 525 °C was not used in the line fit because the rate started to decrease with temperature at this point and therefore departs from arrhenius behavior. The values for the activation energies are reported in Table 6. It should be noted that these activation energies are two to three times lower than expected. One possible explanation is that the experimental data used to calculate these values were taken at temperatures near the reaction rate maximum and were not in the arrhenius region.

Another point worth addressing is why the rates calculated from the decrease in NO do not match those calculated from the increase in N₂ and O₂. From Figure 11 it is seen that N₂ and O₂ are not the only products of the decomposition reaction. Nitrous oxide (N₂O) and nitrogen dioxide (NO₂) also form in significant quantities. It appears that more NO₂ forms than N₂O which would explain why the conversions calculated from N₂ are higher than for O₂. In order to quantitatively confirm this the mass spectrometer needs to be calibrated for N₂O and NO₂.

Table 6 Activation Energies

(kcal/mole)	Decrease in NO Concentration	Increase in N ₂ Concentration	Increase in O ₂ Concentration
Copper Acetate	6.36	5.21	18.6
Copper Ethylene	9.41	10.8	29.3

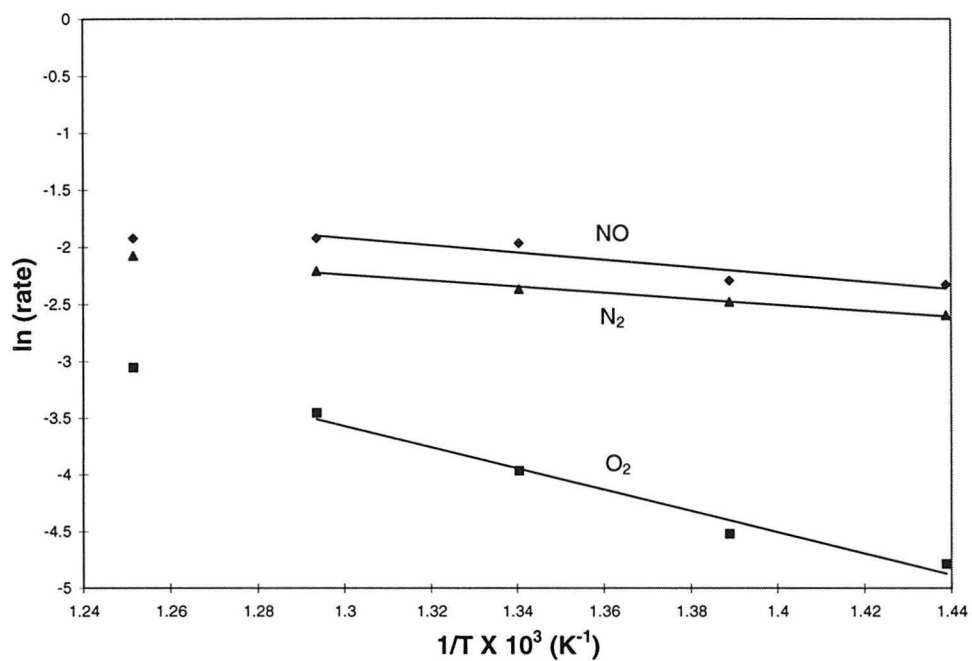


Figure 15 Arrhenius plot for VAW sample 1 exchanged with copper acetate.

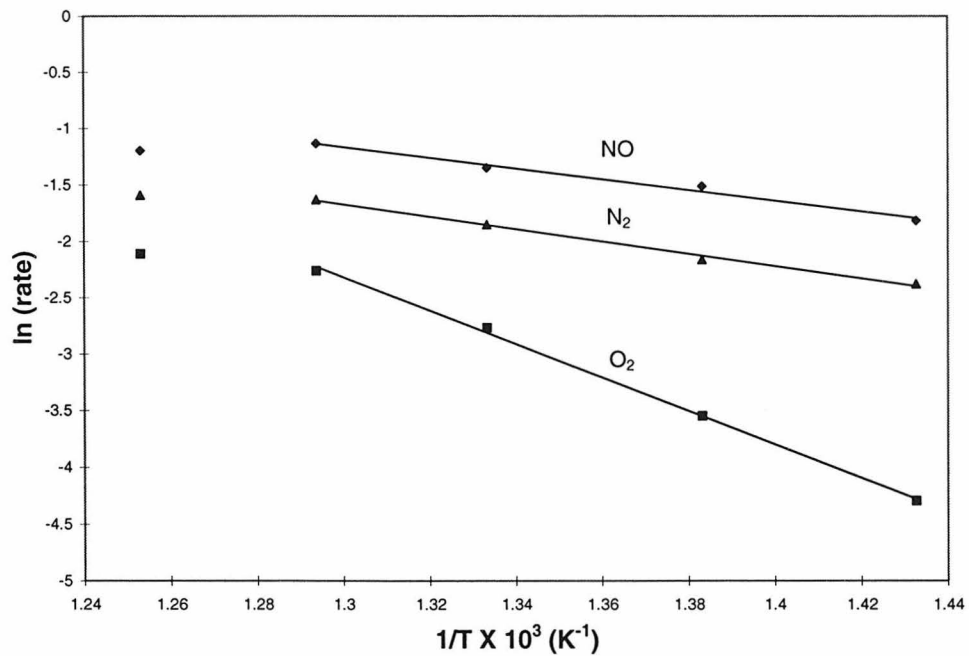


Figure 16 Arrhenius plot for VAW sample 1 exchanged with copper ethylene.

4. Conclusions and Future Directions

4.1 Conclusions

Direct decomposition of nitric oxide by copper ion-exchanged ZSM-5 was investigated. It was found that ion-exchanging with a copper ethylene complex doubles the copper content in the zeolite because copper is in an oxidation state of one, and can only balance the charge from one aluminum atom. The reaction rates also double for these samples, however, the turnover frequencies are similar to those obtained by samples exchanged with copper acetate.

Samples prepared using TPA were found to have poor ion-exchange properties and therefore low activities toward the decomposition of NO. It is probable that TPA forces the aluminum in the framework of ZSM-5 to be more uniformly distributed than in a template free synthesis. It is possible that in the template free samples there is a high concentration of aluminum near the outside of the crystal. Copper can then easily exchange onto these sites, whereas aluminum in the center of the crystal are much harder to ion-exchange with copper.

4.2 Future Directions

4.2.1 Exchange on Different Si/Al Samples

All the ion-exchanges performed have been on samples with Si/Al between 16 and 32. If the charge on a Cu^{+2} ion is balanced by charges created by two framework aluminum atoms, then a sample with a $\text{Si/Al} = 40$ should result in very little or no ion-

exchange. A sample with Si/Al \sim 40, prepared by each of the three methods, could be ion-exchanged and tested for activity. Since high copper loadings are attainable in the VAW sample, it would be desired to attempt ion-exchange on other samples with Si/Al = 12, but it is not possible to synthesize these samples via the Na^+ or F^- templated method.

4.2.2 Temperature Programmed Desorption of Isopropylamine (IPA)

TPD experiments are another method for determining the amount of aluminum in a zeolite and could be conducted in the same fixed-bed reactor described above. TPD is performed on the acid form (H^+) of a zeolite. IPA is chemisorbed onto all the acid sites (Al^- and defect sites SiO^-) and quantitatively measured as it desorbs from these sites during heating. From past experience by Kam-to Wan in our lab, it is known that IPA desorbs from Al^- and SiO^- sites at different temperatures. Thus, TPD will accurately determine both the number of aluminum sites and defect sites in ZSM-5. This technique combined with Si NMR should produce reliable data for defect concentrations.

The procedure is to activate 50-100 mg of sample by heating under a flow of dry He to 300°C at 10°C/min. Next, the sample is cooled to 35°C. 75-150 μl IPA is introduced into the helium stream and the He flow continues over the catalyst for 1.5 hours to allow removal of any physisorbed IPA. The TPD is conducted by elevating the temperature at a rate of 10°C/min to 630°C. The desorbed gases are analyzed by a mass spectrometer.

4.2.3 Activity of Other Copper Ion-Exchanged Zeolites

It was found that NU-87 is active for the direct decomposition of NO. It would be helpful to test other zeolites with similar structure-property relationships for NO reactivity. The objective would be to try and predict which zeolites will be NO active before testing.

Another experiment would be to try and ion-exchange copper onto defect sites. ZSM-5 can be prepared with boro-silicate. The boron can be removed by treatment with HCl, creating a defect site. Sodium can then be exchanged onto the defect sites by exchanging with sodium hydroxide. Copper can be exchanged by the usual procedure. The activity of this sample might determine whether a copper atom must be coordinated with an aluminum atom for the site to be active.

5. References

- ¹ Li, Y.; Hall, W. K. *J. Phys. Chem.* **1990**, *94*, 6145.
- ² Sandler, S. I. *Chemical and Engineering Thermodynamics*, Wiley: New York, NY, **1989**, 604.
- ³ Moelwyn-Hughes, E. A. *Physical Chemistry*, Pergamon: London, **1961**, 989.
- ⁴ Winter, E. R. S. *J. of Catal.* **1971**, *22*, 158.
- ⁵ Davis, M. E. *Ind. Eng. Chem. Res.* **1991**, *30*, 1675.
- ⁶ Thome, R.; Schmidt, H.; Tissler, A. U.S. Patent No. 5,089,243 **1992**.
- ⁷ Larsen, S. C.; Aylor, A.; Bell, A. T.; Reimer, J. A. *J. Phys. Chem.* **1994**, *98*, 11533.
- ⁸ Iwamoto, M.; Yahiro, H.; Tanda, K.; Mizuno, N.; Mine, Y.; Kagawa, S. *J. Phys. Chem.* **1991**, *95*, 3727.
- ⁹ Li, Y.; Armor, J. N. *Appl. Catal. B* **1993**, *2*, 239.
- ¹⁰ Li, Y.; Armor, J. N. *Appl. Catal. B* **1993**, *3*, L1.
- ¹¹ Shapiro, E. S.; Grünert, W.; Joyner, R. W.; Baeva, G. N. *Catal. Lett.* **1994**, *24*, 159.
- ¹² Valyon, J.; Hall, W. K. *Catal. Lett.* **1993**, *19*, 109.
- ¹³ Li, Y.; Armor, J. N. *Appl. Catal. B* **1992**, *1*, L31.
- ¹⁴ Li, Y.; Armor, J. N. *Appl. Catal. B* **1993**, *3*, L55.
- ¹⁵ Bernas, B. *Anal. Chem.* **1968**, *40*, 1968.
- ¹⁶ Corbin, D. R.; Burgess Jr., B. F.; Vega, A. J.; Farlee, R. D. *Anal. Chem.* **1987**, *59*, 2722.
- ¹⁷ Feldman, C. *Anal. Chem.* **1983**, *55*, 2451.
- ¹⁸ Ogura, T. *Inorg. Chem.* **1976**, *15*, 2301.
- ¹⁹ Koller, H.; Lobo, R. F.; Burkett, S. L; Davis, M. E. *J. Phys. Chem.* **1995**, *99*, 12588.
- ²⁰ Hathaway, P. E.; Davis, M. E. *J. of Catal.* **1989**, *116*, 263.

Appendices

Appendix I. List of Chemicals Used

Aluminum hydroxide: Reheis Inc.

Aluminum nitrate nonahydrate: 98+%, Aldrich

Ammonium fluoride: 97%, Aldrich

Cesium iodide: 99.999%, Aldrich

Colloidal silica (SiO₂): Ludox AS-40, 40% SiO₂ in aq. solution, DuPont

Copper powder - 150 mesh: 99.5%, Aldrich

Copper(II) perchlorate hexahydrate: 98%, Aldrich

Cupric acetate monohydrate: EM Science

Fumed-silica (SiO₂): 99.8%, Cab-O-Sil M5, Cabot Corp.

ICP Standards: aluminum, calcium, copper, scandium, silicon, sodium 1000 PPM, VWR

L-Tartaric acid: 99.5%, Aldrich

Lithium Metaborate: 99.995%, Aldrich

Methyl alcohol anhydrous: 99.9%, Mallinckrodt

Nitric Acid: 69.6%, Mallinckrodt

Nitric oxide: 14.8% balance helium, Matheson

Potassium carbonate: 99.99%, Aldrich

Sodium chloride: 99+%, Em Science

Sodium hydroxide: 50% (w/w), Mallinckrodt

Sodium hydroxide: Em Science

Tetrapropylammonium bromide (TPABr): 98%, Aldrich

Water: distilled and deionized

Appendix II. List of Samples

Sample No	Synthesis Method	Gel Si/Al	PS ^a Samples	HK ^b Samples
1	VAW	-----	-----	-----
2	Na+ / TPA	20	PS001 PS007 PS013 PS015	HK113
3	Na+ / TPA	40	PS003 PS008	HK114
4	F- / TPA	14.9	PS005 PS009 PS014 PS016	HK109
5	F- / TPA	23.8	PS004 PS010	HK108
6	F- / TPA	40	PS006 PS011	HK110
7	Na+ template free	18	PS012A	-----

^aSamples prepared by Peter Seidel

^bSamples prepared by Hubert Koller

Appendix III. Characterization of Samples

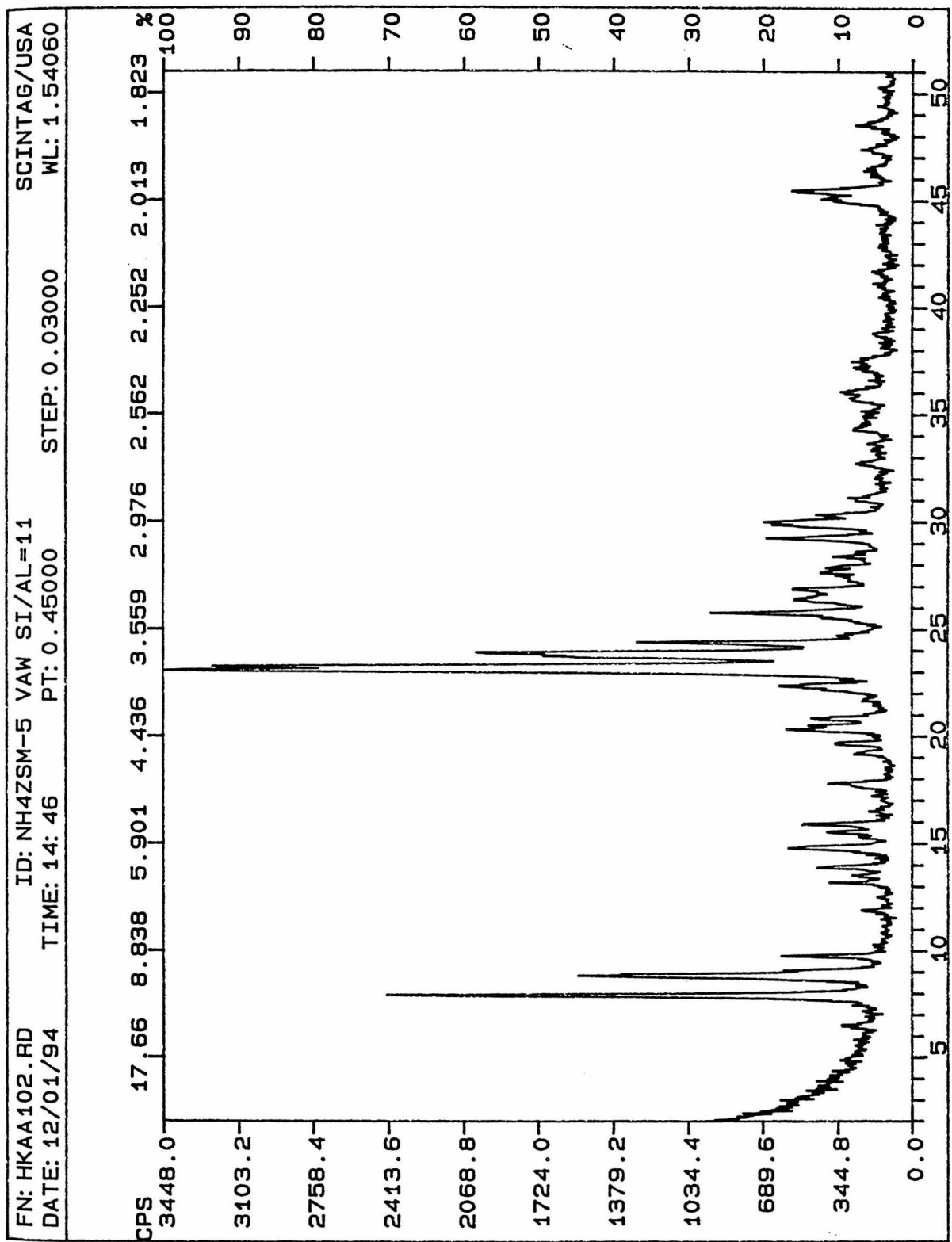
Sample	XRD			TGA		NMR				Elemental Analysis		
	as made		Calcined			as made		Calcined		Galb	Peter Seidel	
	as made	Calc	after TGA	as made	Calc [*] Na ⁺	²⁹ Si	²⁷ Al	²⁹ Si	²⁷ Al	as made	as made	Calc [*] Na ⁺
VAW	x			x	x	x	x	x	x		x	
PS001	x	x	x	x	x							x
PS003	x			x	x							x
PS004	x		x	x	x							x
PS005	x	x		x	x							x
PS006	x			x	x							x
PS007	x				x							x
PS008	x											
PS009	x				x							x
PS010	x											
PS011	x											
PS012	x			x							x	
PS013	x											
PS014	x											
PS015	x											
PS016	x											
HK113	x	x		x		x	x	x	x	x		
HK114	x			x		x	x	x	x			
HK109	x	x		x		x	x	x	x	x		
HK108	x			x		x	x	x	x			
HK110	x	x		x		x	x	x	x	x		

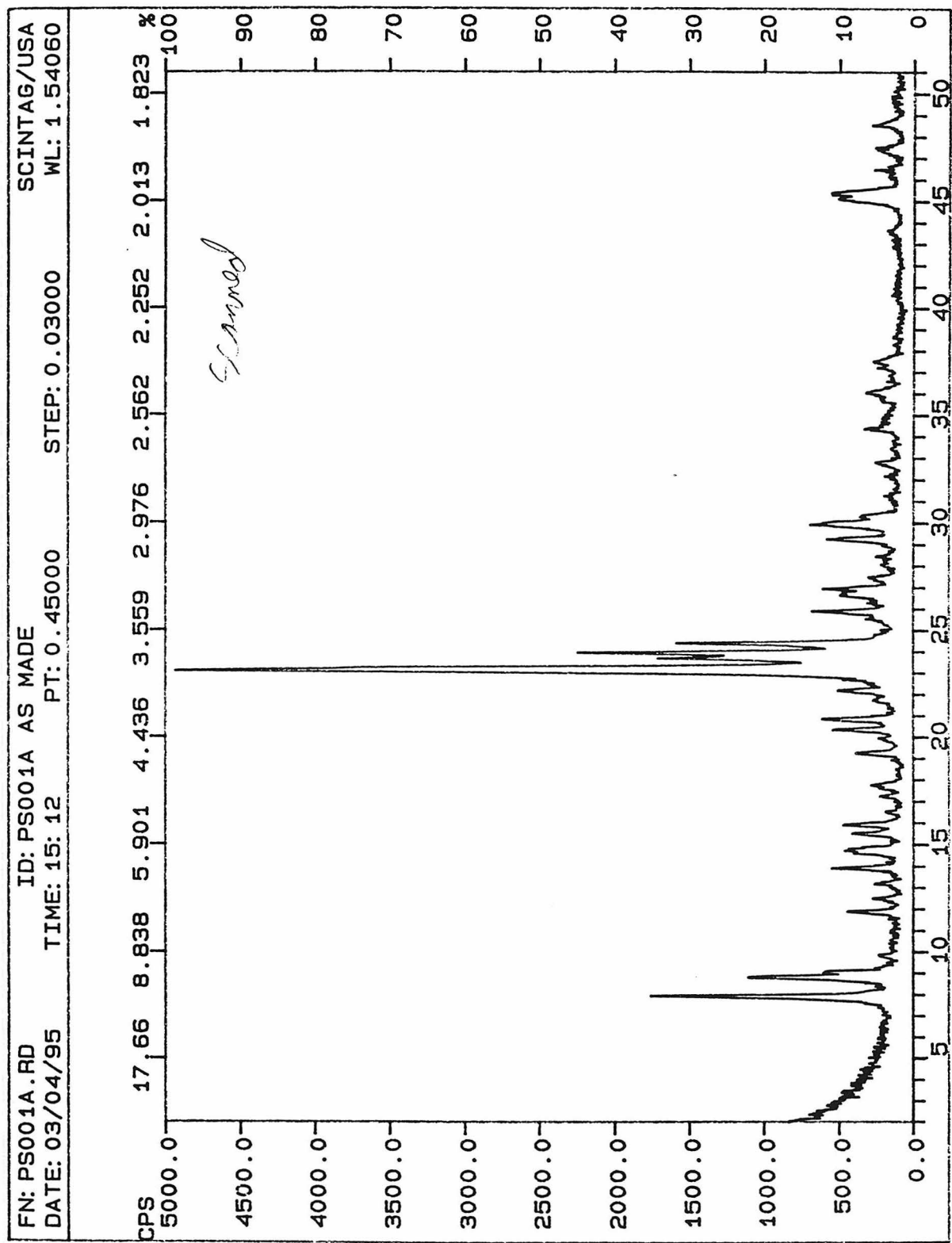
*Samples were calcined and ion-exchanged with sodium chloride

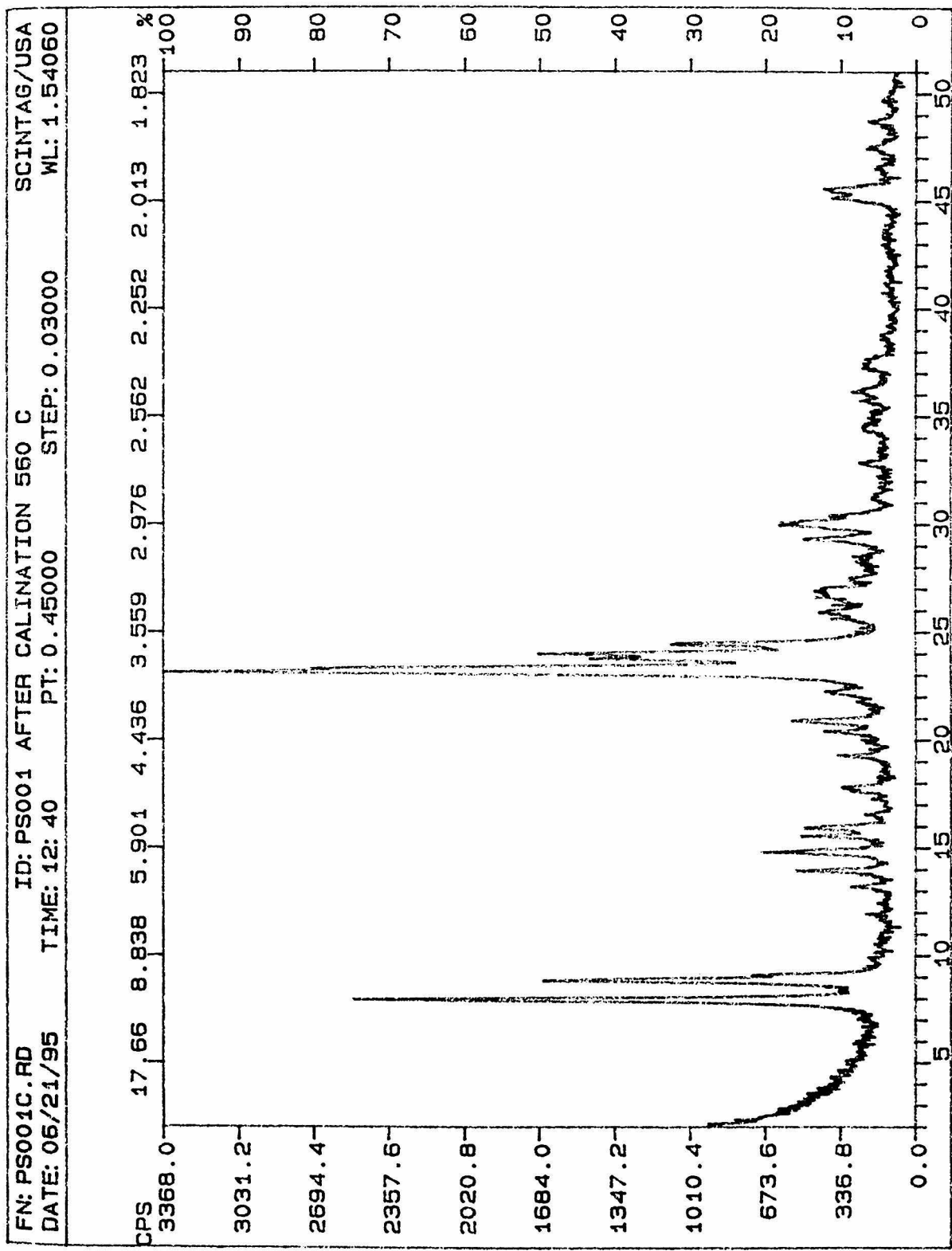
Appendix IV. X-ray Powder Diffraction Patterns

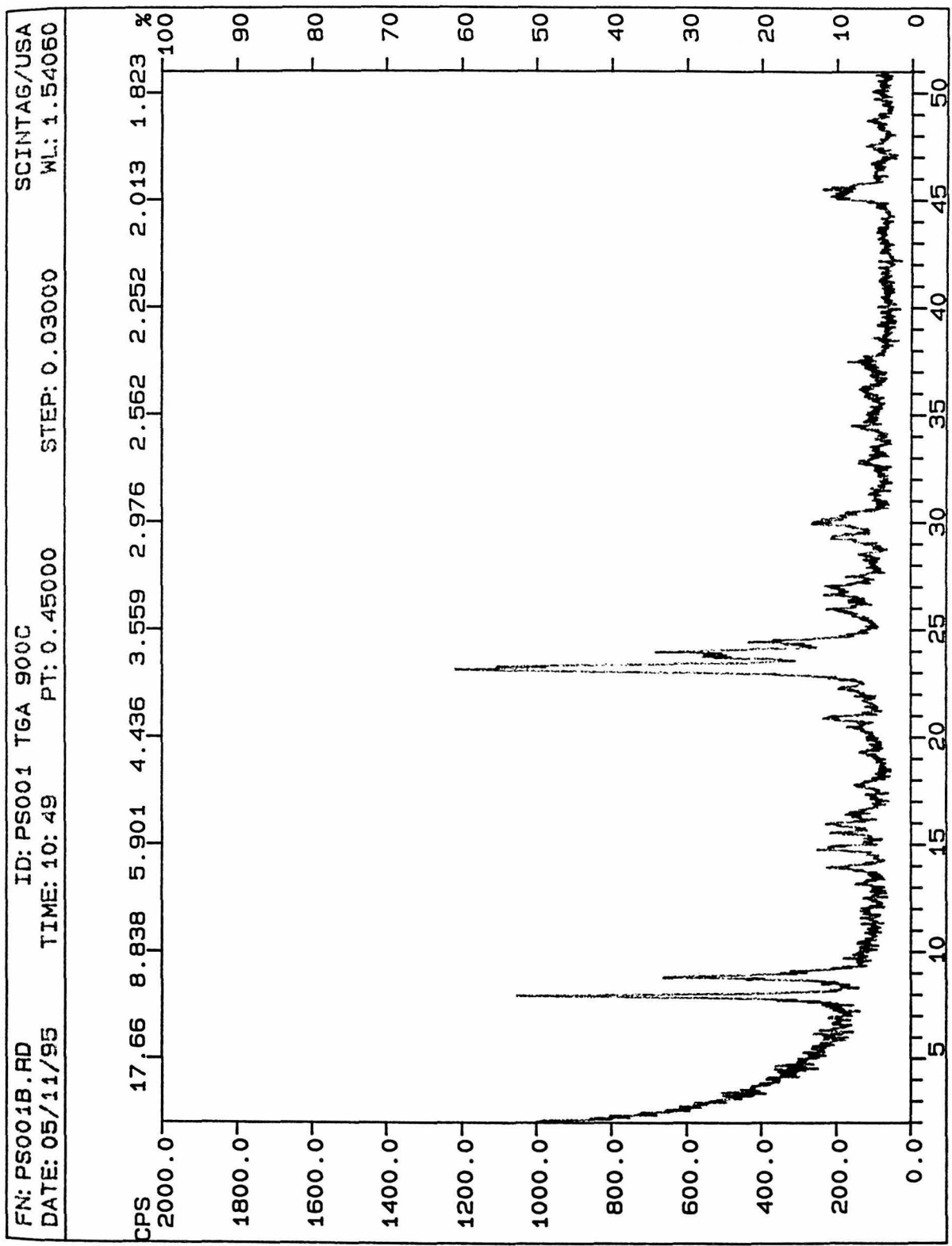
VAW NH₄⁺

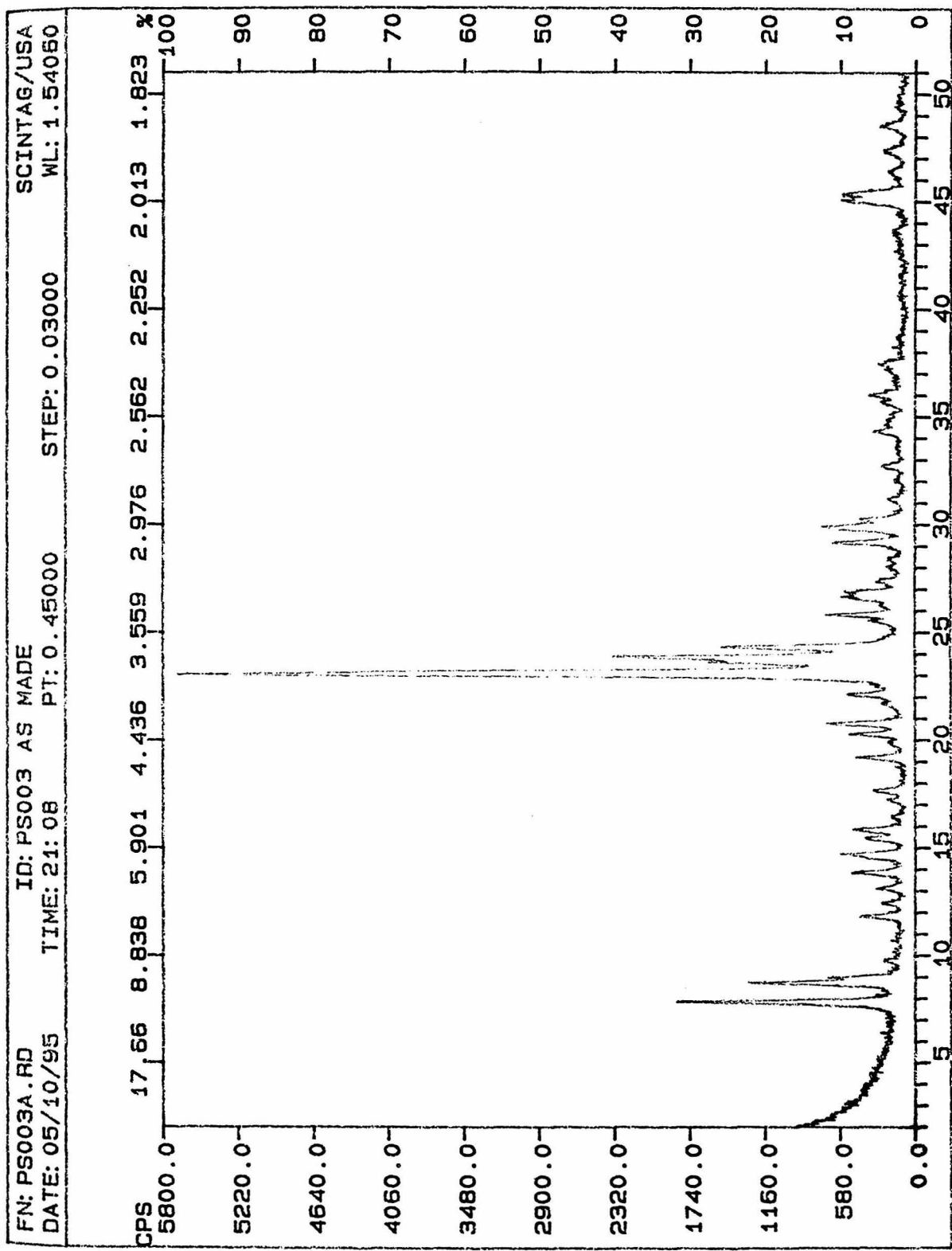
PS001 as made	PS001 Calcined	PS001 after TGA
PS003 as made		
PS004 as made		PS004 after TGA
PS005 as made,	PS005 Calcined	
PS006 as made		
PS007 as made		
PS008 as made		
PS009 as made		
PS010 as made		
PS011 as made		
PS012 as made		
PS013 as made		
PS014 as made		
PS015 as made		
PS016 as made		

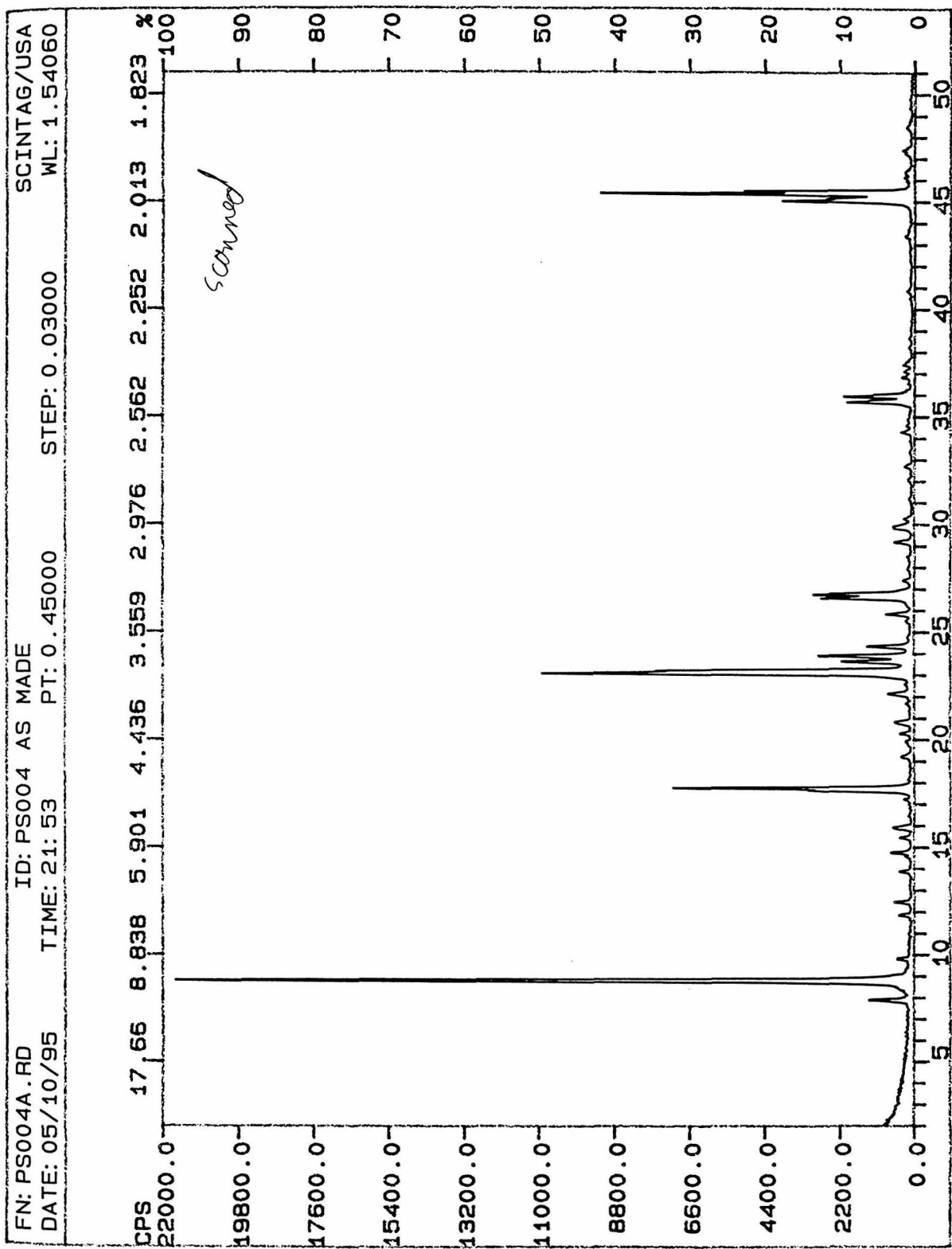


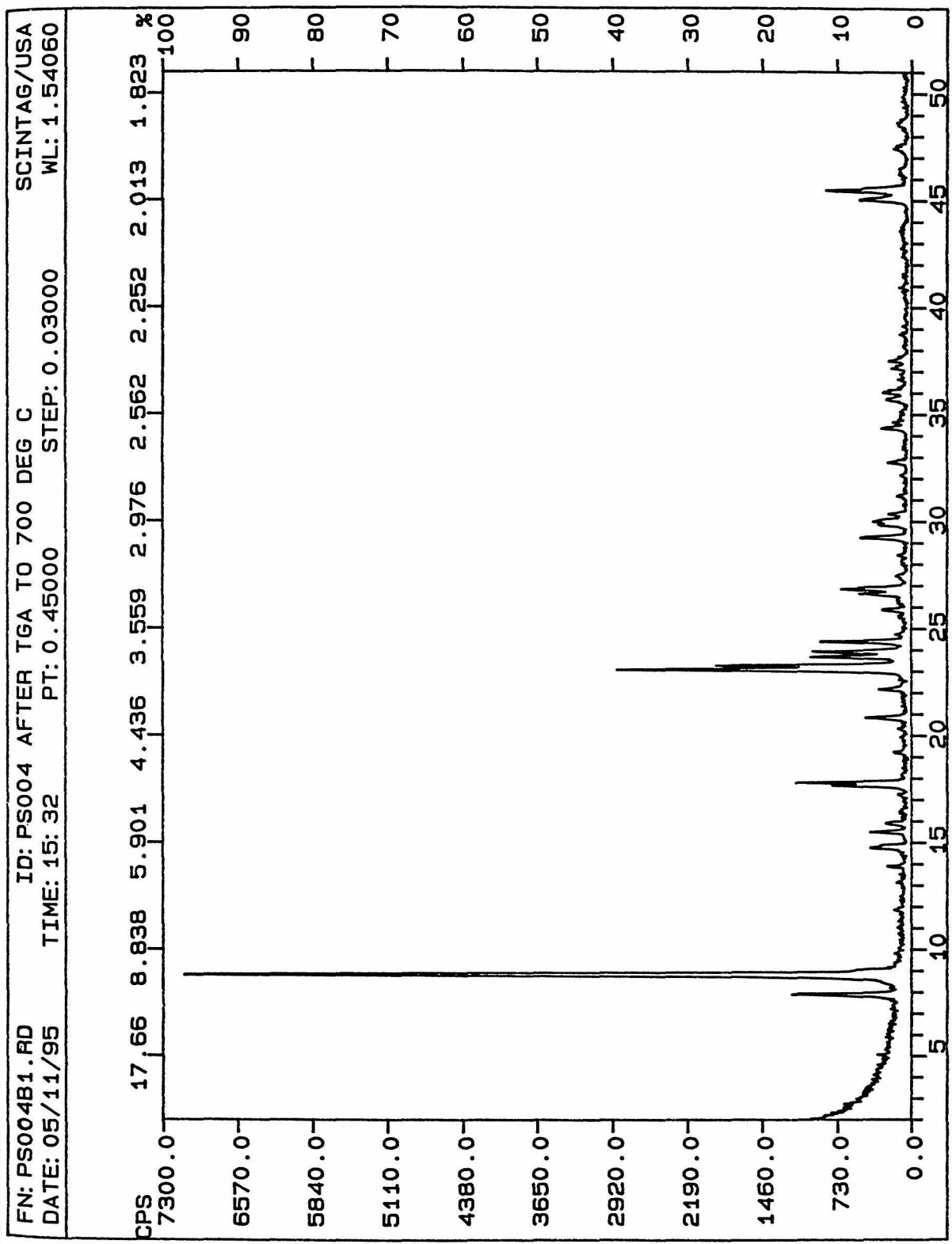


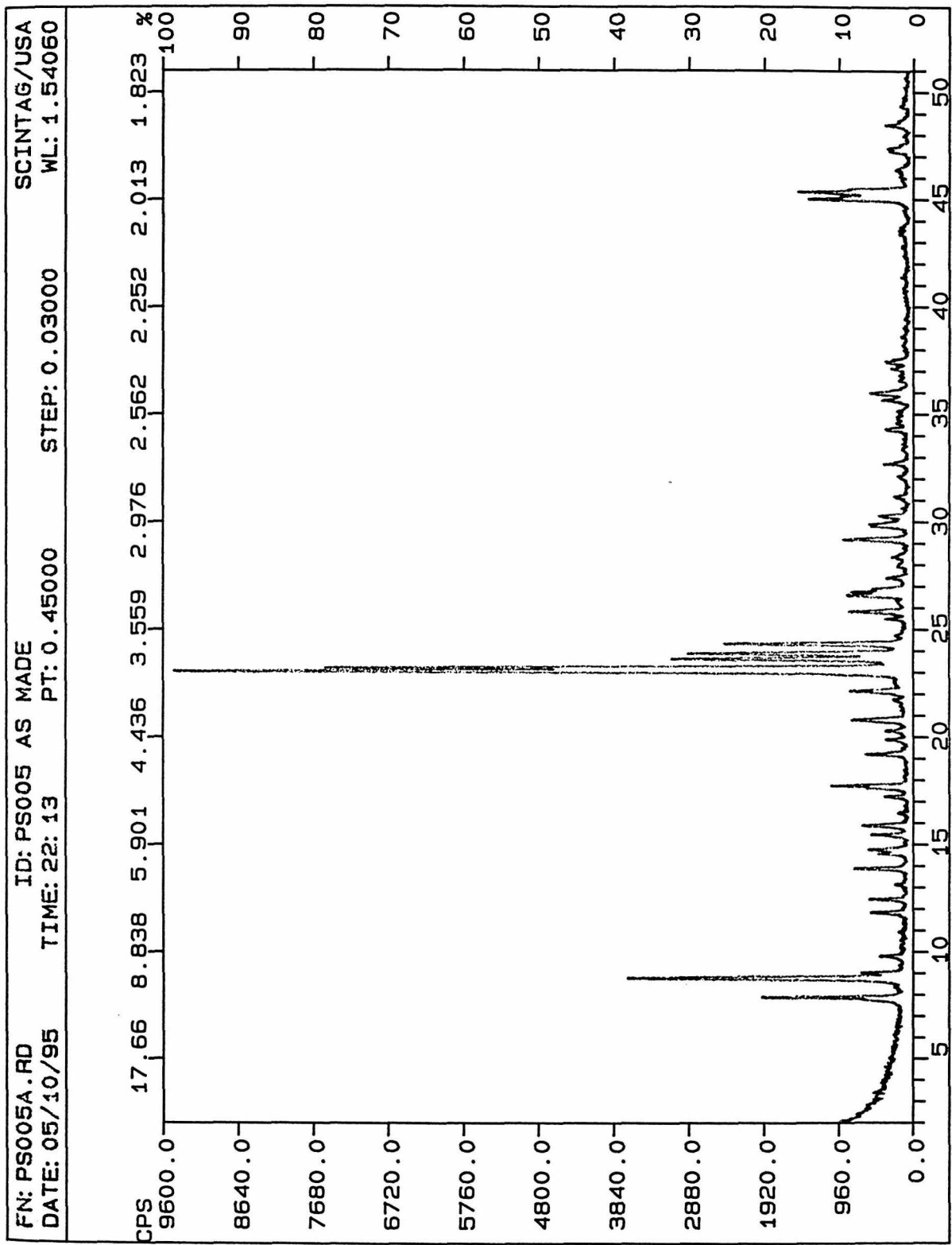


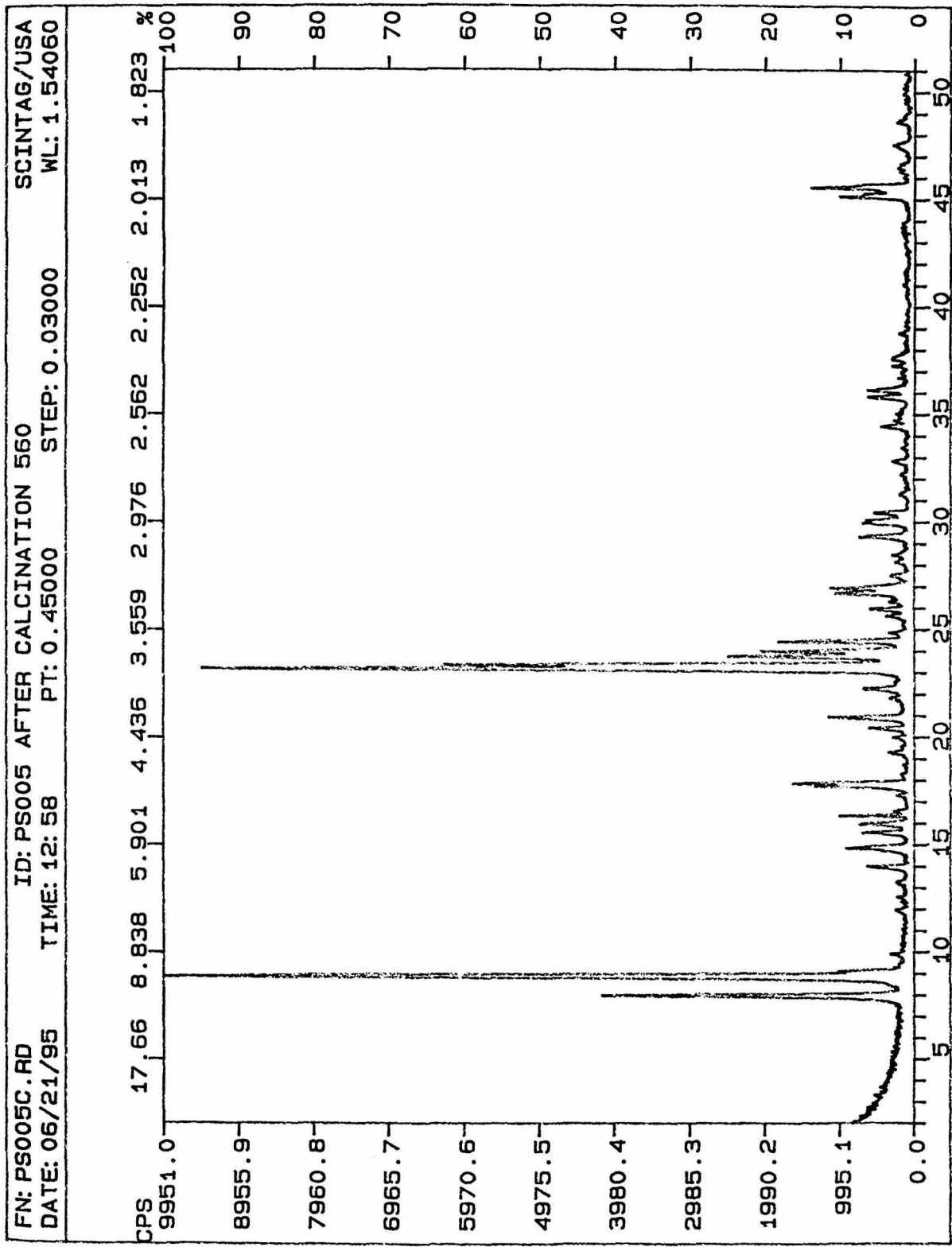


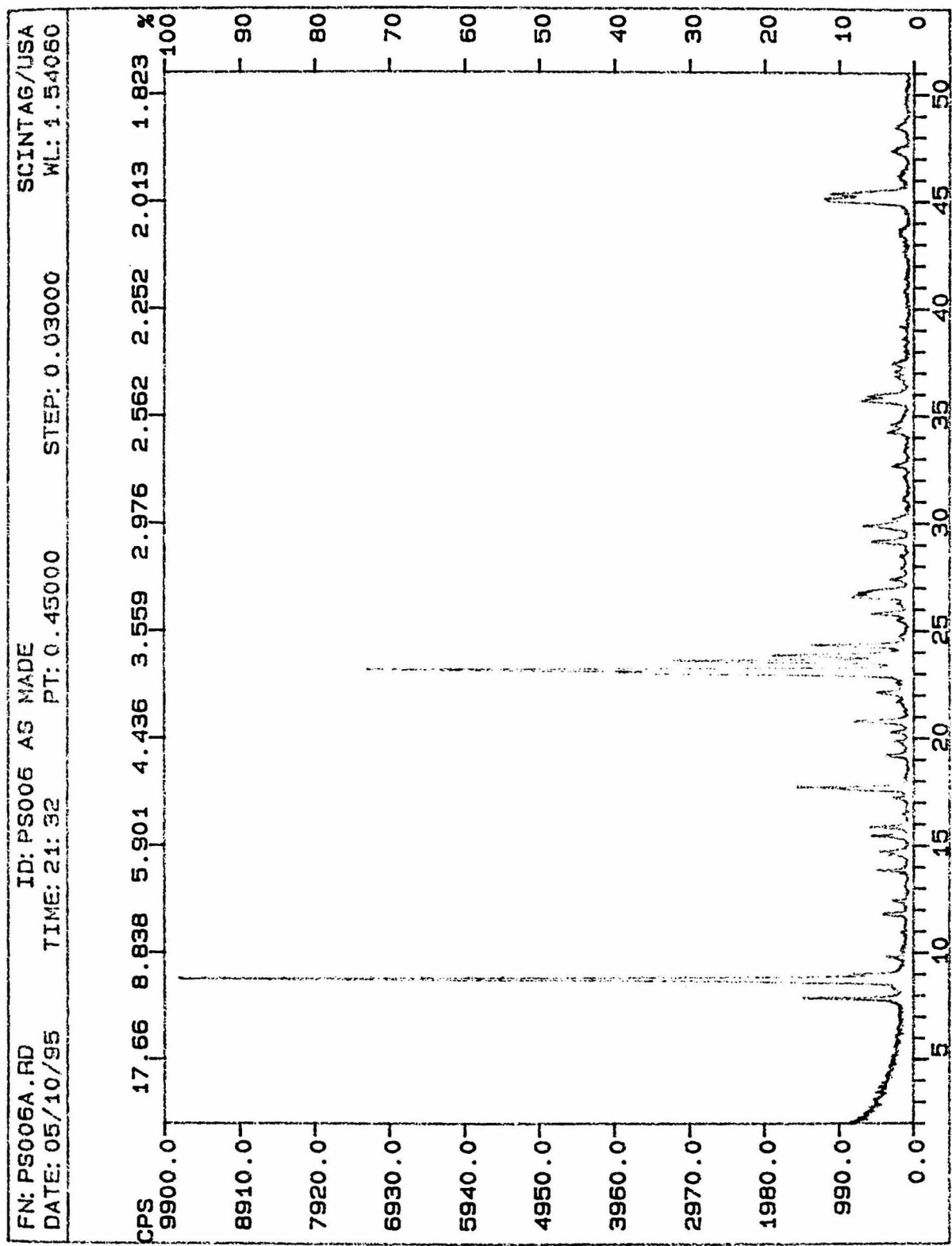


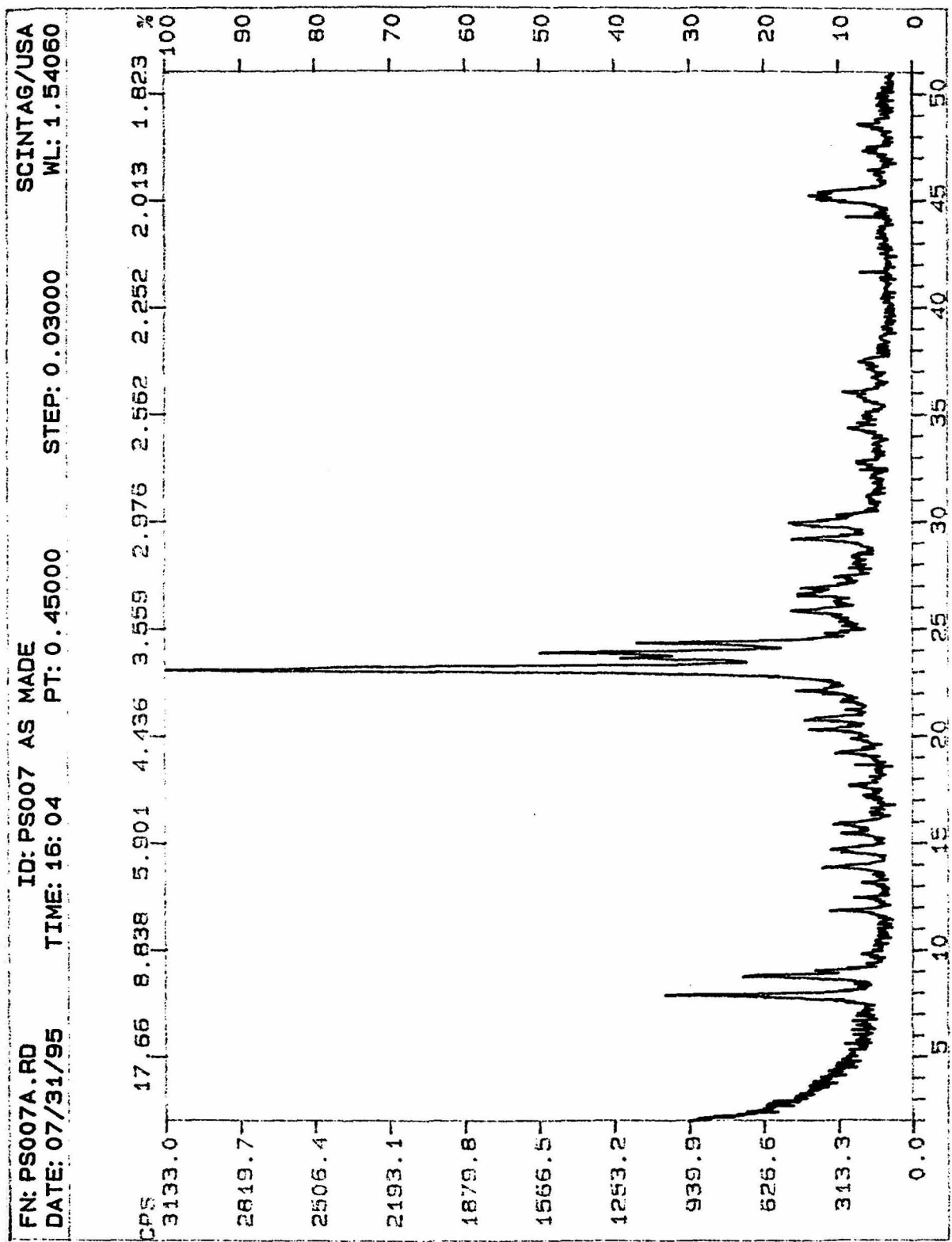


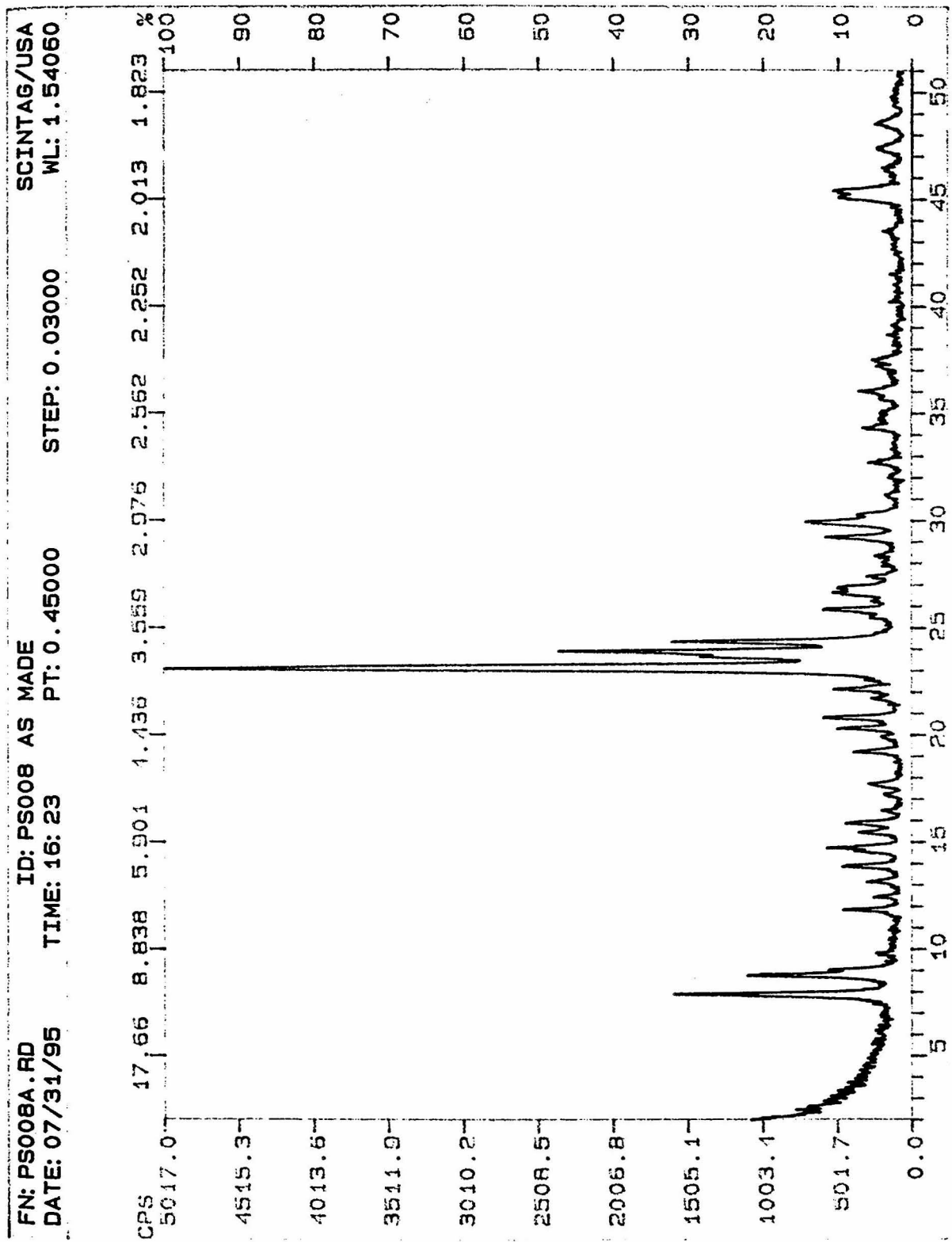


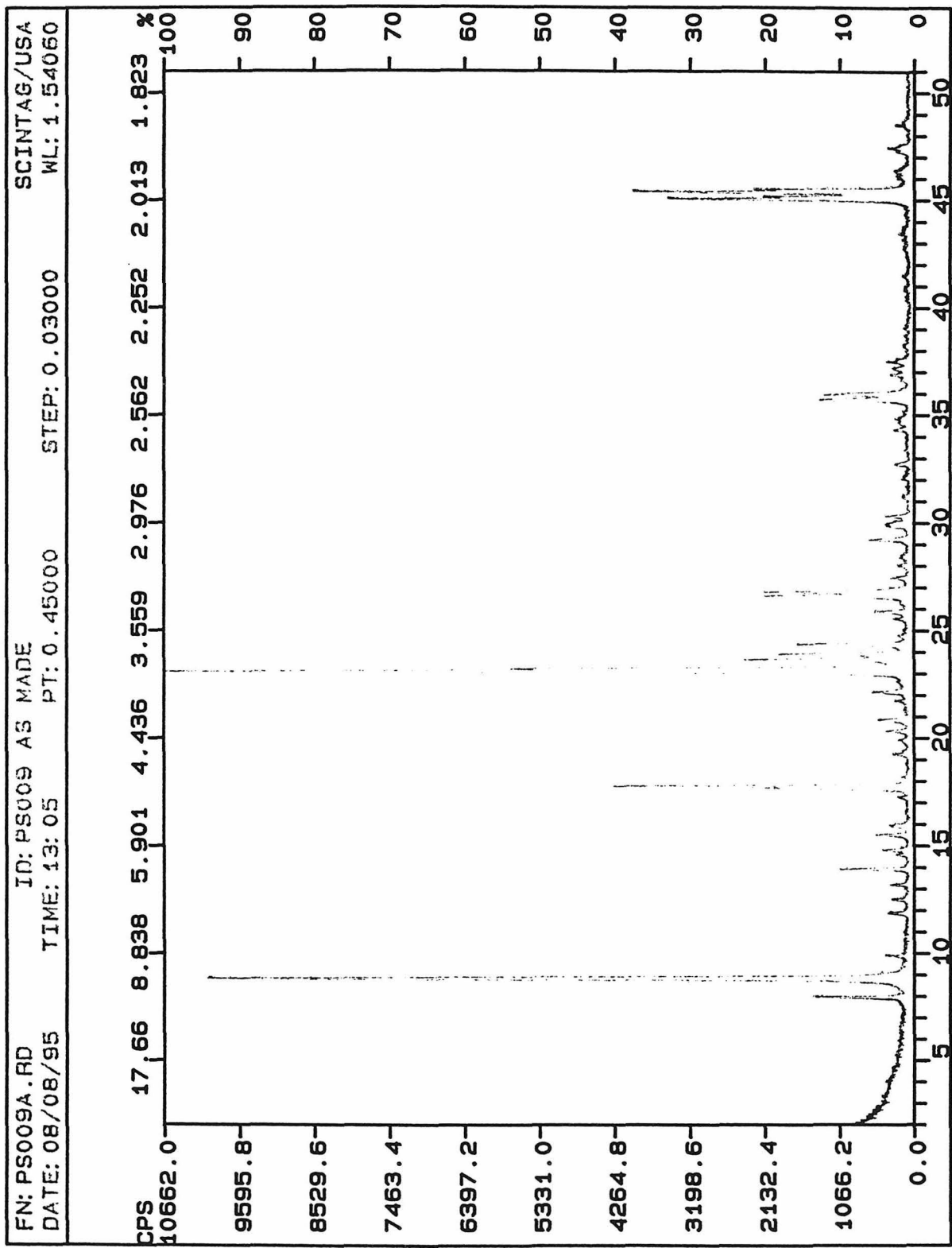




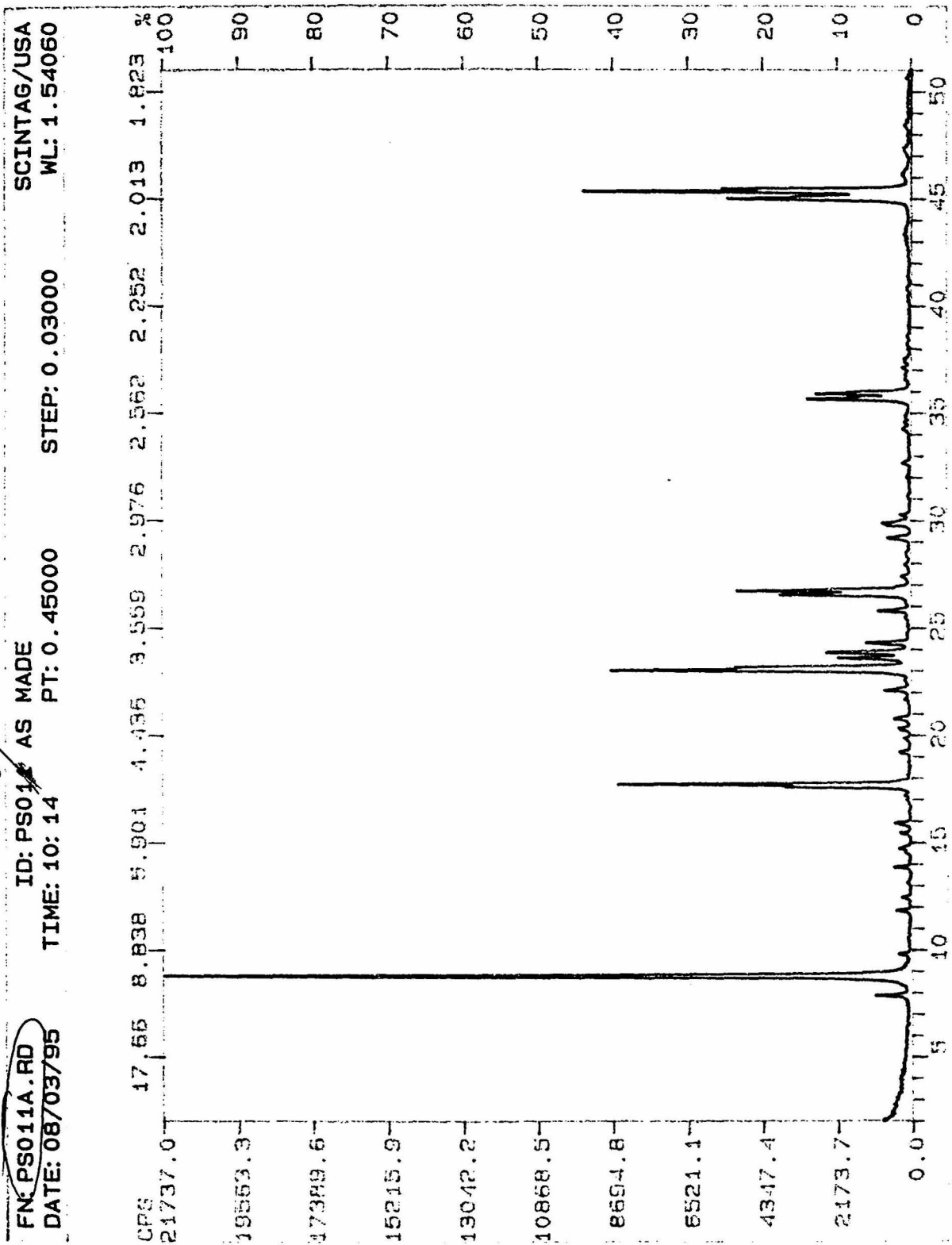




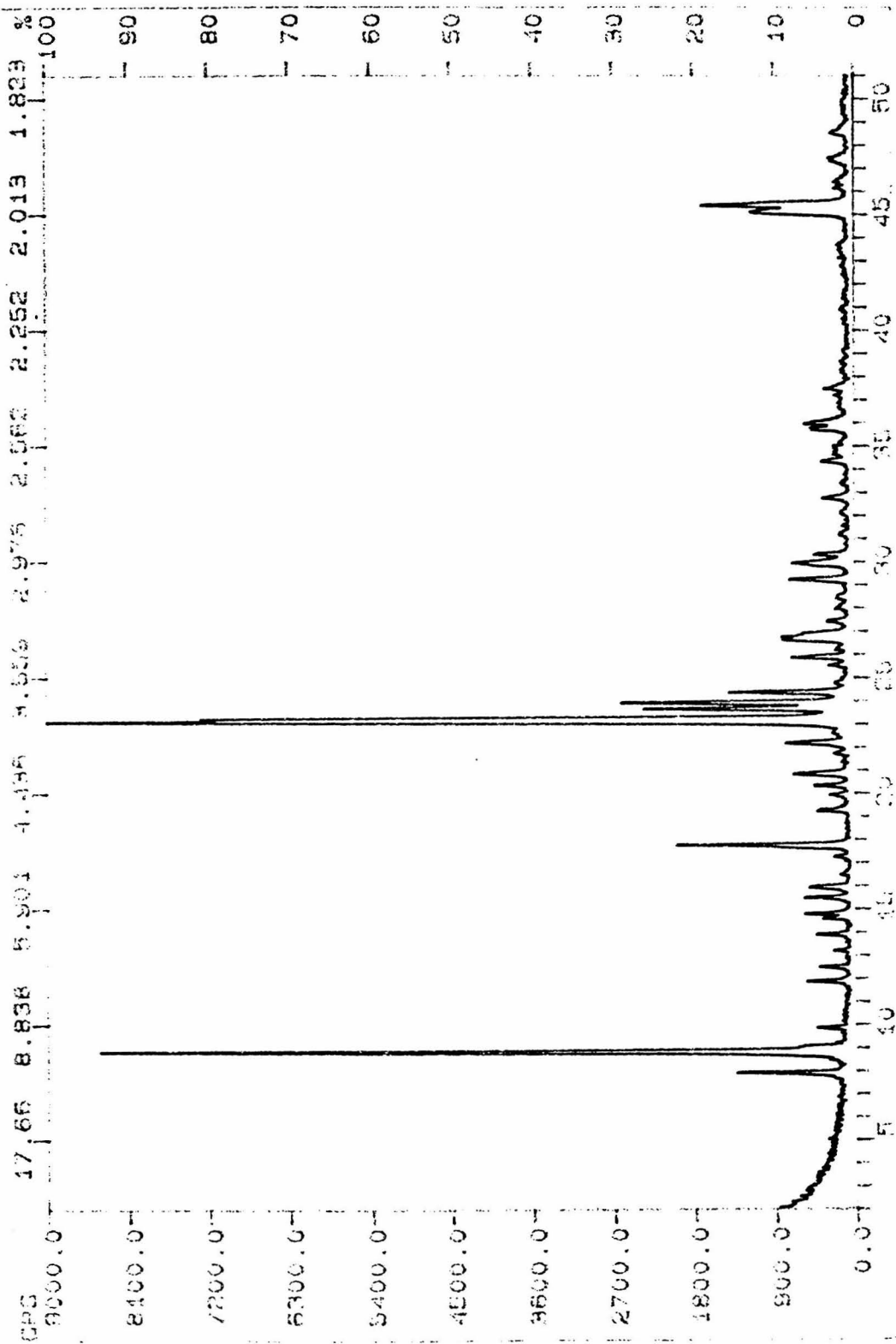


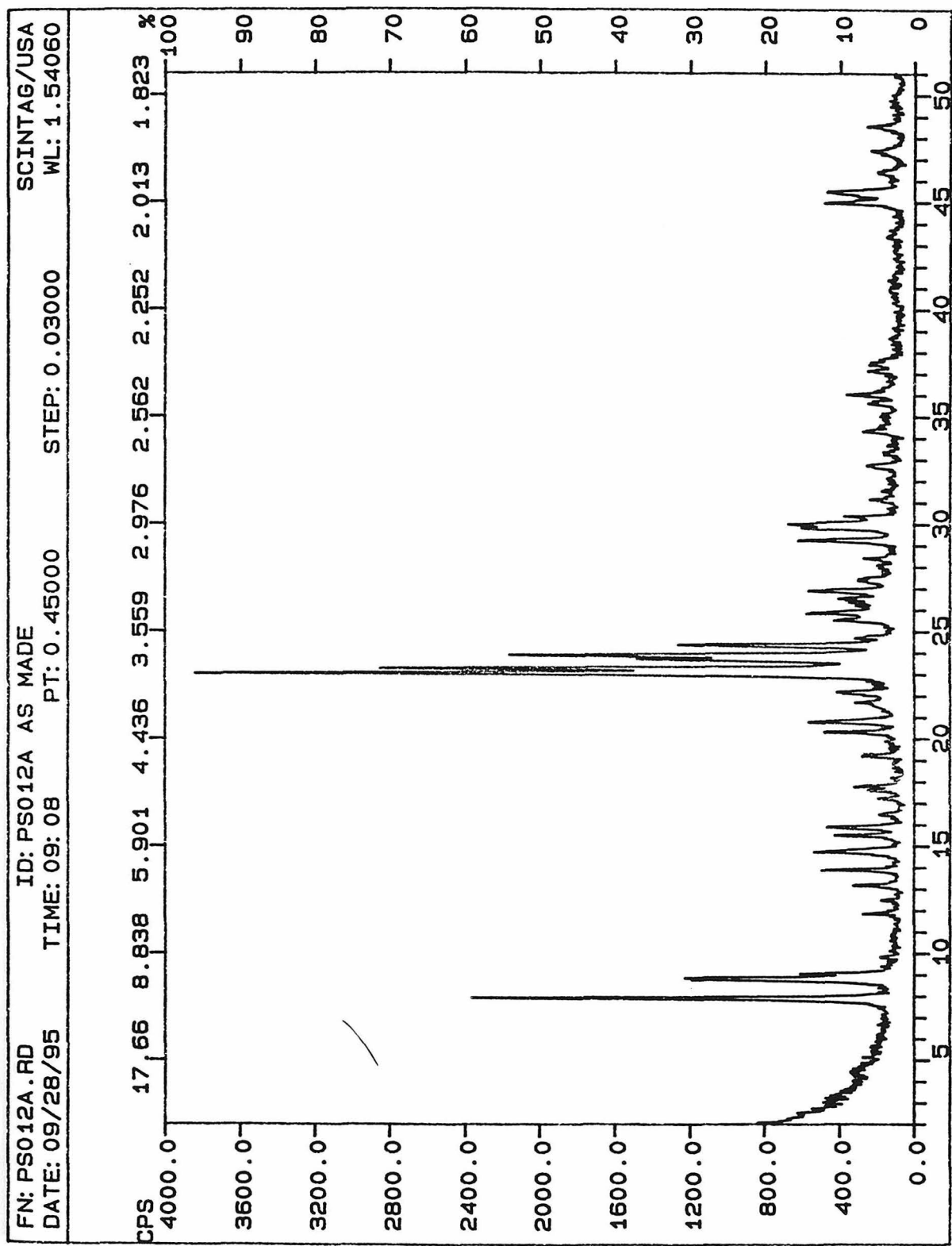


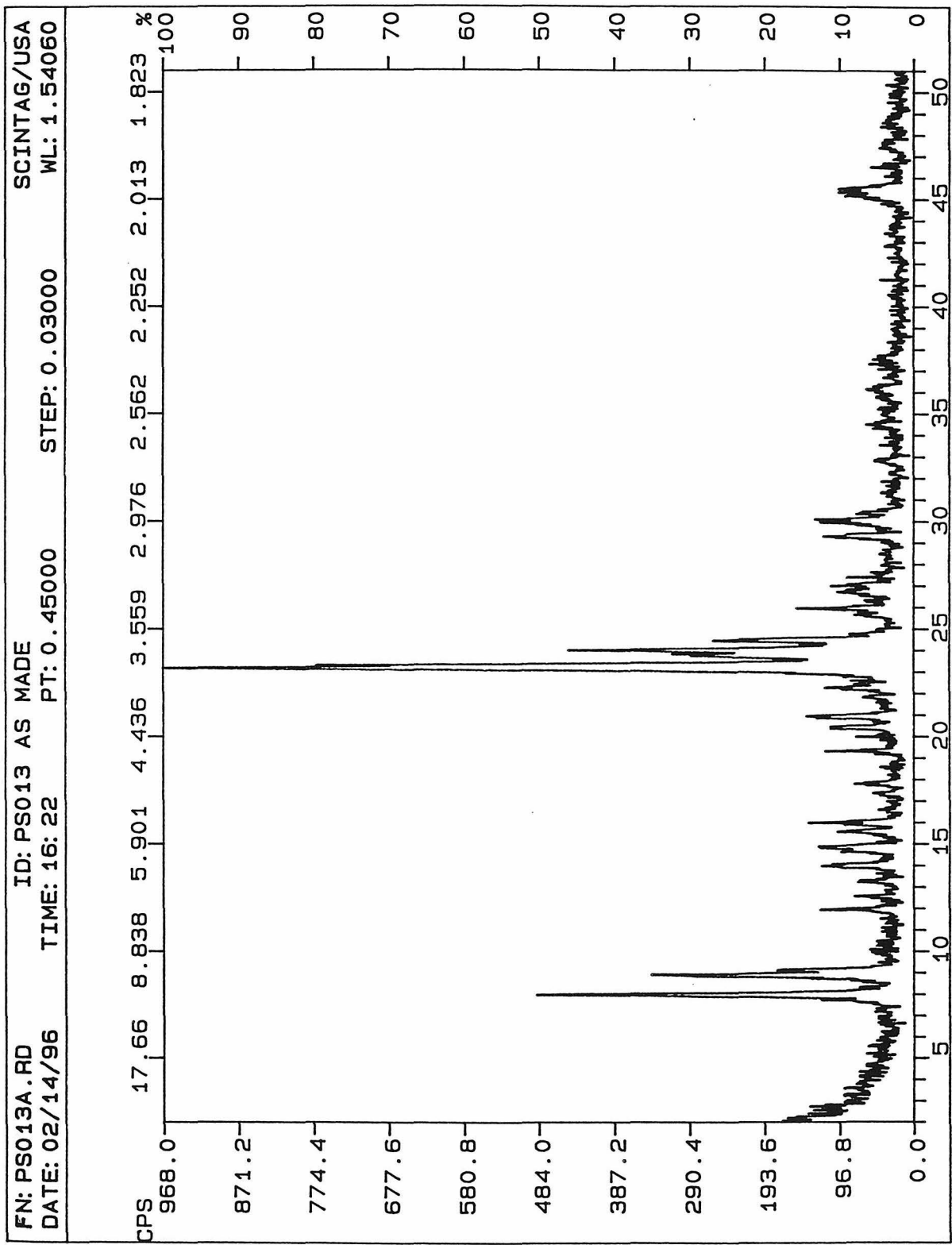
10/
 FN: PS011A.RD ID: PS011 AS MADE
 DATE: 08/03/95 TIME: 10: 14 PT: 0.450000 STEP: 0.03000

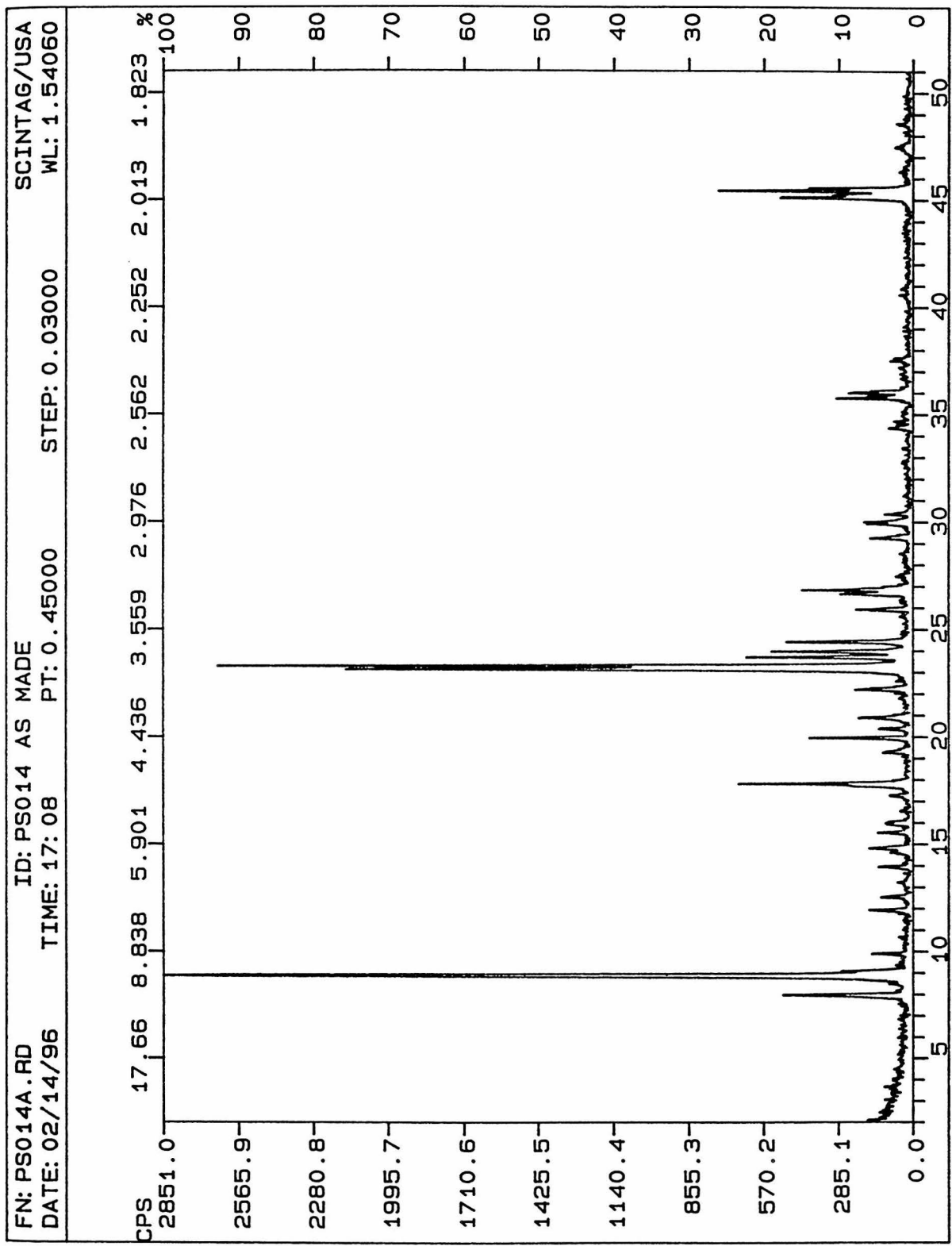


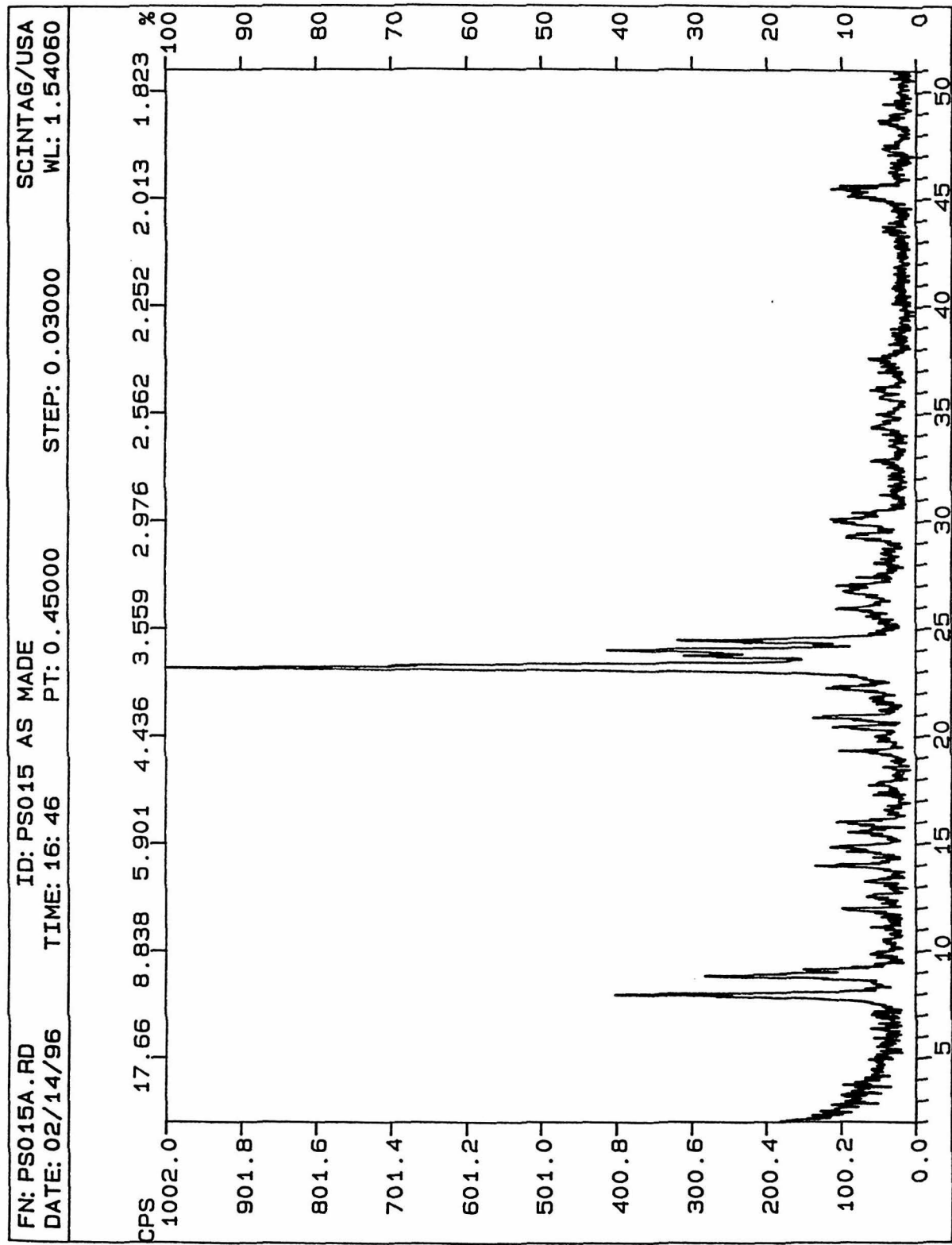
Economy
2 PS010A.RD ID: PS011 AS MADE
 DATE: 08/04/95 TIME: 13:47 PT: 0.45000
 STEP: 0.03000
 SCINTAG/USA
 WL: 1.54060

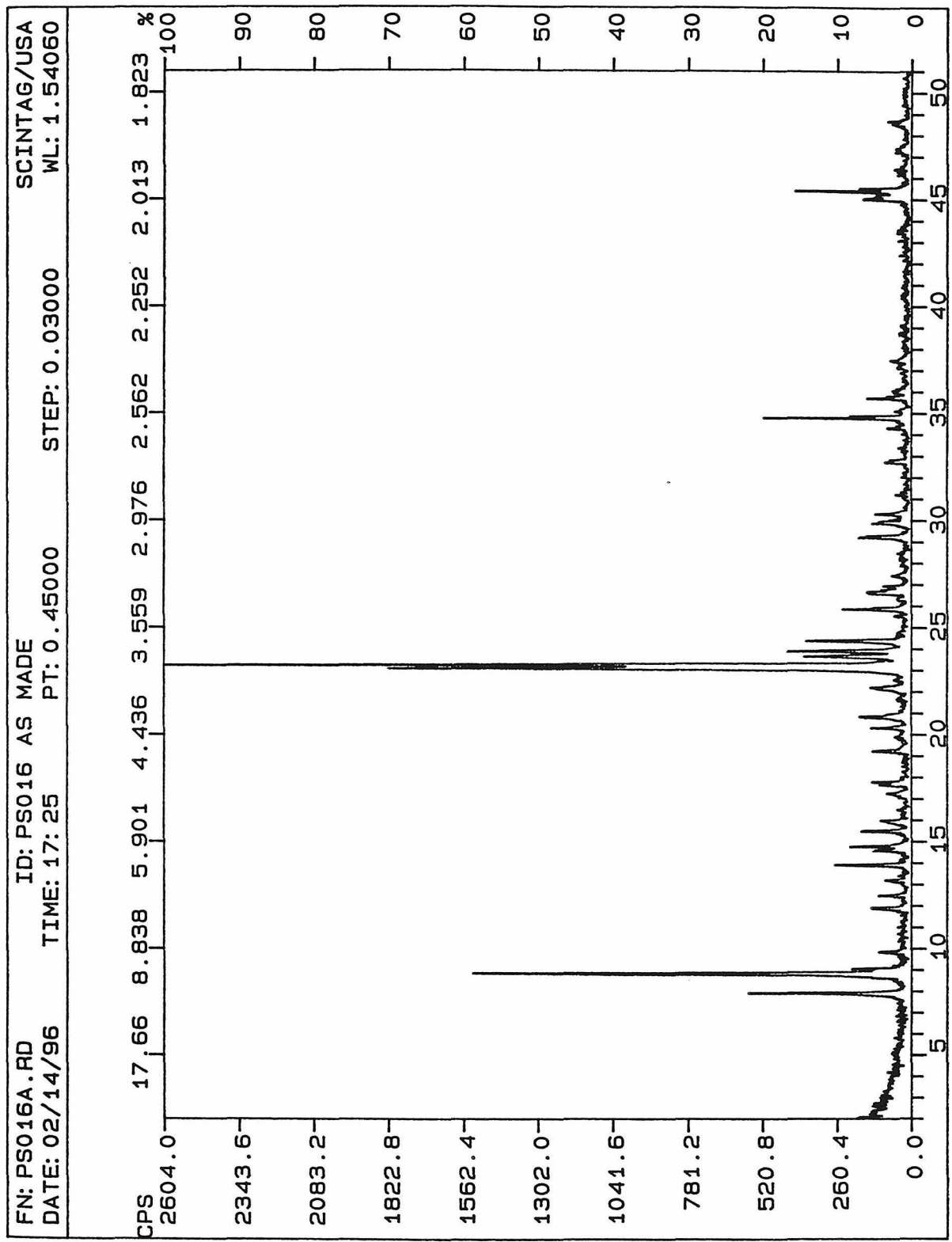












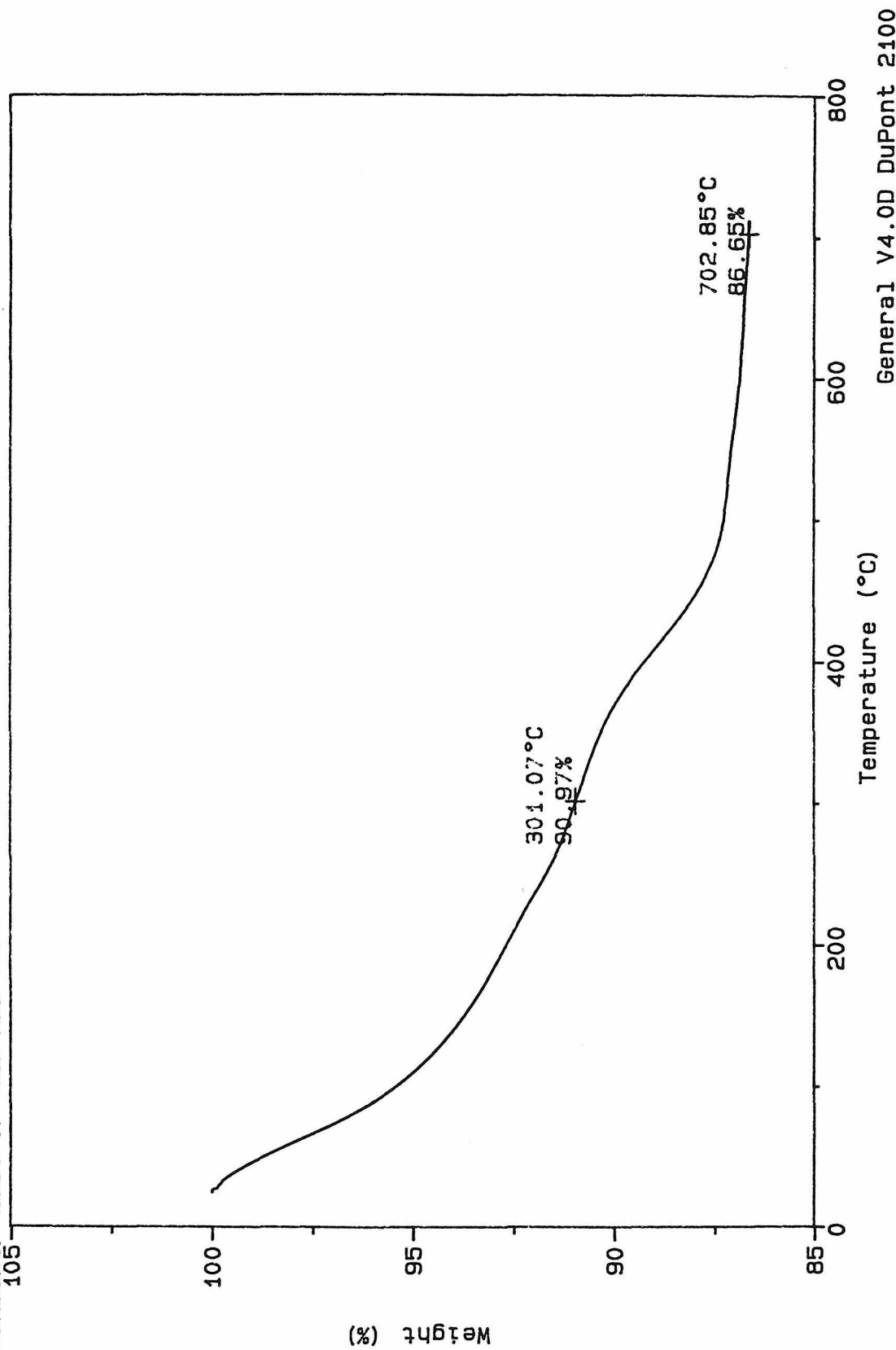
Appendix V. Thermogravimetric Analyses

VAW NH ₄ ⁺	VAW Na ⁺ exchanged
PS001 as made	PS001 Calcined and Na ⁺ exchanged
PS003 as made	PS003 Calcined and Na ⁺ exchanged
PS004 as made	PS004 Calcined and Na ⁺ exchanged
PS005 as made	PS005 Calcined and Na ⁺ exchanged
PS006 as made	PS006 Calcined and Na ⁺ exchanged
	PS007 Calcined and Na ⁺ exchanged
	PS009 Calcined and Na ⁺ exchanged
PS012 as made	

Sample: NH4-ZSM5 VAW 7461-05-43
Size: 11.3370 mg
Method: 10 DEG C/MIN TO 700 DEG C
Comment: LOSS OF H2O AND NH4+
105

TGA

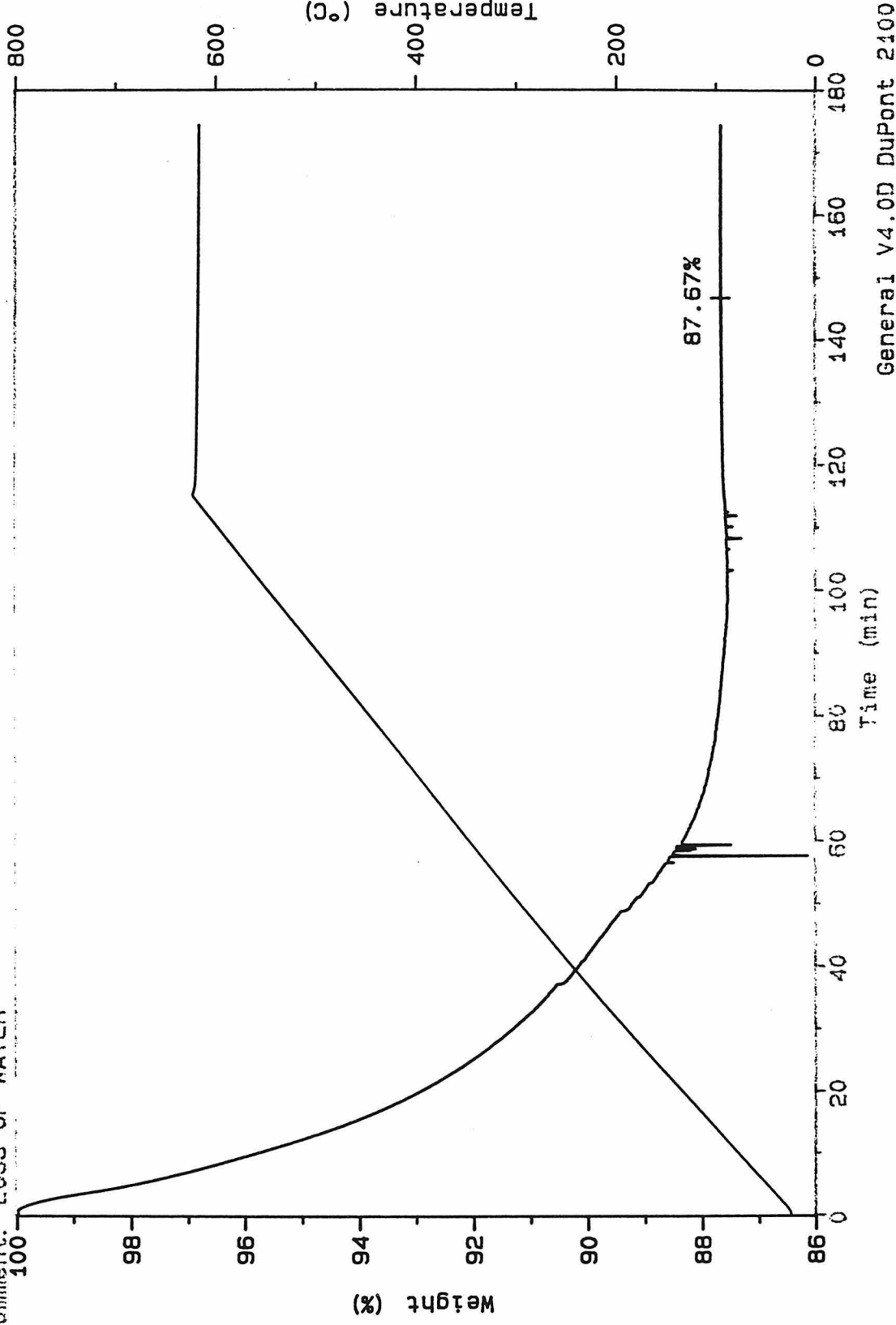
File: A:HKVAW.002
Operator: HK
Run Date: 10-Feb-95 09: 24



File: A:VAWZSMNA.001
 Operator: JCL
 Run Date: 26-Jun-95 22:38

TGA

Sample: VAWZSMNA
 Size: 12.1830 mg
 Method: 5C/MIN 600 ISO 60 MIN
 Comment: LOSS OF WATER

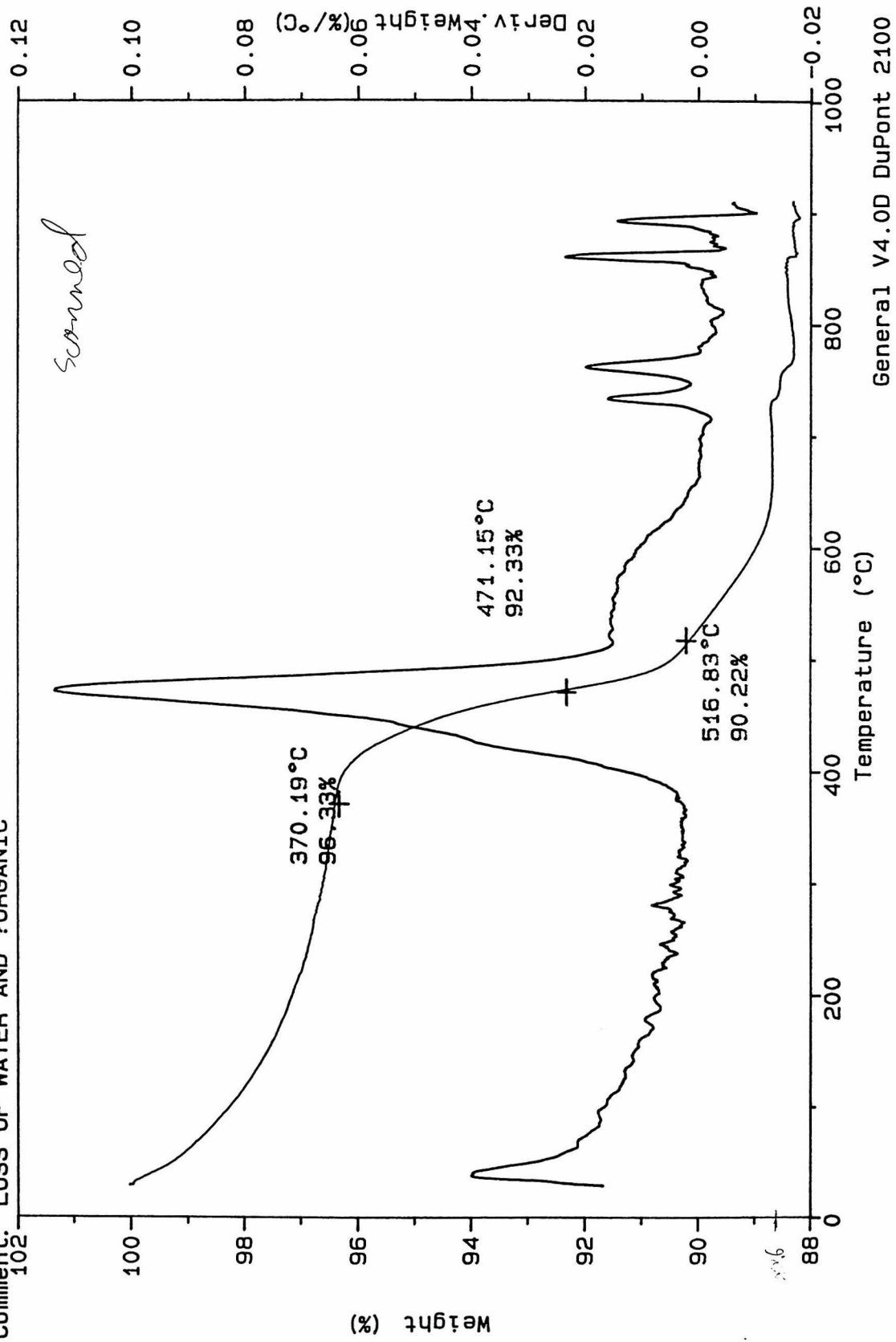


General V4.0D DuPont 2400

Sample: PS001 NA-TPA-AL-ZSM-5
Size: 9.8390 mg
Method: 10 DEG C/MIN TO 900 DEG C
Comment: LOSS OF WATER AND ?ORGANIC
102

TGA

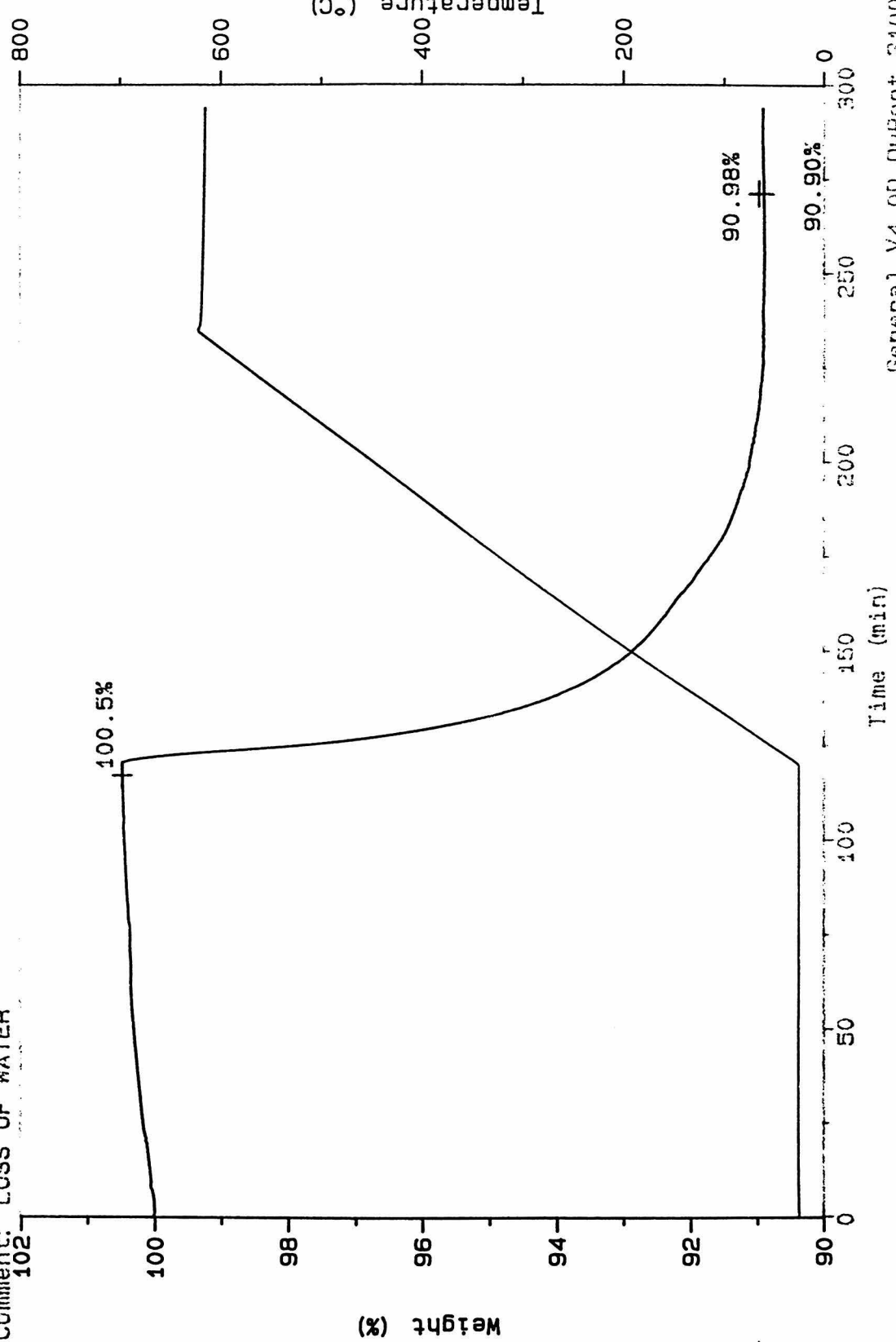
File: C:PS001A
Operator: PS
Run Date: 10-May-95 22:12

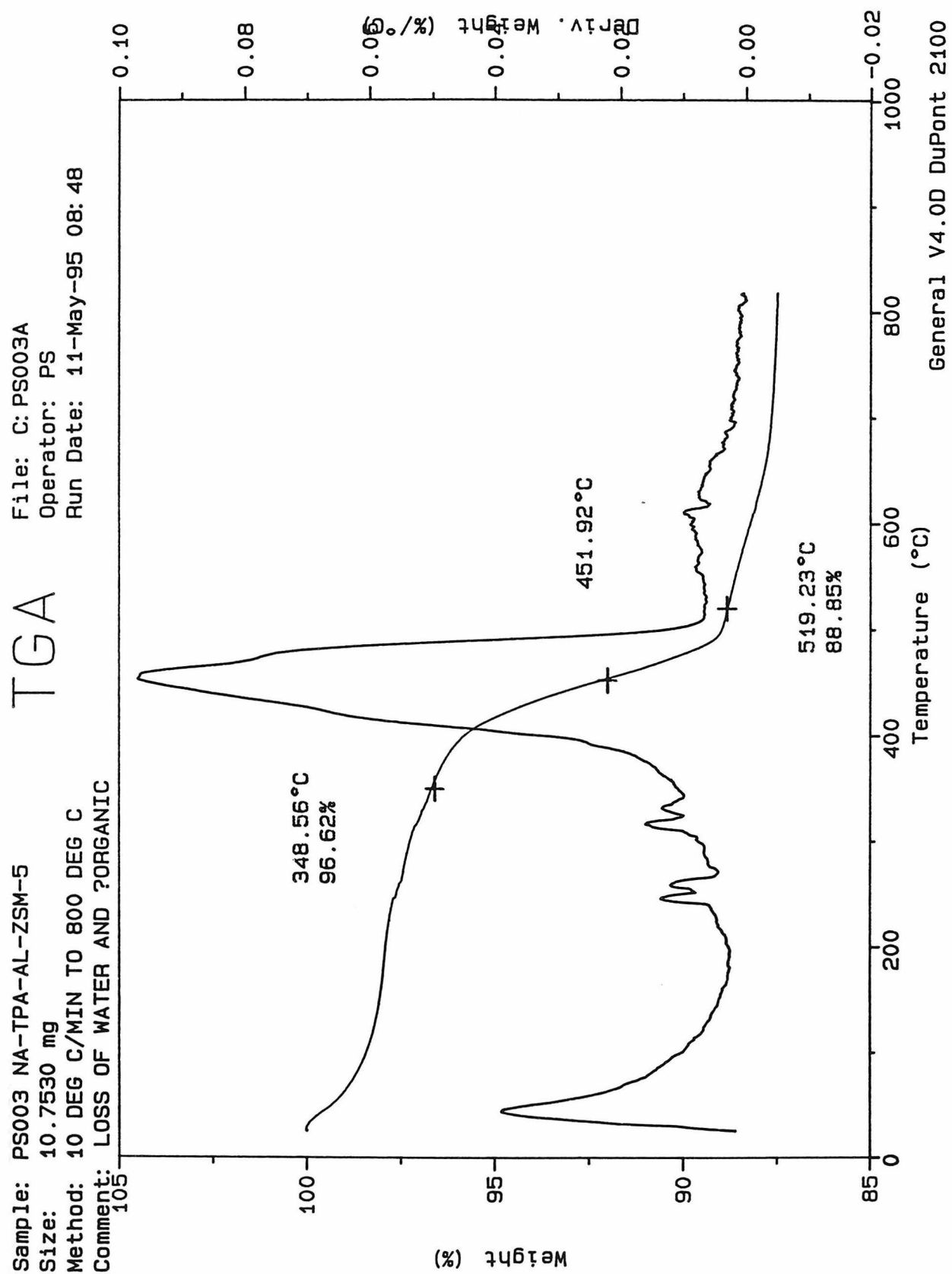


Sample: PS001GNA.004
Size: 10.9440 mg
Method: 50/MIN 600 ISO 60 MIN
Comment: LOSS OF WATER
102

TGA

File: A:PS001GNA.004
Operator: JCL
Run Date: 26-Jun-95 22:03





Sample: PC003CNA
Size: 12.7990 mg
Method: 5C/MIN 600 ISO 60 MIN
Comment: LOSS OF WATER AFTER NA EX
102

TGA

File: A:PC003CNA.001

Operator: JCL

Run Date: 2-Jul-95 10:57

Temperature (°C)

400

200

0

General V4.0D DuPont 2100

Weight (%)

100

98

96

94

92

90

Time (min)

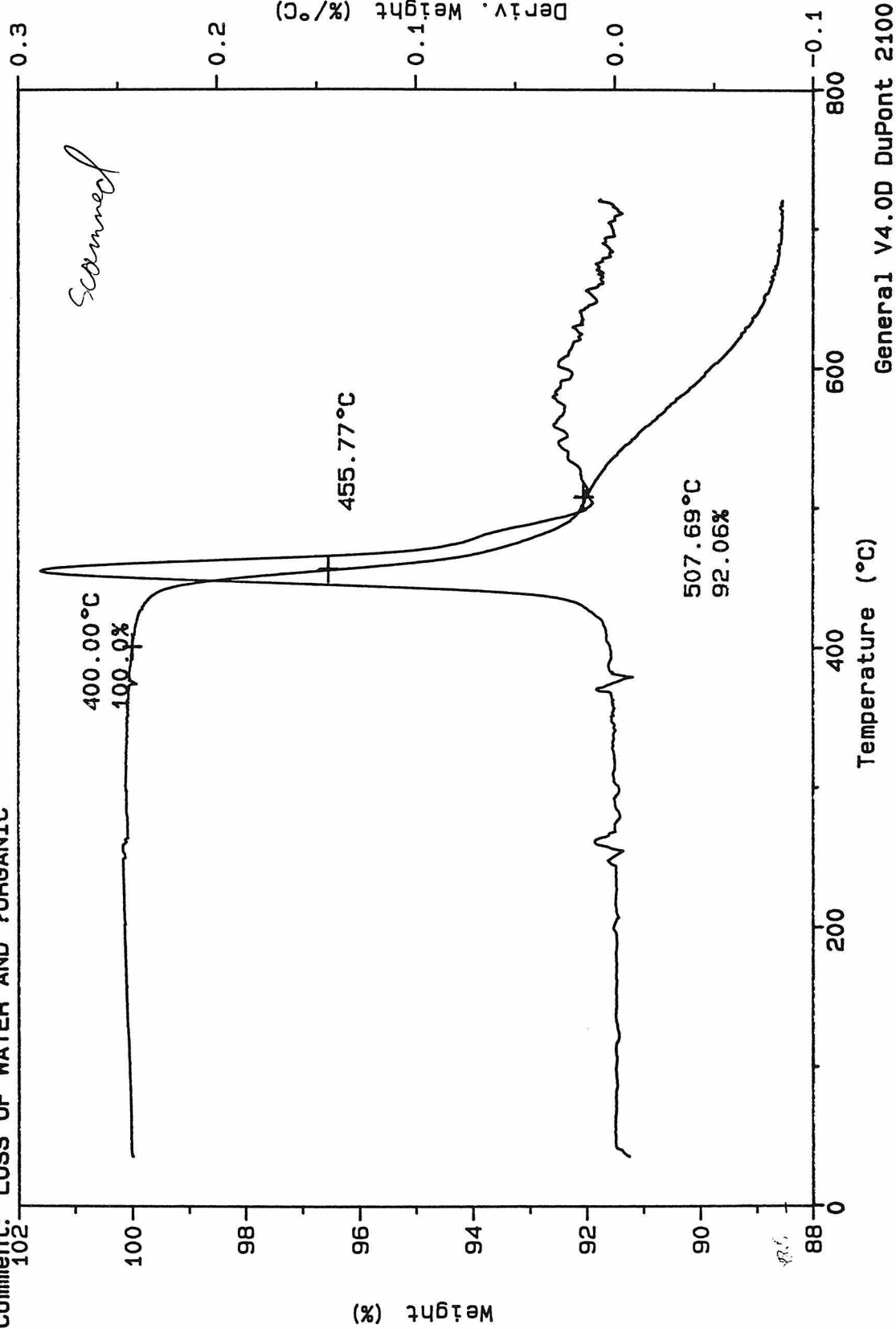
20 40 60 80 100 120 140 160 180

0 200 400 600 800

90.87%

Sample: PS004 NA-TPA-AL-ZSM-5
Size: 15.9770 mg
Method: 10 DEG C/MIN TO 700 DEG C
Comment: LOSS OF WATER AND ?ORGANIC

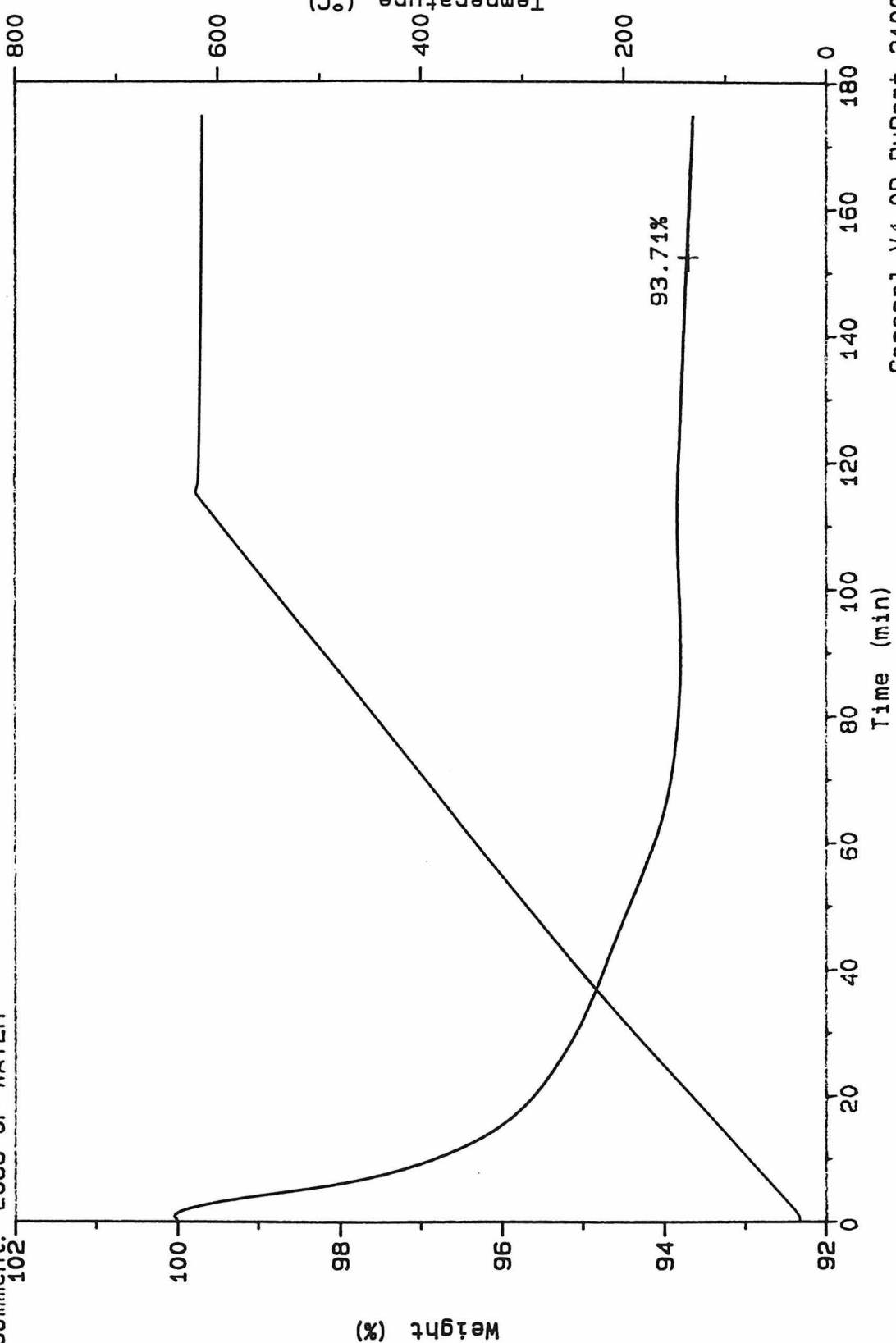
TGA



Sample: PS004C
Size: 12.3650 mg
Method: 5C/MIN 600 ISO 60 MIN
Comment: LOSS OF WATER
102

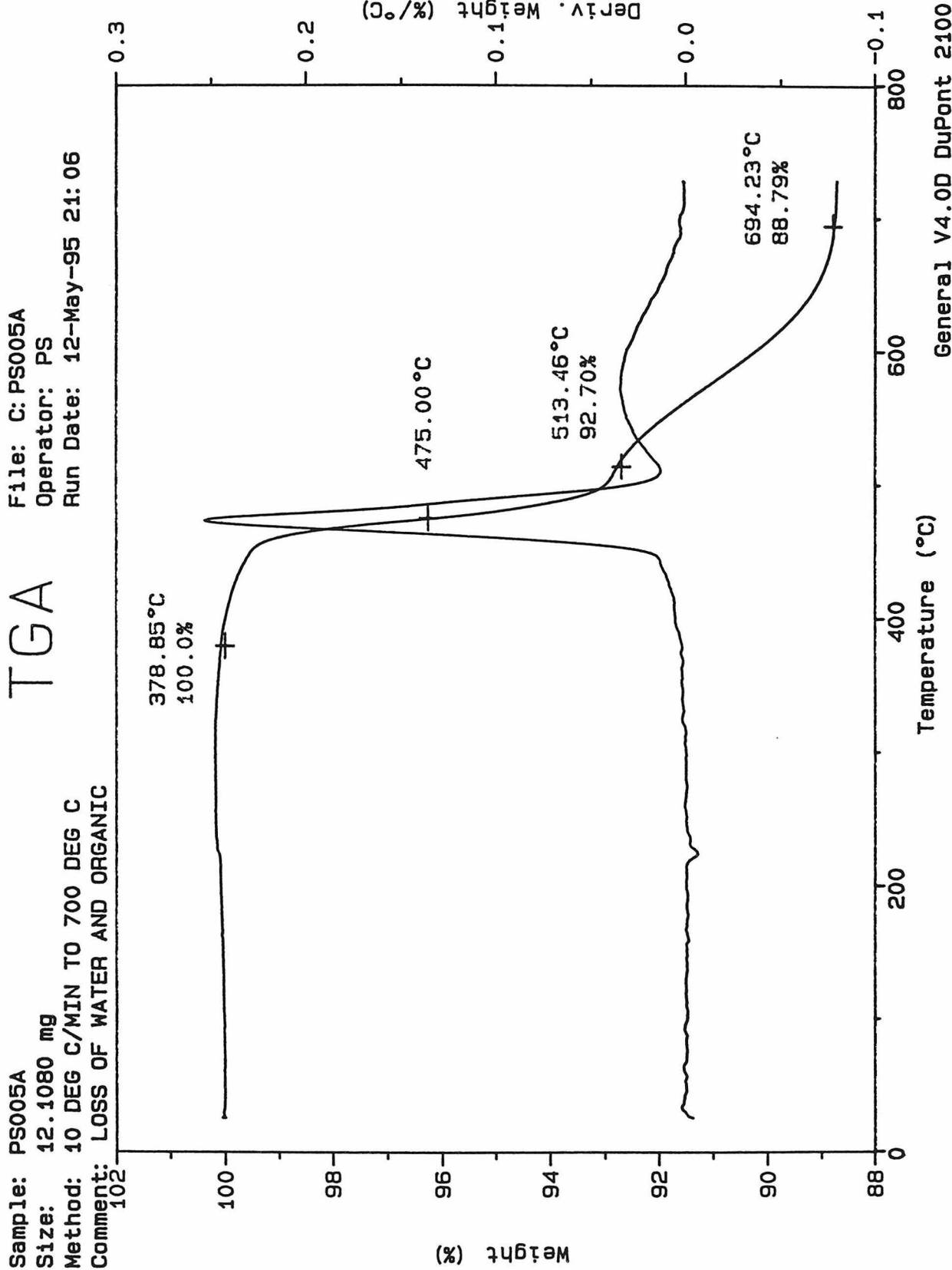
TGA

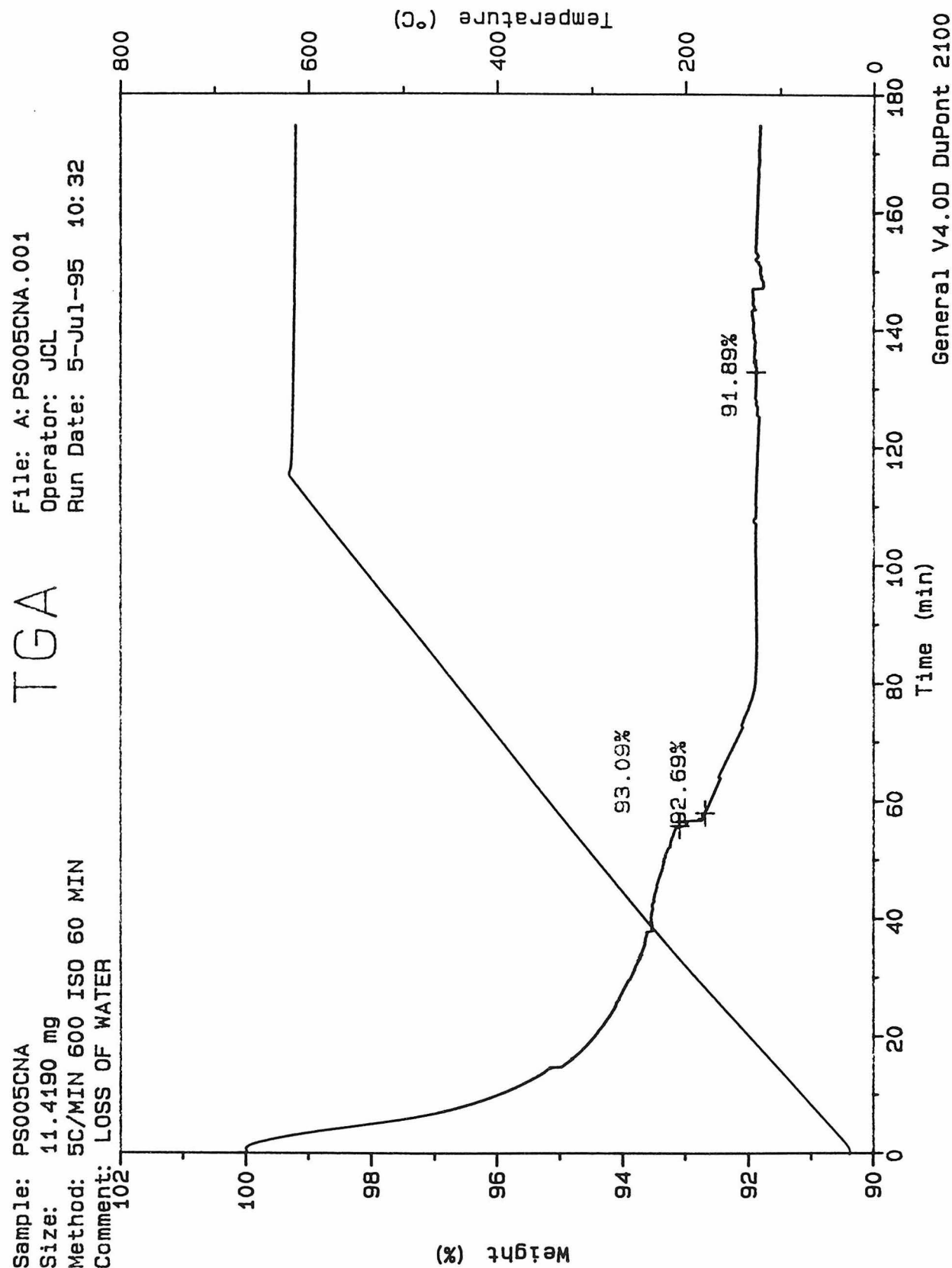
File: A:PS004CNA.001
Operator: JCL
Run Date: 11-Jul-95 22:45



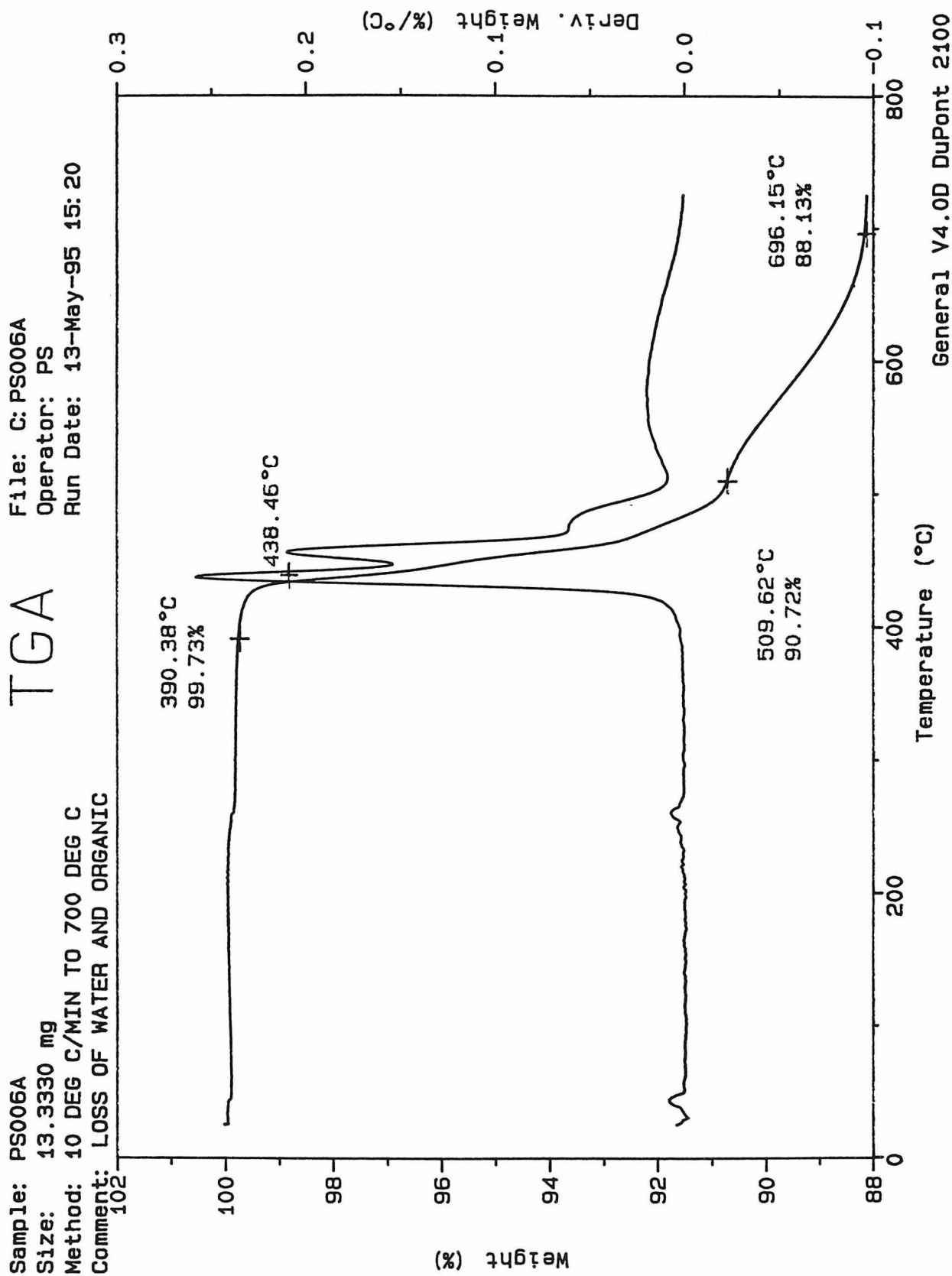
Sample: PS005A
Size: 12.1080 mg
Method: 10 DEG C/MIN TO 700 DEG C
Comment: LOSS OF WATER AND ORGANIC
102

TGA





$S_i(A) = 2.5$



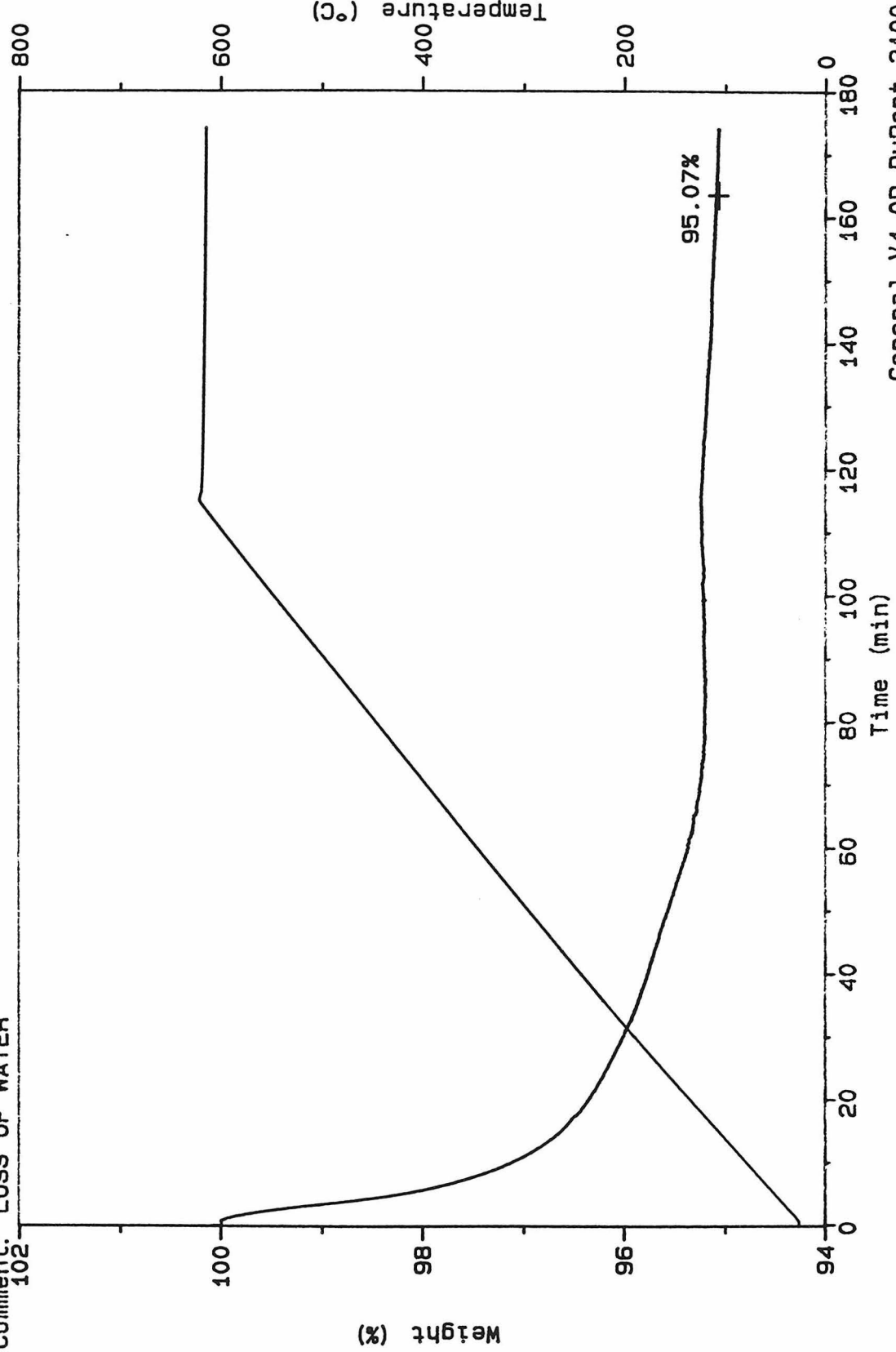
Sample: PS006C
Size: 10.3960 mg
Method: 5C/MIN 600 ISO 60 MIN
Comment: LOSS OF WATER

TGA

File: A:PS006CNA.001

Operator: JCL

Run Date: 28-JUL-95 15:05



General V4.0D DuPont 2100

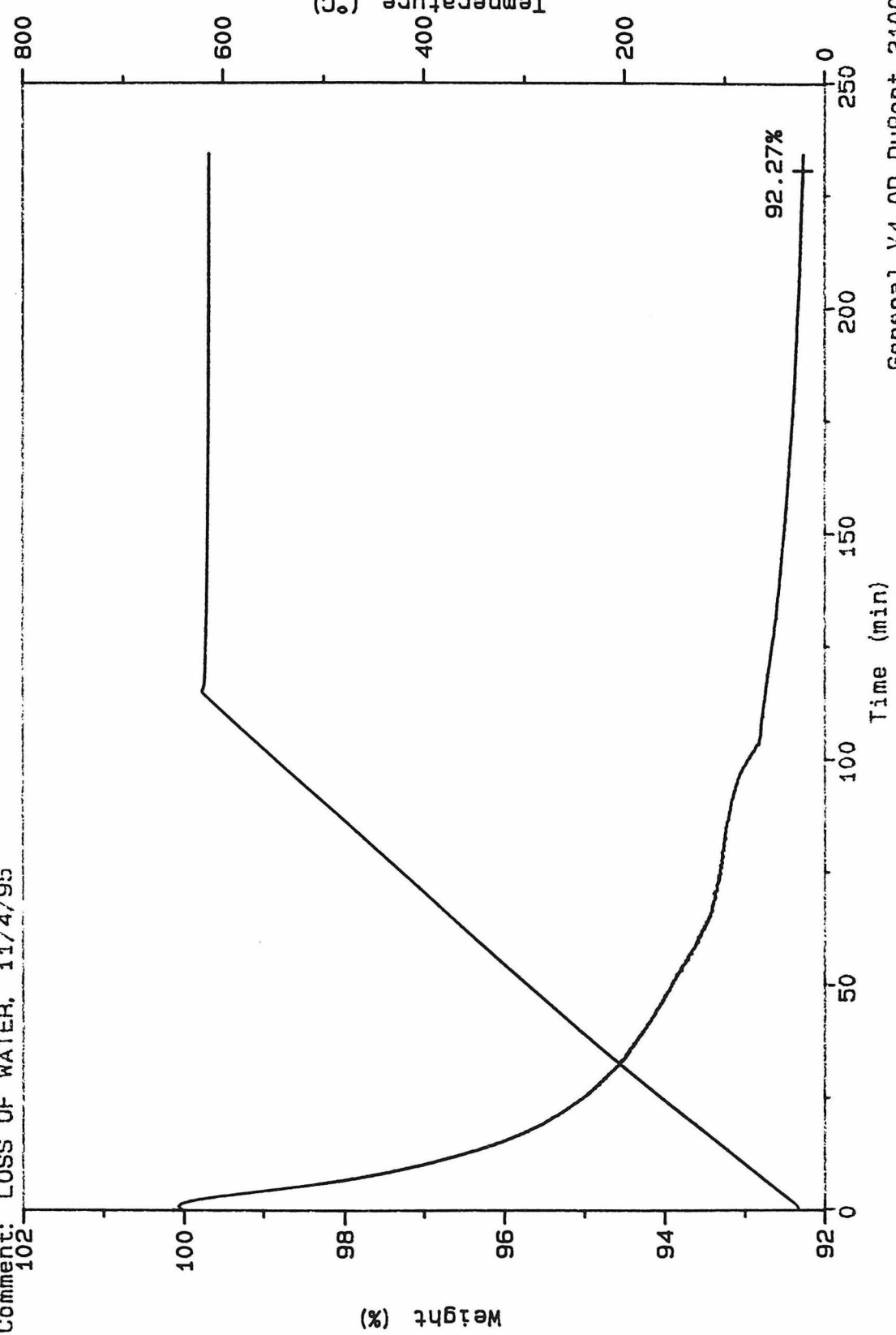
Sample: PC007C NAEKED (PS001)
Size: 11.4500 mg
Method: 5C/MIN 600C ISO 120 MIN
Comment: LOSS OF WATER, 11/4/95
102

TGA

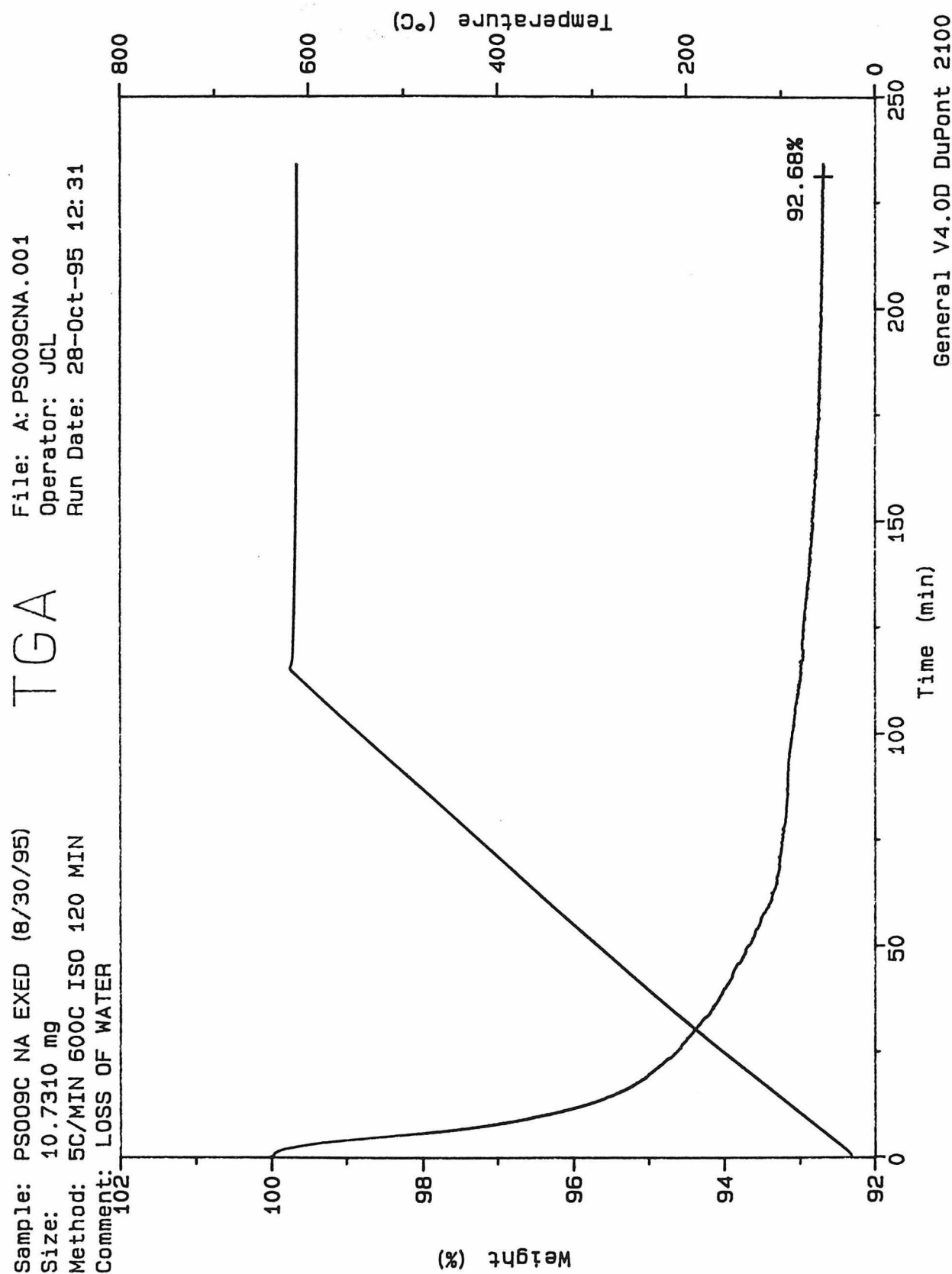
File: A:PS007CNA.001

Operator: JCL

Run Date: 10-Nov-95 14:48

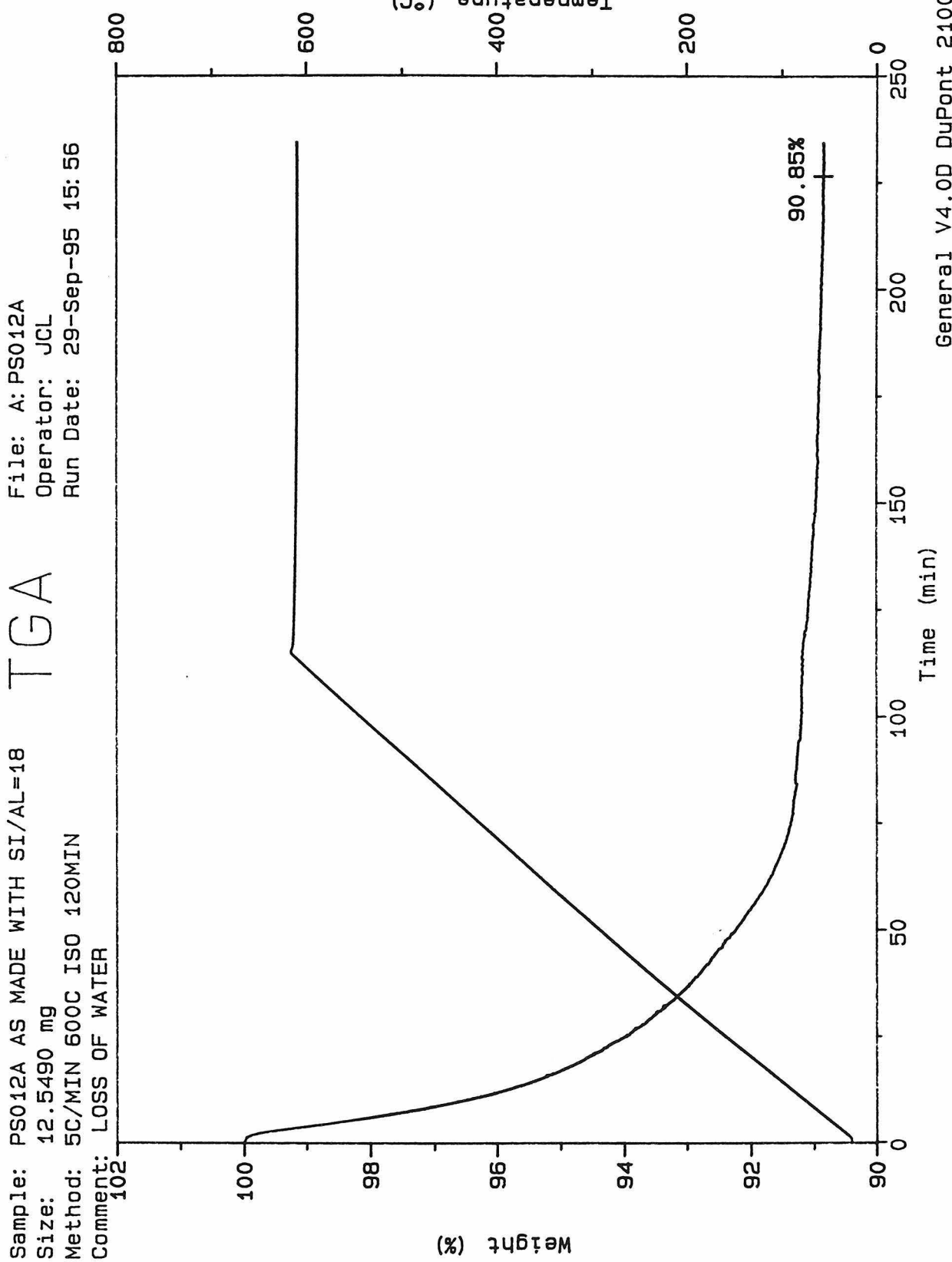


General V4.0D DuPont 2100



Sample: PS012A AS MADE WITH SI/AL=18
Size: 12.5490 mg
Method: 5C/MIN 600C ISO 120MIN
Comment: LOSS OF WATER

TGA

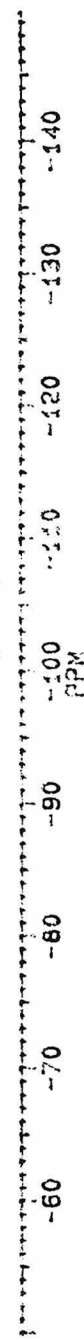


Appendix VI. NMR Spectra

VAW	NH_4^+	^{29}Si MAS	^{27}Al MAS	
	calcined	^{29}Si MAS	^{27}Al MAS	
HK113	as made	^{29}Si MAS	^{27}Al MAS	
	calcined	^{29}Si MAS	^{27}Al MAS	
HK114	as made	^{29}Si MAS	^{27}Al MAS	
	calcined	^{29}Si MAS	^{27}Al MAS	^{29}Si CPMAS
HK109	as made	^{29}Si MAS	^{27}Al MAS	
	calcined	^{29}Si MAS	^{27}Al MAS	
HK108	as made	^{29}Si MAS	^{27}Al MAS	
	calcined	^{29}Si MAS	^{27}Al MAS	
HK110	as made	^{29}Si MAS	^{27}Al MAS	
	calcined	^{29}Si MAS	^{27}Al MAS	

HKZSMVAM.001
AU PROG:
SOLIDCYC.AU
DATE 22-11-94
TIME 9:25

SF	59.628
SI	22500.000
TD	2048
SW	500
HW/PT	16666.667
AB	.015
RE	640
TE	289
DP	5787.000
PL	51.20
LB	0.0
GB	0.0
WL	297.05
SR	27263.90
DI	20.000000
P4	40.00
P1	4.00
RD	0.0
PW	0.0
DE	40.00
NS	3382
DS	0



NH4-2SX-5 YAW ID: 7464-05-43 SI/AL=42, 27AL WAS 8KHz. 4MM

54,6329

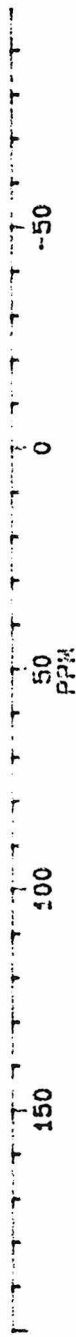
PPM

BAKER

HKZSM5VA.001
AU PHOG:
SOLIDCYC:AU
DATE 17-11-94
TIME 18:24

SF 78.206
01 38301.338
SI 4096
TD 1024
SW 100000.000
HZ/PT 48.828
AG .005
RG 640
TE 289
02 19741.000
DP 3L P0
LB 50.000
GB 0.0
MI 1.02
HZ/CM 1.171E3
SR 34700.26
D1 -.5000000
P4 40.00
P1 3.50
RD 0.0
PW 0.0
DE 8.75
NS 4355
DS 0

75



-112.239

B
R
U
K
E
R

HKVAW.001
AU PROG:
SOLIDCY.C.AU
DATE 25-1-95
TIME 17:56

SF 59.631
01 26000.000
SI 4096
TD 500
SW 16666.667
HZ/PT 8.138

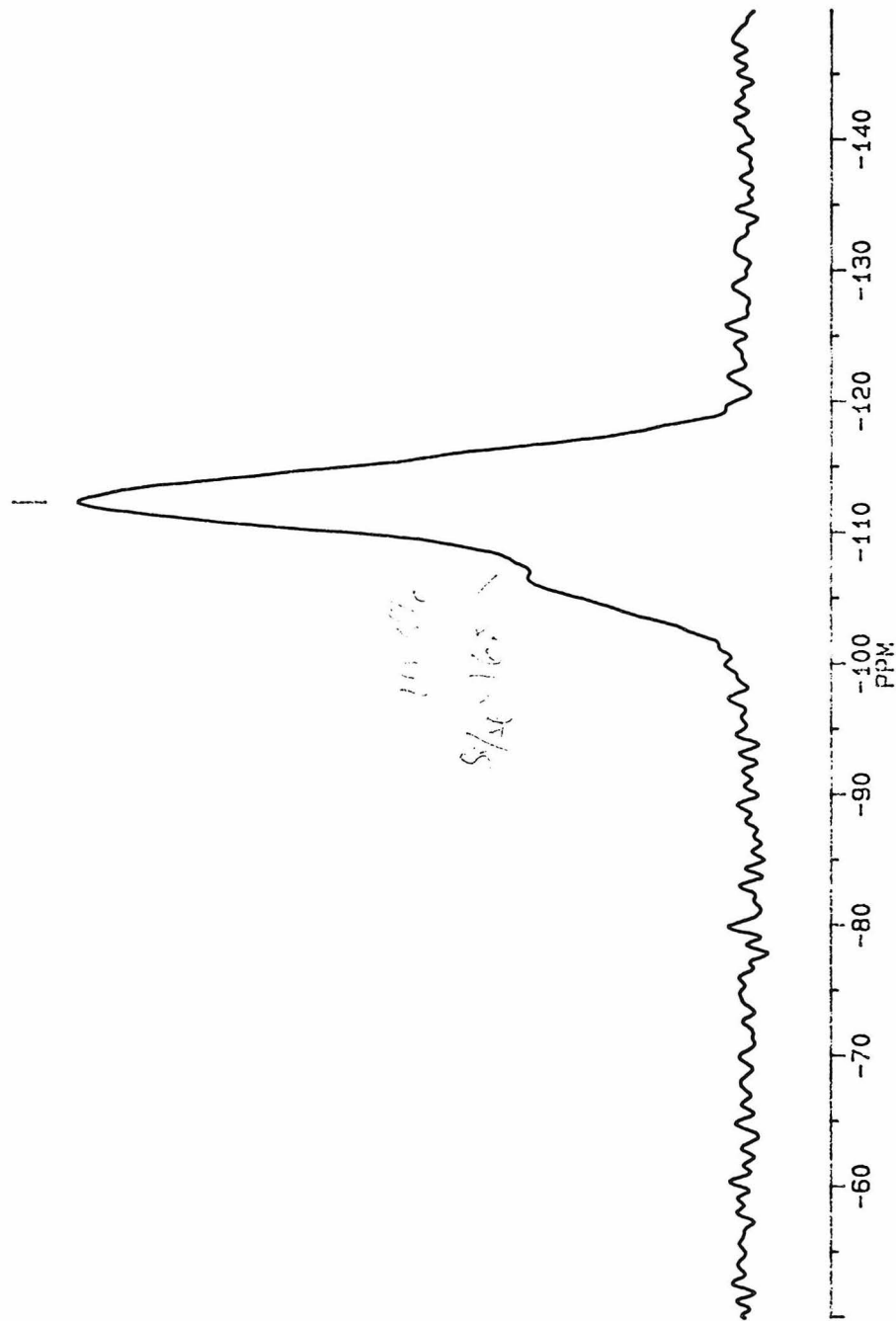
AG .015
RG 640
TE 289

02 5787.000
DP 5L P0

LB 0.0
GB 0.0
MI .04
HZ/CM 297.852
SR 29817.23

D1 5.000000
P4 40.00
P1 4.00
RD 0.0
PW 0.0
DE 40.00
NS 1145
DS 0

PPM



VAW ZSM-5 CALC 550C, 27AL MAS 8KHZ, 4MM

53.7553

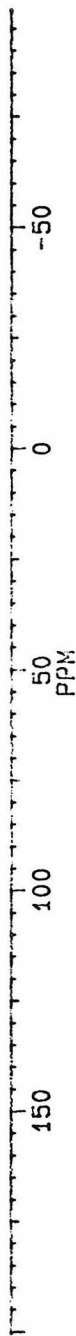
-4.7443

BRUKER

HKVANZSM.001
AU PROG:
SOLIDCYC.AU
DATE 20-1-95
TIME 15:34

SF 78.209
01 38093.818
SI 8192
TD 1024
SW 100000.000
HZ/PT 24.414
AQ .005
RG 200
TE 289
02 49741.000
DP 3L P0
LB 40.000
GB 0.0
MI 0.03
HZ/CM 1.471E3
SR 38093.82
D1 1.0000000
P4 40.00
P1 4.00
RD 0.0
PW 0.0
DE 8.75
NS 7263
DS 0

77



869,577

C. R. A.
B. R. A.

HK443SI.004
AU PROG;
SOLIDCYC.AU
DATE 18-1-95
TIME 13:01

SF	59.628
SI	22500.000
TD	4096
SW	300
Hz./PT	25000.000
Hz.	12.207
AO	.042
RG	640
TE	289
CA	5787.000
DP	4L 10
LB	20.000
SB	0.0
MX	297.03
SR	29834.30
DA	10.000000
PP	40.00
PA	4.00
PW	0.0
DE	27.50
NS	1402
SC	0



HK413 TPA--AL-ZSM-5, 27AL MAS 8KHZ, 4032

51.3439

PPM

BRIDGE R

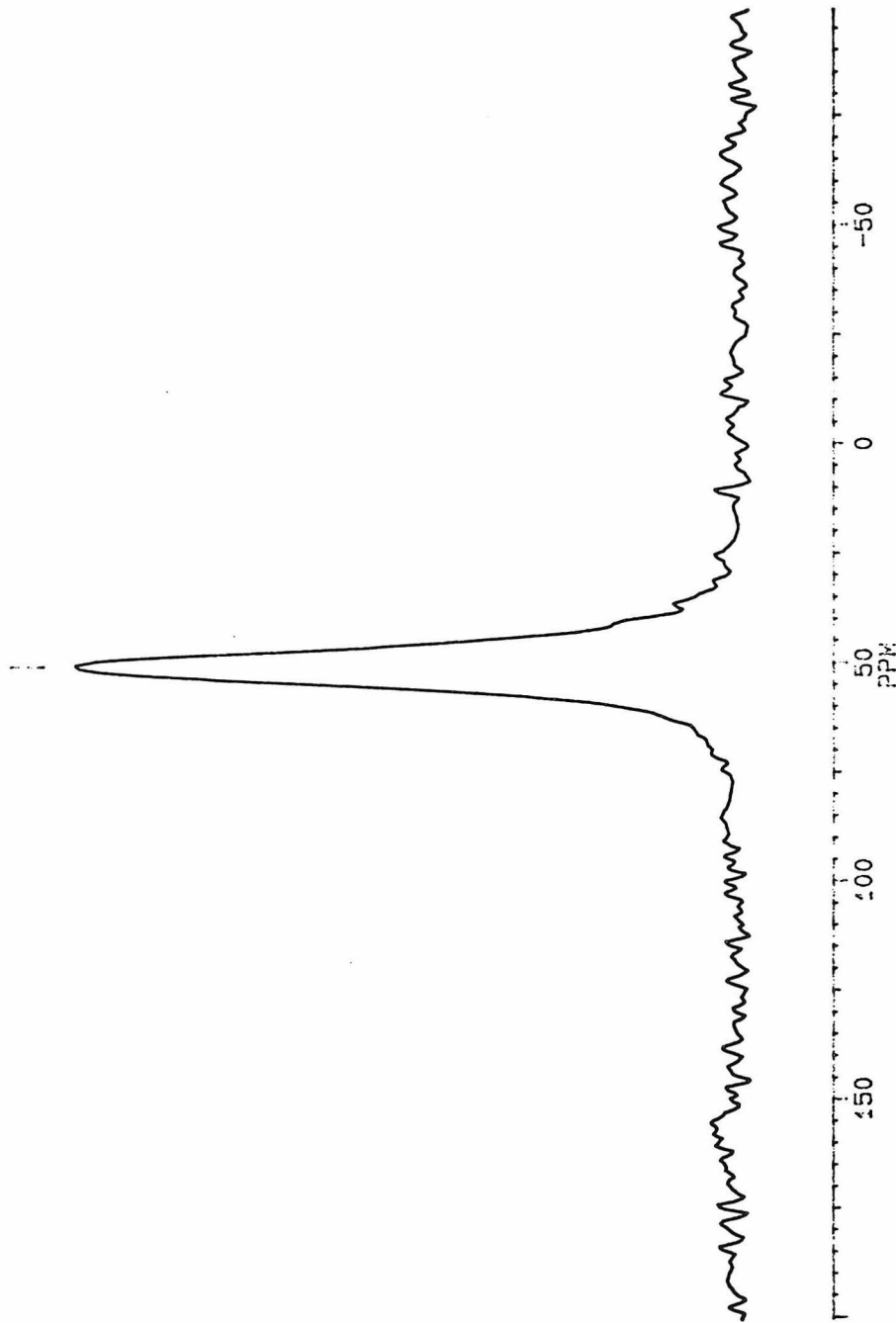
HK413 AL.001
AU PRO6:
SOLIDCYC.AU
DATE 20-1-95
TIME 9:55

SF 78.209
OY 38093.818
SI 8192
TD 1024
SW 400000.000
HZ/PT 24.414

AG .005
RG 200
TE 289
DP 49744.000
3L P0

LB 40.000
GB 0.0
WT 1.471E3
HZ/CM 1.471E3
SR 38093.82
D1 1.0000000
D4 40.00
P1 4.00
AD 0.0
DW 0.0
DE 8.75
NS 4455
DS 0

79



HK113 (TPA) -AL-ZSM-5 CALC 600C, 29Si MAS 3KHz, 7MM

-112.934

BRUNER

HK143SI.002
AU PROG:
SOLIDCYC.AU
DATE 28-1-95
TIME 17: 56

SF 59.631
01 26000.000
SI 4096
TD 1024
SW 16666.667
HZ/PT 8.138

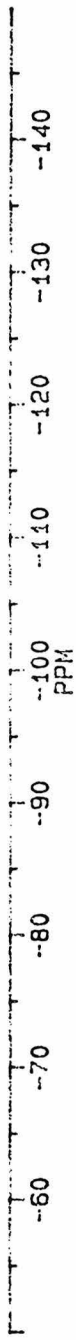
AQ .034
RG 640
TE 289

02 5787.000
DP 5L P0

LB 0.0
GB 0.0
MI .02
HZ/CM 297.852
SR 29817.20

D1 20.000000
P4 40.00
P1 4.00
RD 0.0
PW 0.0
DE 40.00
NS 652
DS 0

80



ppm

HK443 AL-ZSM-5 CALC 600C, 27AL MAS 8KHZ, 4MM

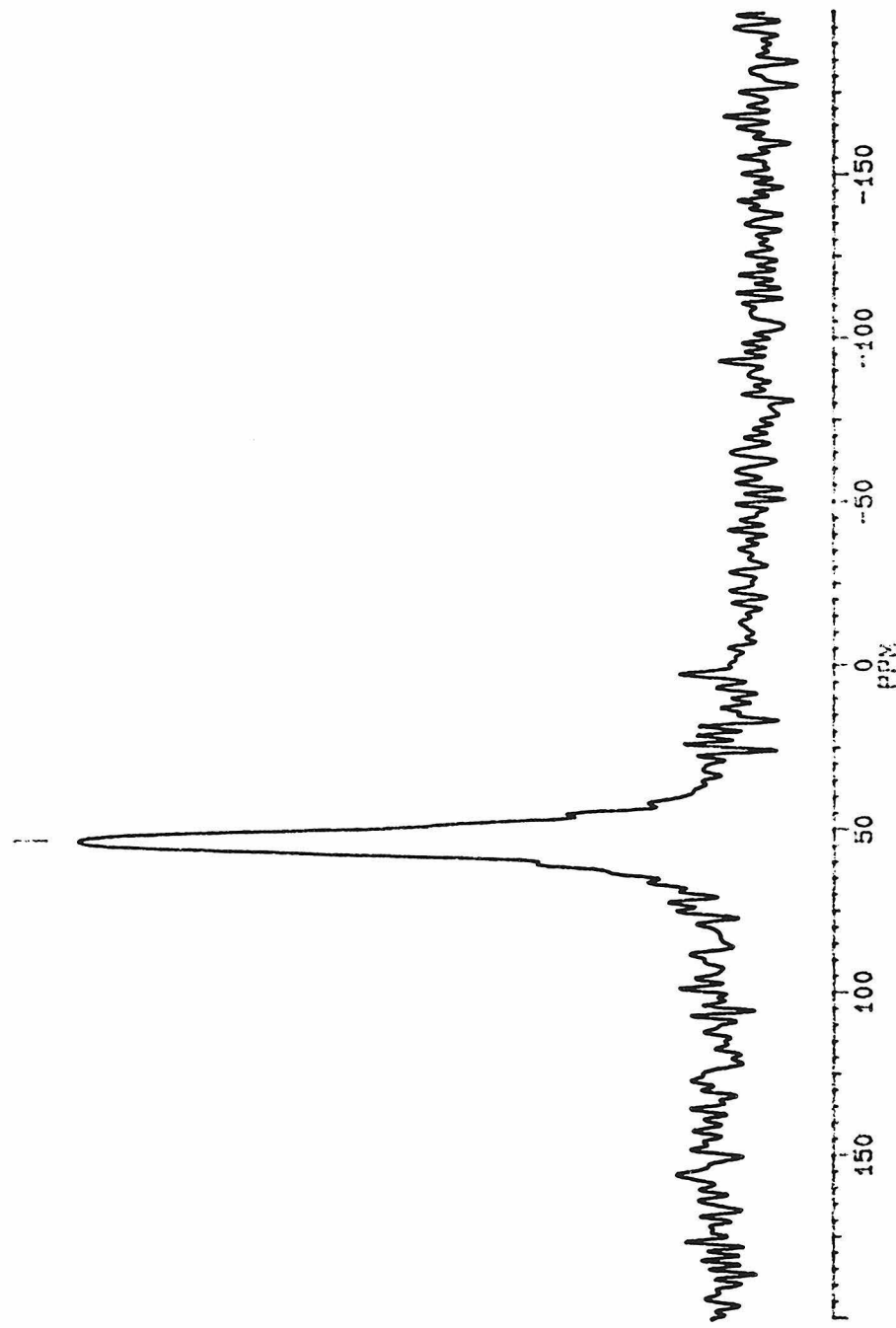
53,8857

PP

BRUGER

HK443 AL. 002
AU PROG:
SOLIDCYC.AU
DATE 2-2-95
TIME 14: 03

SF 78.209
04 38301.338
SI 4096
TD 500
SN 50000.000
HZ/PT 24.414
AQ .005
RG 640
TE 289
02 19741.000
DP 31. P0
LB 0.0
GB 0.0
MI 1.563E3
HZ/CM 1.563E3
SA 38093.80
D1 1.0000000
P4 40.00
P1 4.00
RD 0.0
PW 0.0
DE 15.00
NS 8693
DS 0



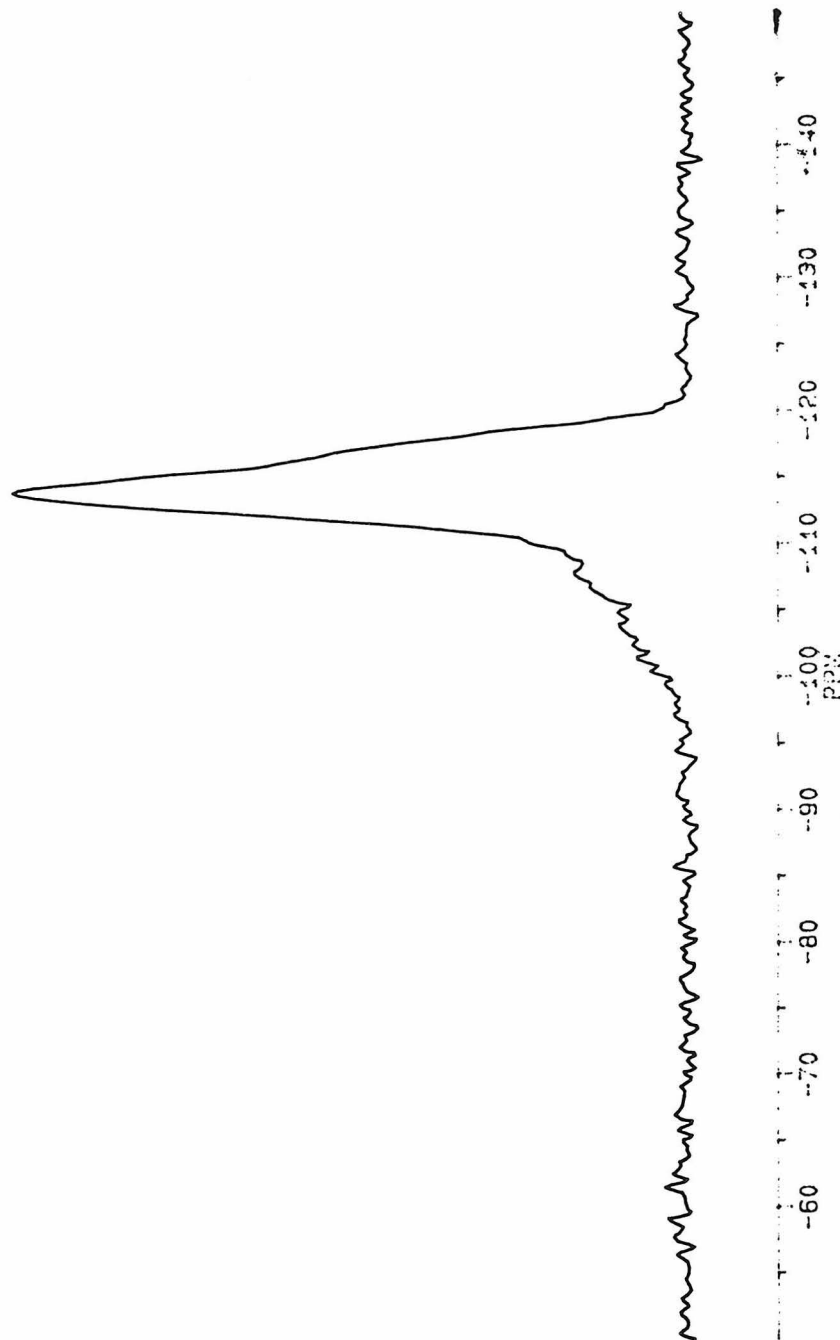
-163.728

BRUNER

HK444SL.004
AU PROG:
SOLIDCYC.AU
DATE 18-4-95
TIME 14:56

SF 59.634
04 22500.000
SF 4096
TD 1024
SX 25000.000
HZ, PT 12.207

AG .020
RG 640
TE 289
02 5787.000
DP 4.70
13 0.0
63 0.0
WT/GW 297.852
SR 29894.30
D4 10.0000000
D2 40.00
P1 4.00
AD 0.0
PW 0.0
DE 27.50
NS 1668
DS 0

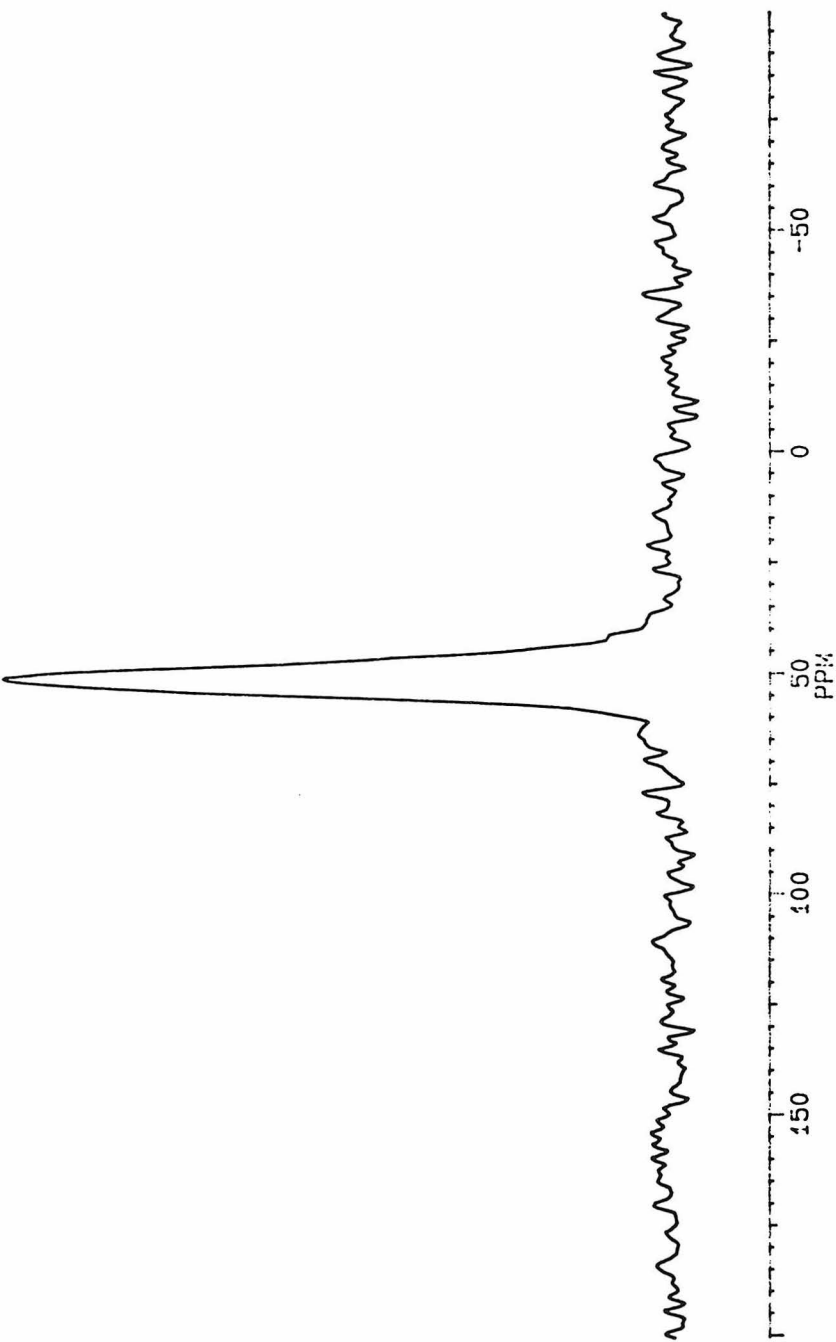


Zd

BRIKES

HK114AL.004
 AU PROG:
 SOLIDYC.AU
 DATE 20-1-95
 TIME 11:01

SF 78.209
 01 38093.818
 SI 8492
 TD 1024
 SW 100000.000
 HZ/PT 24.414
 AQ .005
 RG 200
 TE 289
 02 19741.000
 DP 3L P0
 LB 40.000
 GB 0.0
 XI 24
 HZ/CM 1.171E3
 SR 38093.82
 01 1.000000
 P4 40.00
 P1 4.00
 RD 0.0
 PW 0.0
 DE 8.75
 NS 3435
 DS 0



HK114 CALC 600C, 29SI MAS 3KHZ, 7MM

-83.435

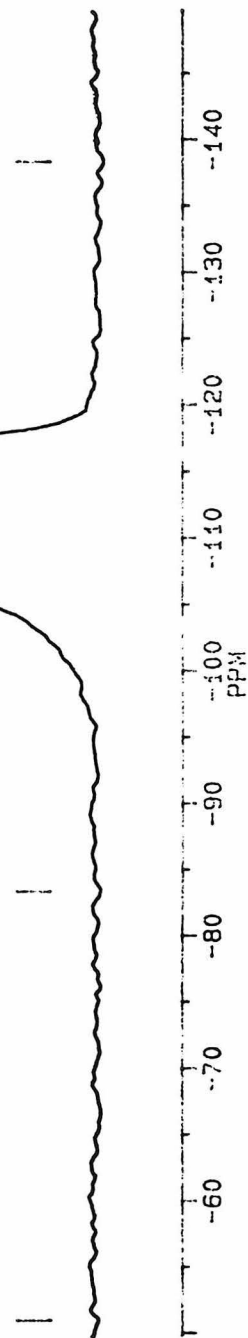
-142.670

-138.369

BRUKER

HK114SI.002
AU PROG:
SOLIDCYC.AU
DATE 29-1-95
TIME 11:34

SF	59.631
SI	26000.000
SI	4096
TD	600
SW	16666.667
HZ/PT	8.138
AQ	.018
RG	640
TE	289
DP	5787.000
PL	P0
LB	30.000
GB	0.0
MI	.01
HZ/CM	297.852
SR	29817.20
DI	5.0000000
P4	40.00
P1	4.00
RD	0.0
PW	0.0
DE	40.00
NS	479
DS	0



-51.028

-111.813
-103.044

BRUKER

HK114SI.003
AU PROG:
CPMAS,AU
DATE 30-1-95
TIME 9:13

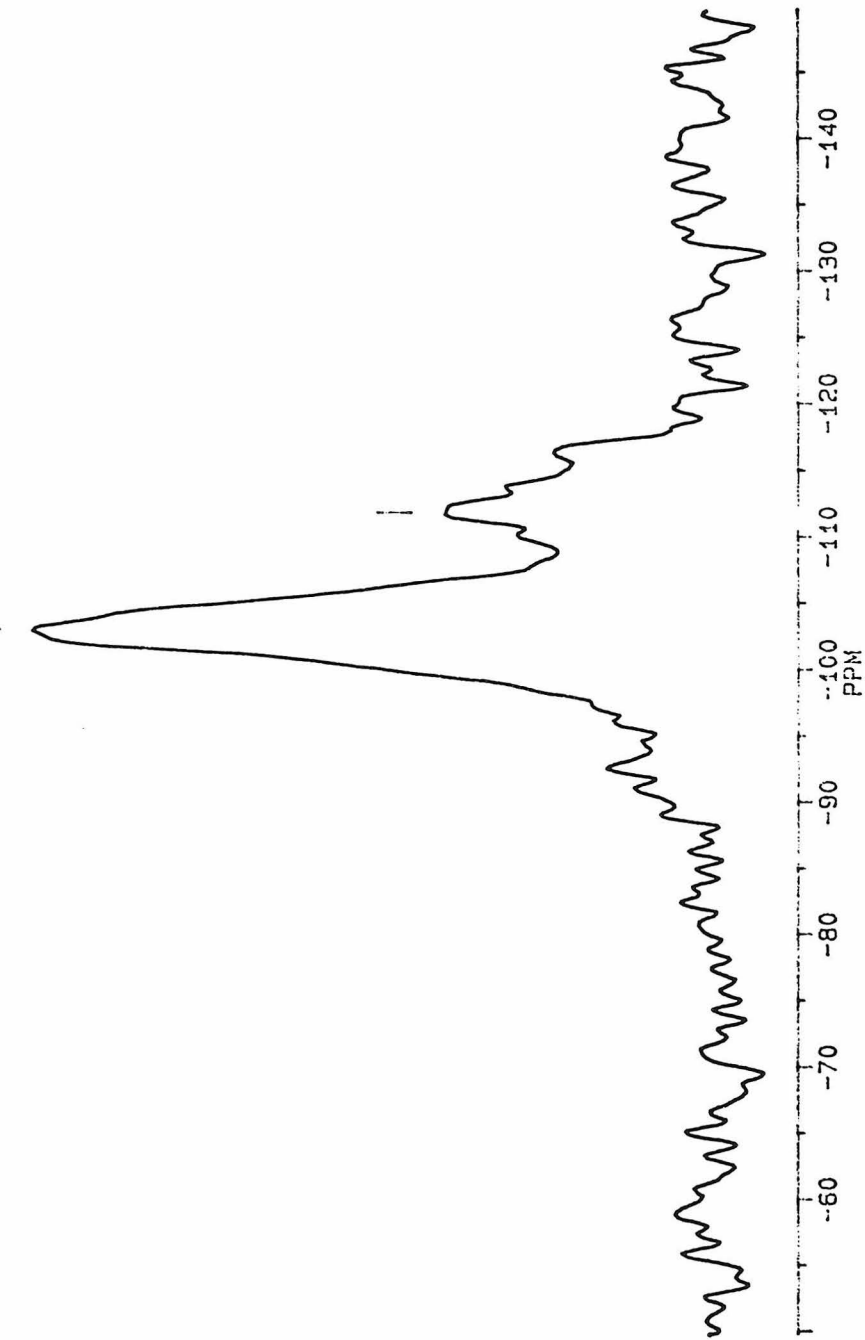
SF 59.631
01 26000.000
SI 4096
TD 500
SW 16666.667
HZ/PT 8.138

AQ 0.015
RG 640
TE 289

02 5787.000
DP 5L P0

LB 30.000
GB 0.0
NI 0.08
HZ/CM 297.852
SR 29817.20

D1 5.0000000
P4 40.00
P1 8.50
P2 3000.00
RD 0.0
PW 0.0
DE 40.00
NS 15327
DS 0
D3 .0030000



54,3962

BRUKER

HK114AL.002
 AU PROG:
 SOLIDCYC.AU
 DATE 2-2-95
 TIME 17:22

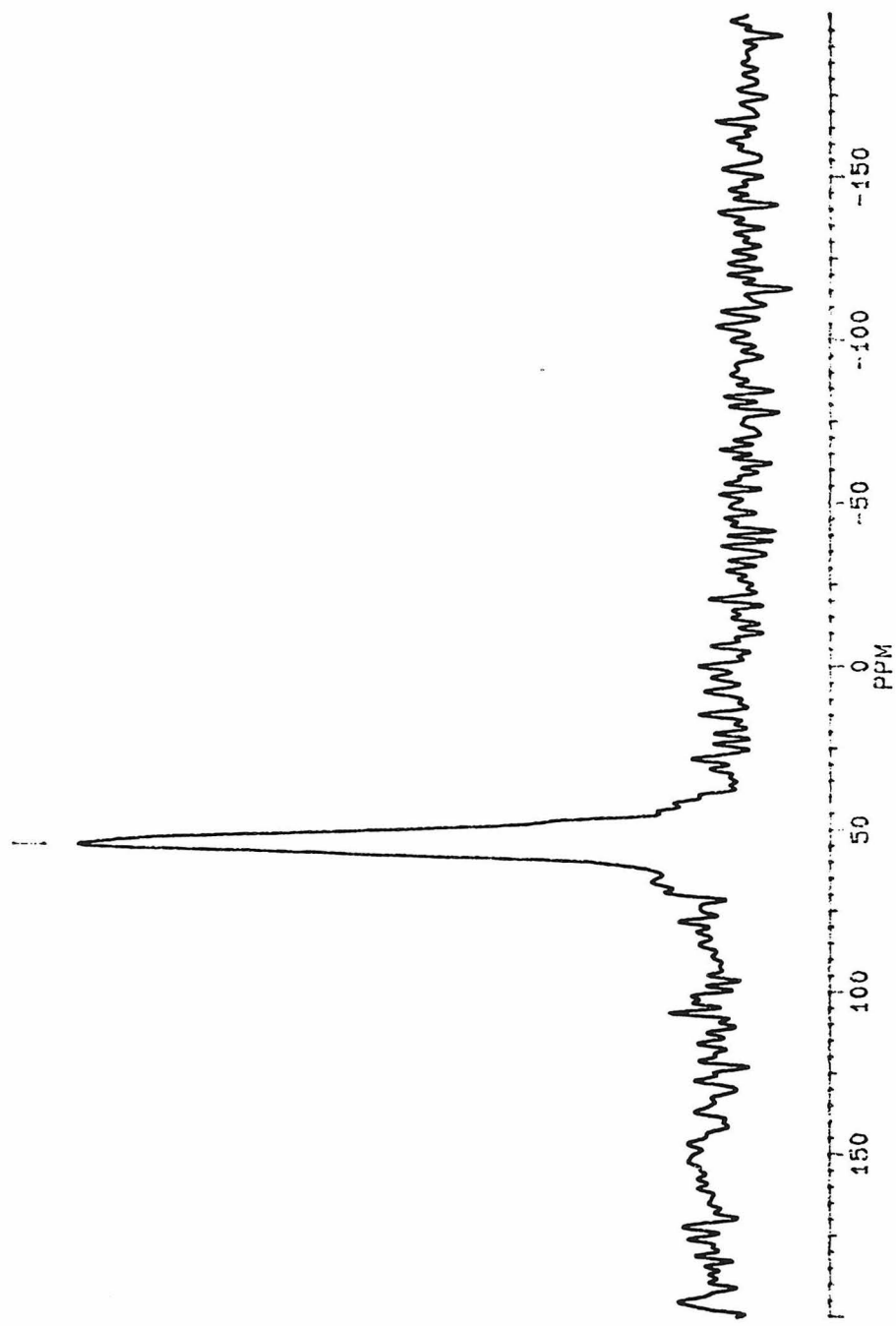
SF 78.209
 01 38301.338
 SI 4096
 TD 500
 SW 50000.000
 HZ/PT 24.414

AQ .005
 RG 640
 TE 289

02 19741.000
 DP 3_ P0

LB 30.000
 GB 0.0
 WI .26
 HZ/CM 1.563E3
 SR 38093.80

D1 1.0000000
 P4 40.00
 P1 4.00
 RD 0.0
 PW 0.0
 DE 15.00
 NS 6869
 DS 0



HK409 TPAF-AL-2S15, 29SI NAS 3KHZ, 7W

143.726

PPM

BRUNN

HK409SI.001
AU PRO6;
SOLIDCYC.AU
DATE 17-4-95
TIME 16:52

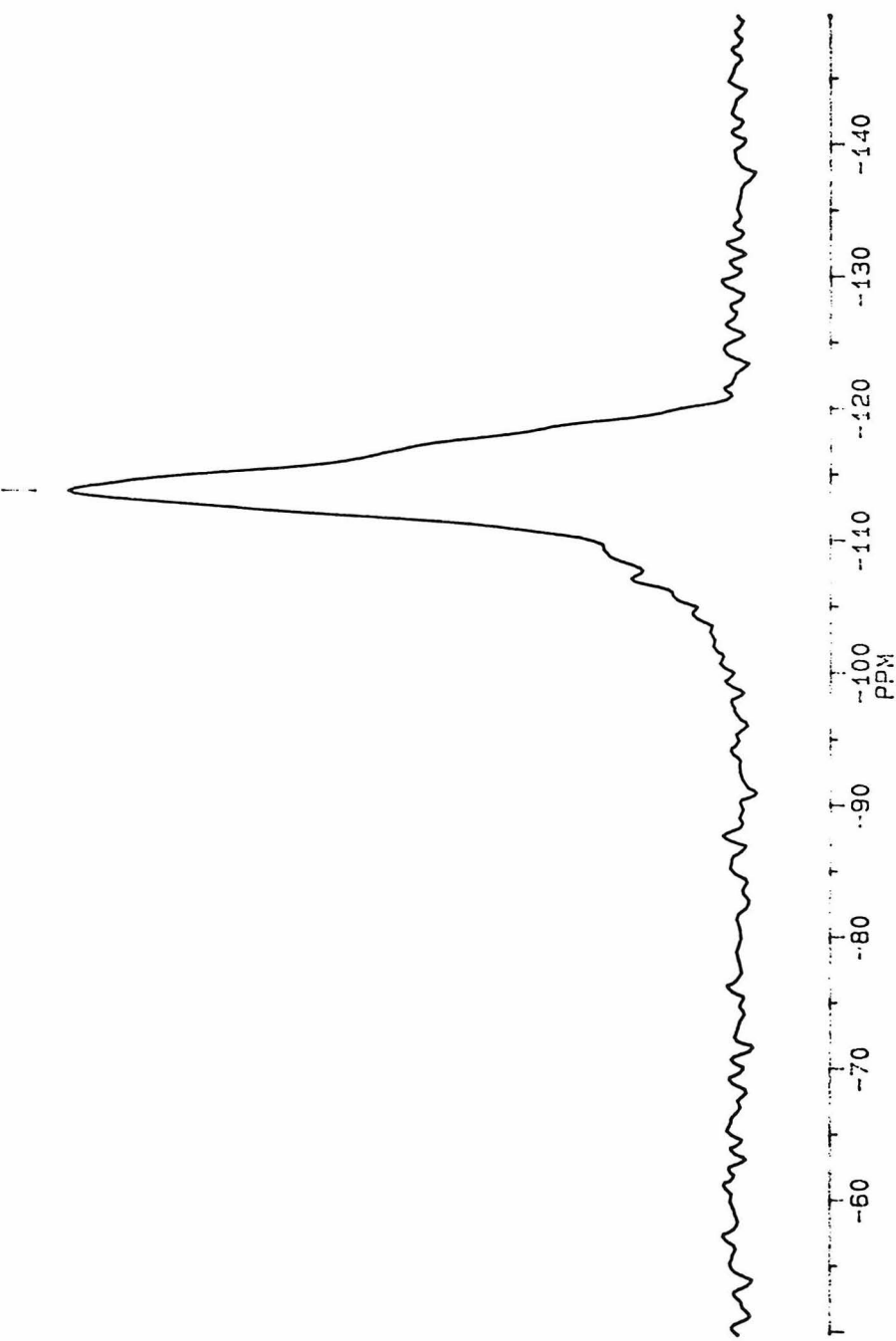
SF 59.628
01 22500.000
ST 4096
TD 700
SW 25000.000
HZ/PT 42.207

AG 640 .044
RG 289
TE

02 5787.000
DP 4L P0

LB 0.0
GB 0.0
MI 0.02
HZ/CM 297.852
SR 29891.30

D1 10.0000000
P4 40.00
P1 4.00
RD 0.0
PW 0.0
DE 27.50
NS 2493
CS 0



HK109 TPAF-Al-ZSM-5, 27AL MAS 8KHz, 4MM

90.0

80.0

70.0

60.0

50.0

40.0

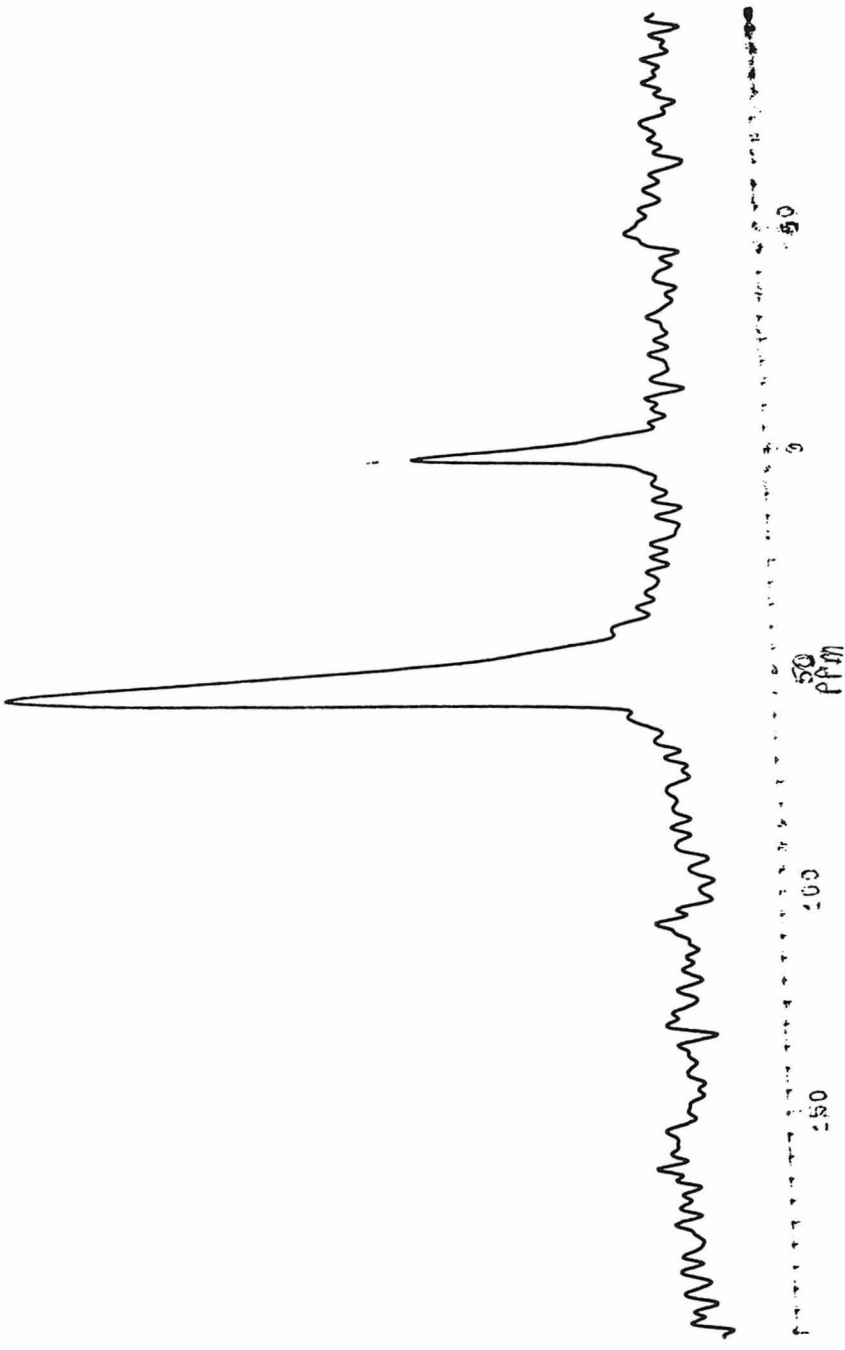
30.0

20.0

10.0

0.0

88



200

150 100 50 0

PPM

HK409 (TPAFO-AL-ZSW-5 CALC 600C, 29ST M/S 34H7, 7NM

-106.576

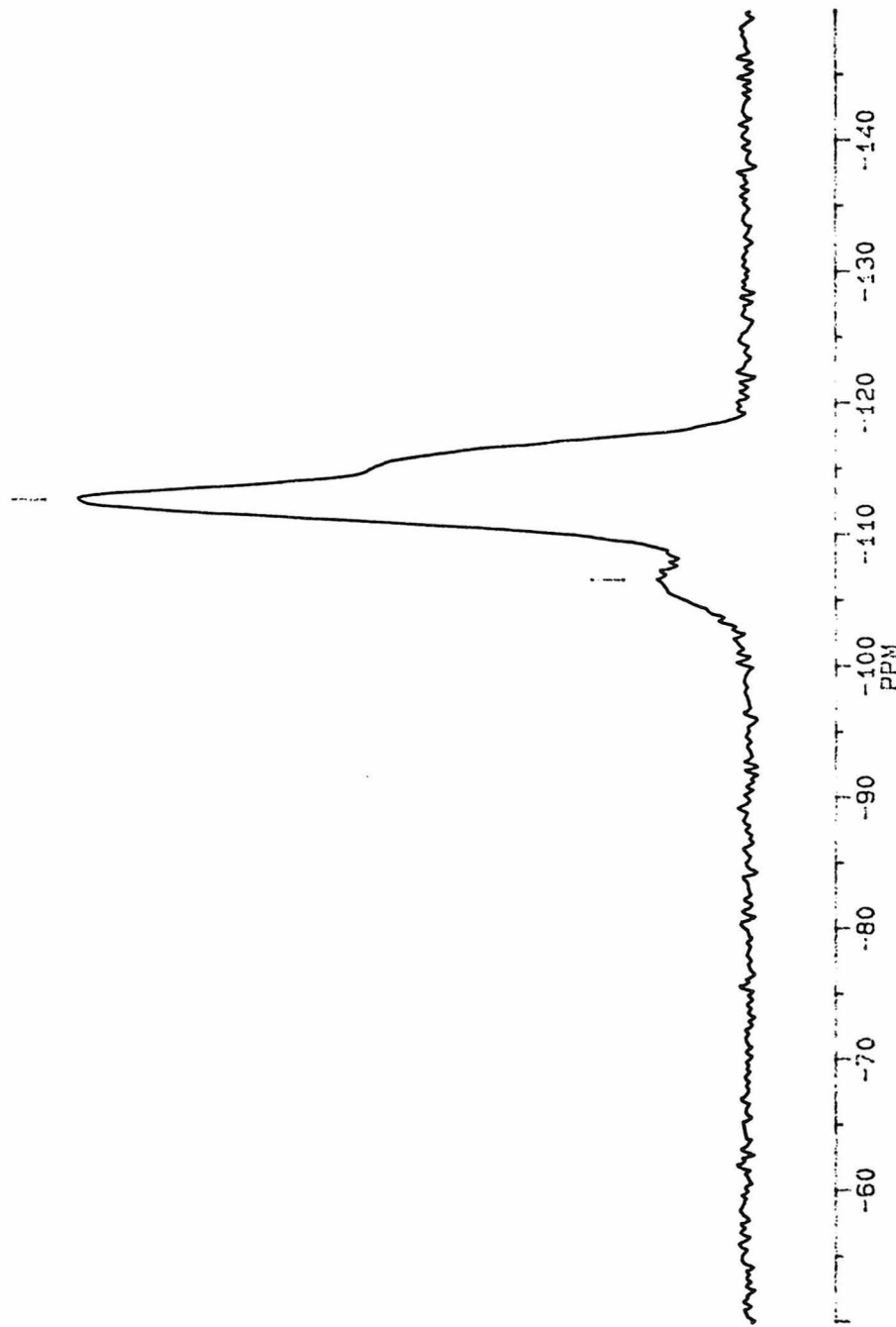
-412.633

PPM

BRUKER

HK409SI.002
AU PRO6;
SOLIDCYC.AU
DATE 26-1-95
TIME 12: 29

SF 59.631
01 26000.000
SI 4096
TD 1024
SW 16666.667
HZ/PT 8.138
AQ 640 .031
RG 289
TE 02 5787.000
DP 5L P0
LB 0.0
GB 0.0
XI 297.01
HZ/CW 29817.23
SR 0
D1 5.0000000
P4 40.00
P1 4.00
RD 0.0
PW 0.0
DE 40.00
NS 1016
DS 0



HK109 CALC 600C. 27AL MAS 8KHZ. 4MM

53.5834

PPM

BRUKER

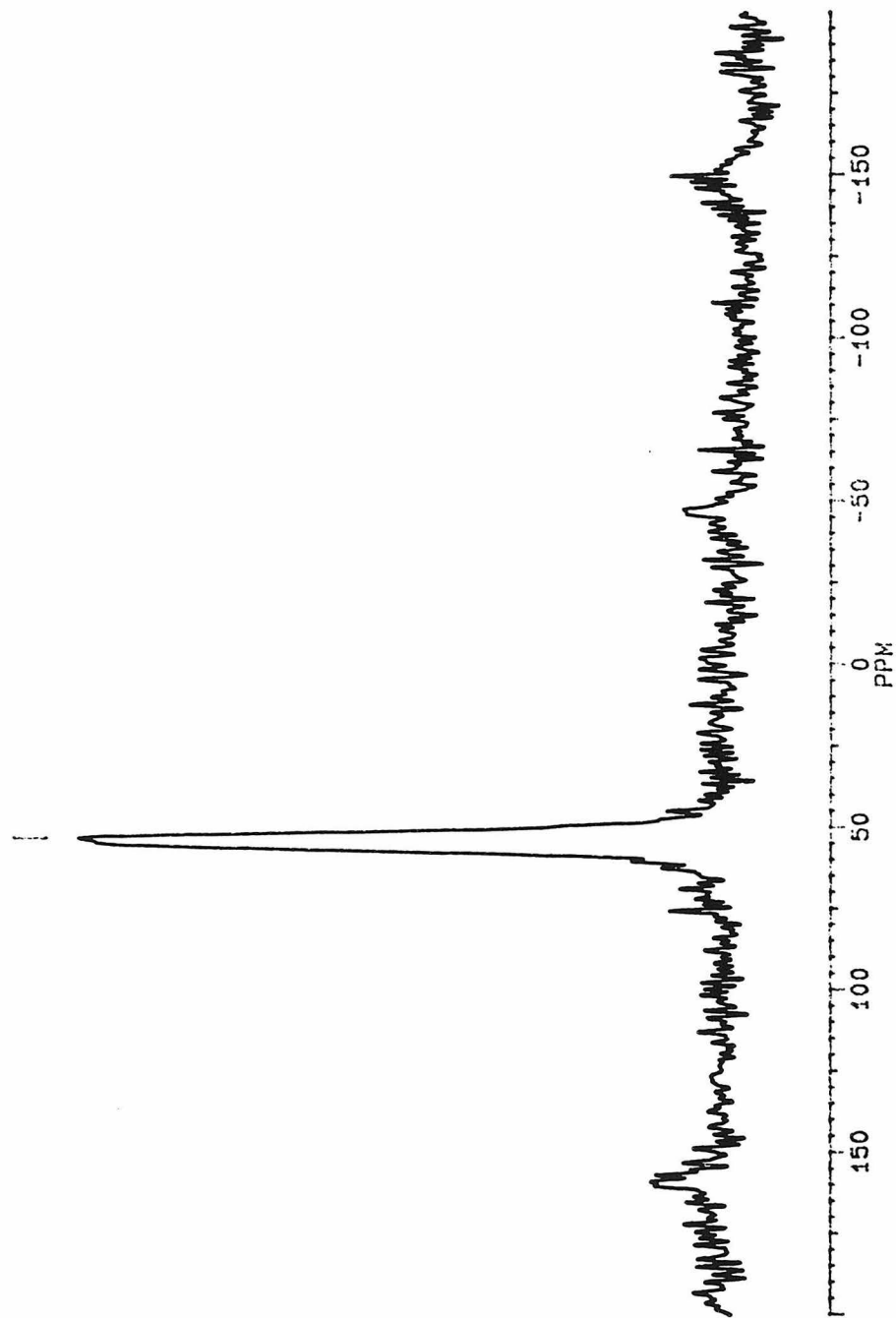
HK109AL.002
AU PROG:
SOLIDCYC.AU
DATE 1-2-95
TIME 20:24

SF 78.209
01 38301.338
SI 8192
TD 800
SW 50000.000
HZ/PT 12.207

AQ .008
RG 640
TE 289

02 19741.000
DP 3L P0
LB 0.0
GB 0.0
XI 1.20
HZ/CM 1.564E3
SA 38093.80

D1 1.000000
P4 40.00
P1 4.00
RD 0.0
PW 0.0
DE 15.00
NS 11445
DS 0



HK408 TPAFF-AL-ZSM-5, 29SI MAS 3KHz, 7MN

-453.751

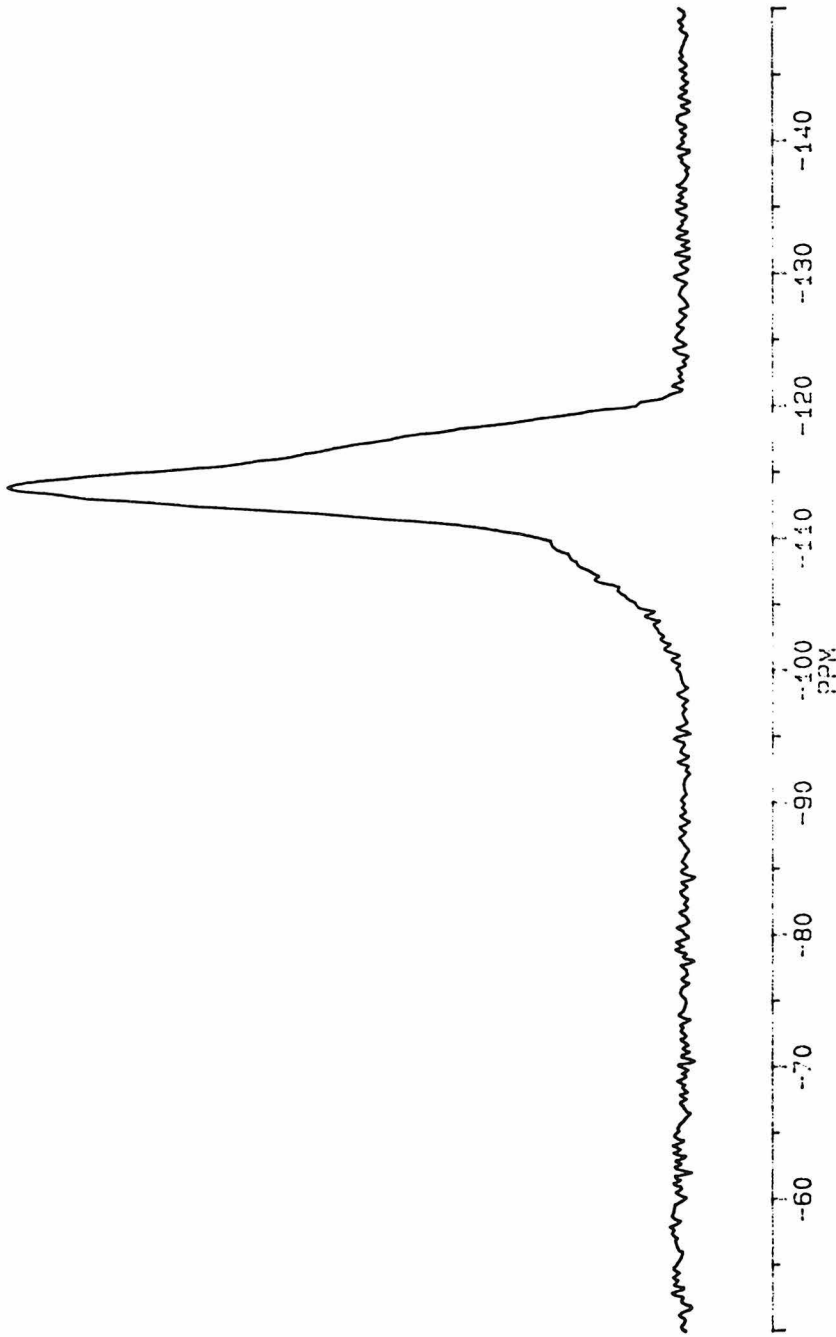
PPM

BLISTER

HK408SI.001
AU PROG:
SOLIDCYC.AU
DATE 12-1-95
TIME 14:48

SF 59.631
01 22500.000
SI 4096
TD 1024
SW 16666.667
HZ/PT 8.138

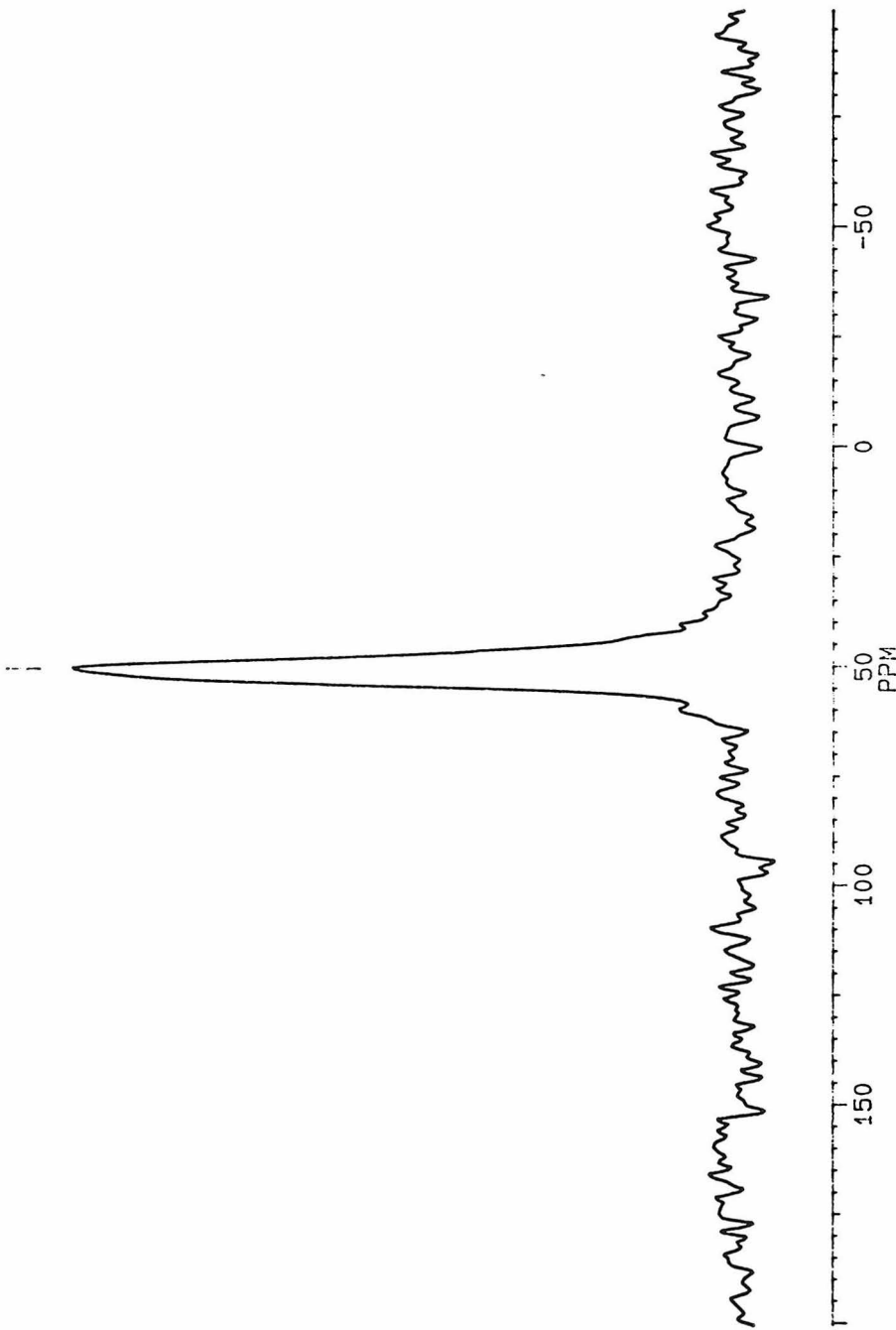
AQ .031
RG 640
TE 289
02 5787.000
DP 42 P0
LB 0.0
GB 0.0
WT 03
HZ/CM 298.258
SR 29891.30
D1 20.0000000
P4 40.00
P1 4.00
RD 0.0
PW 0.0
JE 40.00
NS 37.60
DS 0





HK108AL.001
AU PROG:
AU SOLIDCYC.AU
DATE 19-1-95
TIME 17:43

SF 78.209
01 38093.818
SI 8492
TD 1024
SW 100000.000
HZ/PT 24.414
AQ .005
RG 200
TE 289
02 19741.000
DP 3L P0
LB 50.000
GB 0.0
MI 0.29
HZ/CM 1.174E3
SR 38093.82
DS 0
D1 1.0000000
P4 40.00
P1 4.00
RD 0.0
PW 0.0
DE 8.75
NS 1401
DS 0



HK108 AL--(TPAF)--ZSM-5 CALC 600C, 29SI MAS 3KHZ, 7MM

142.717
105.896

PPM

BRUKER

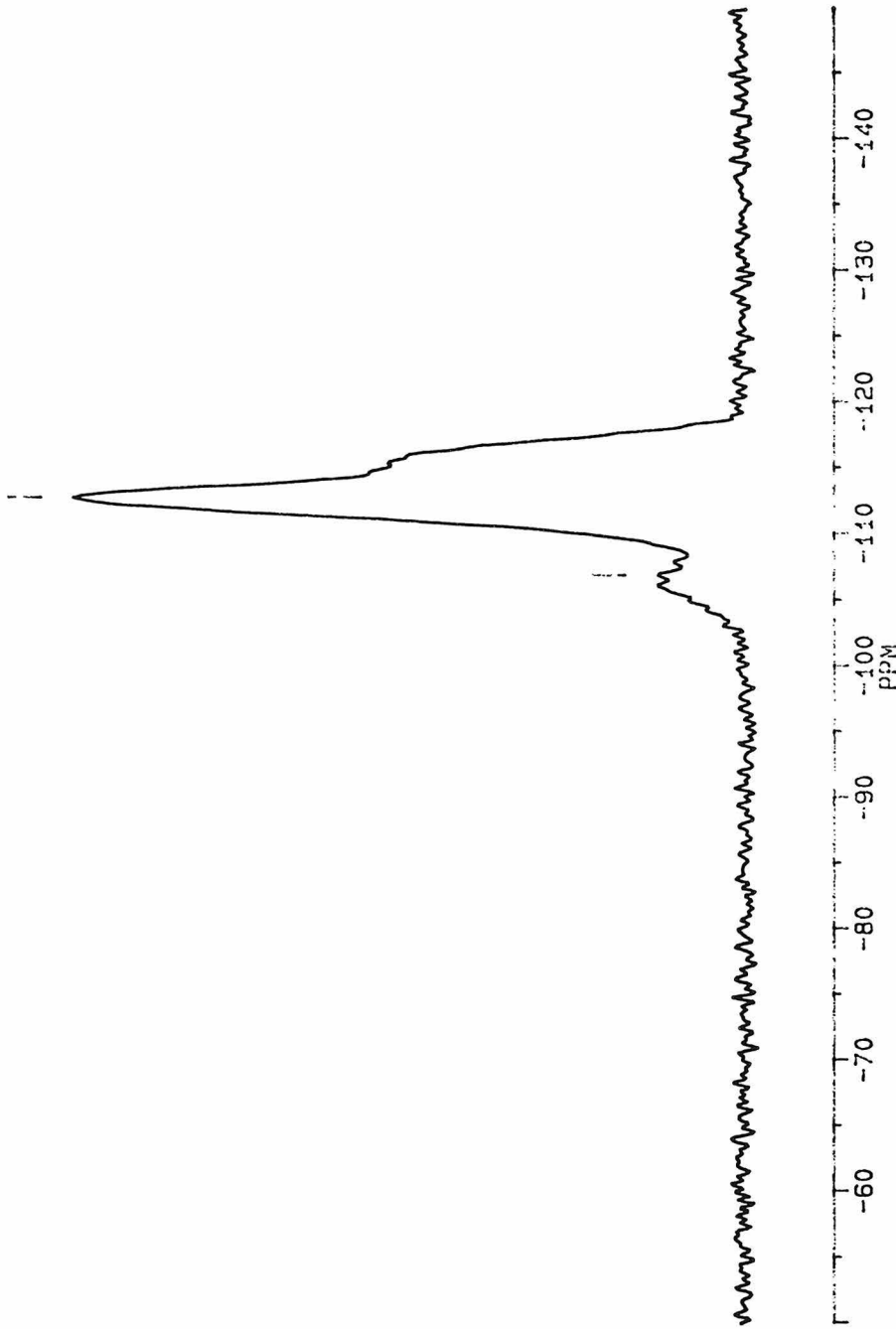
HK108SI.002
AU PROG:
SOLIDCYC.AU
DATE 25-1-95
TIME 18:34

SF 59.634
04 26000.000
SI 4096
TD 1024
SW 16666.667
HZ/PT 8.138

AQ .031
RG 640
TE 289
02 5787.000
DP 5L P0

LB 0.0
GB 0.0
MT 297.852
HZ/CM 29817.23

D1 5.000000
P4 40.00
P1 4.00
RD 0.0
PW 0.0
DE 40.00
NS 373
DS 0



HK108 CALC 600C, 27AL MAS 8KHZ, 4MM

53.9636

2pp

BRUKER

HK108AL.002
AU PROG:
SOLIDCYC:AU
DATE 22-1-95
TIME 12:06

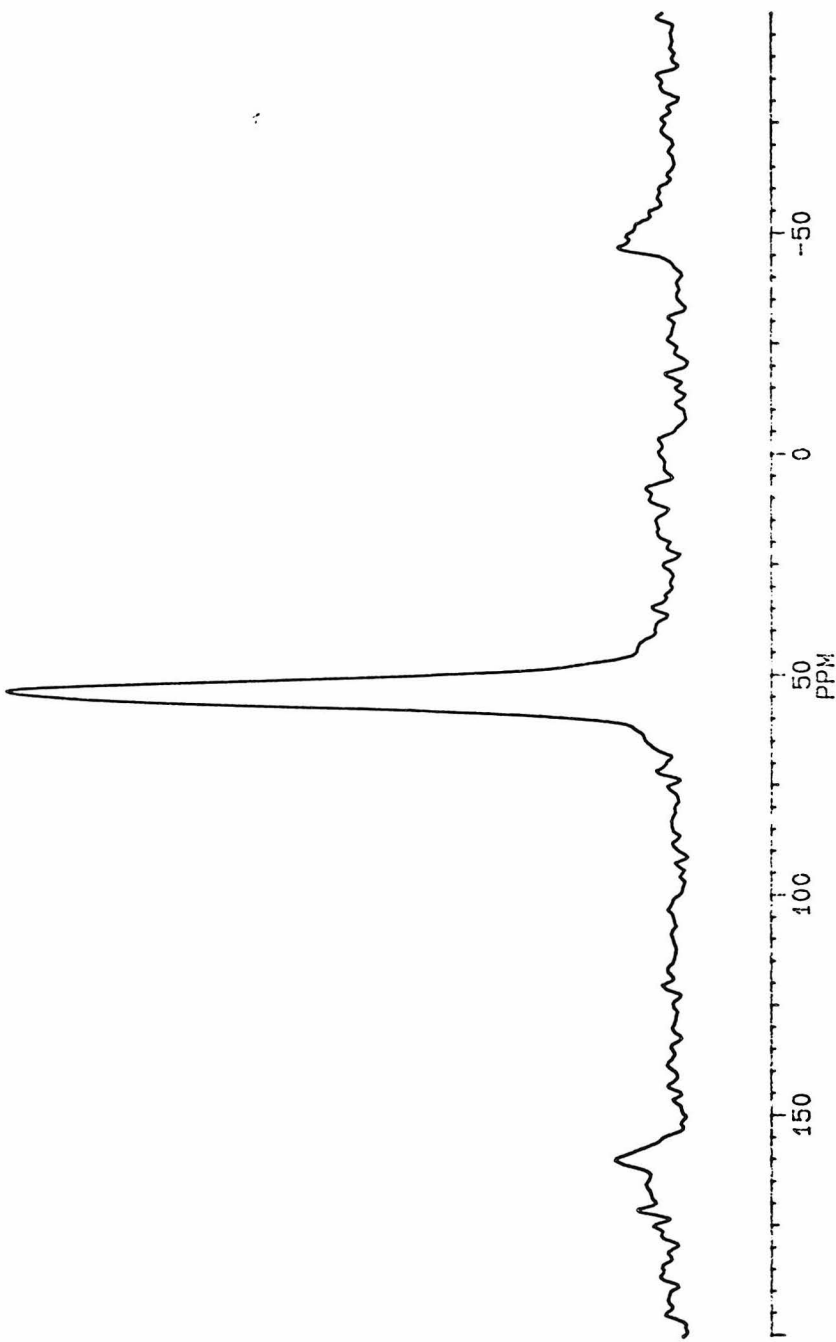
SF 78.209
01 38093.818
SI 8192
TD 1024
SW 100000.000
HZ/PT 24.414

AQ .005
RG 640
TE 289

02 19741.000
DP 3L P0

LB 40.000
GB 0.0
MT 0.06
HZ/CM 1.47453
SR 38093.82

D1 1.0000000
P4 40.00
P1 4.00
RD 0.0
PW 0.0
DE 8.75
NS 4934
DS 0



HK110 TRAF-ZSM-5, 29SI MAS 3442, 7884

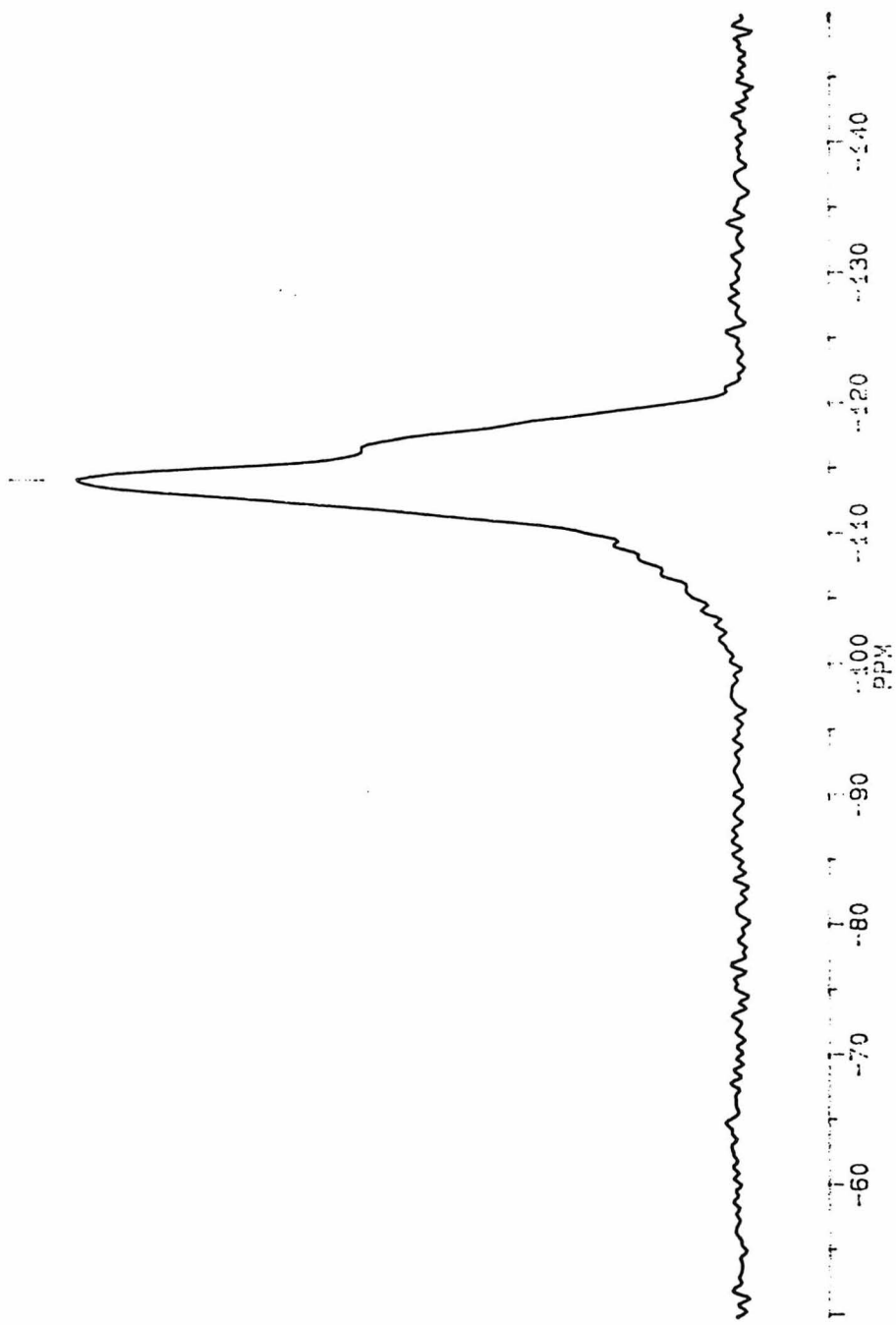
250-777-

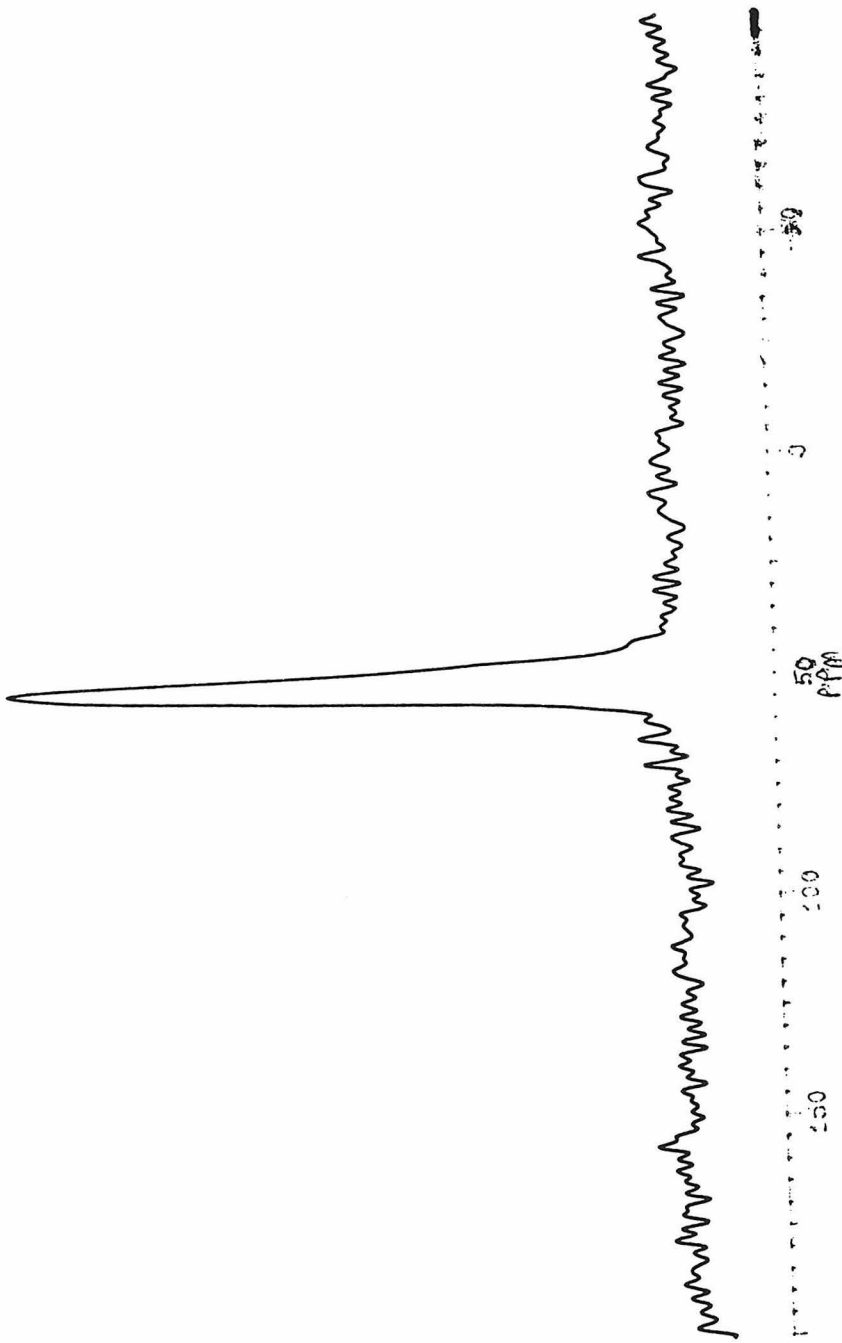
340

HK140ST.001
AU PROG;
SOLIDCYC.AU
DATE 18-4-95
TIME 9:48

SF	59.628
04	22500.000
STD	4096
MSR	1024
Hz/PT	25000.000
	12.207

95





HK110 TAF-AL-ZSM-5. 37A) m/s 8MHz 4mm

210

HK110 AL-(TPAF)-ZSM5 CALC 600C. 29SE MAS 3KHz. 7MM

106.311

443.210

PPM

BRUKER

HK110SI.002
AU PROG:
SOLIDYC/AU
DATE 25-1-95
TIME 14:48

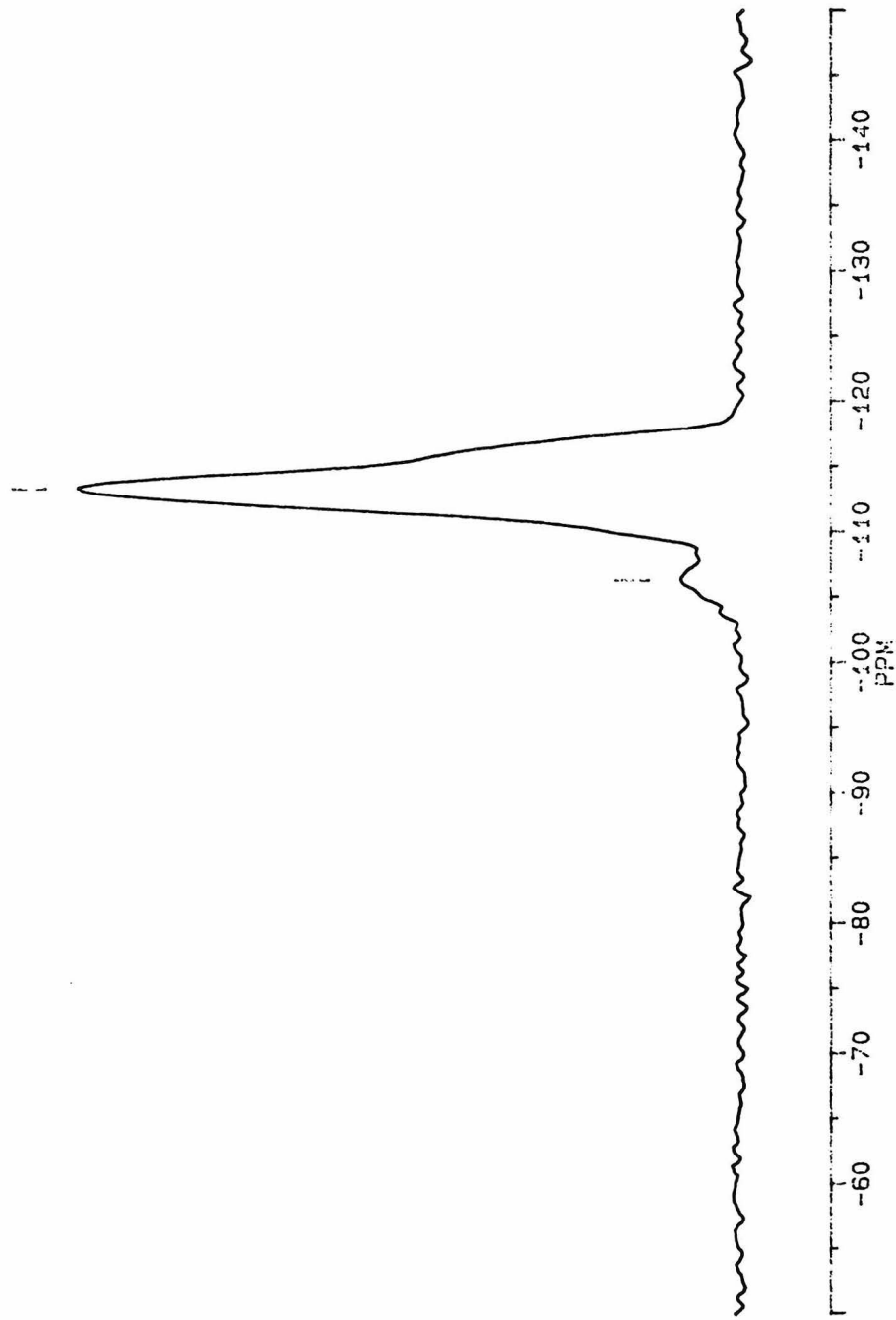
SF 59.634
01 22500.000
SF 4096
TD 500
SW 16666.667
HZ/PT 8.138

AQ .045
RG 640
TE 289

02 5787.000
DP 5L P0

L3 0.0
GB 0.0
K1 .02
HZ/CM 298.258
SR 29847.23

D1 5.0000000
P4 40.00
P1 4.00
RD 0.0
PK 0.0
DE 40.00
NS 444
DS 0



HK110 AL-ZSM-5 CALC 600C, 27AL MAS 8KHZ, 4MM

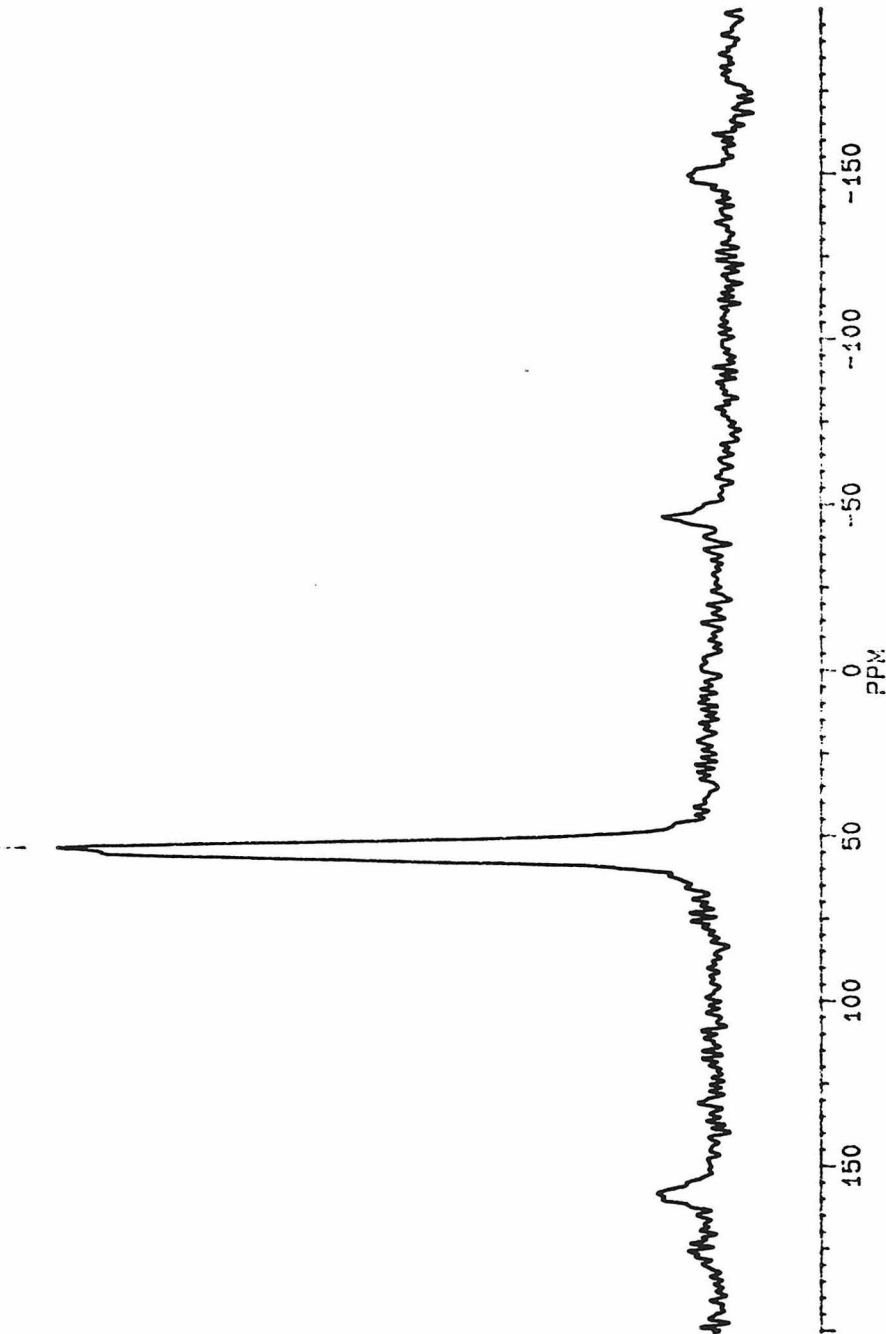
53, B404

PPM

BRUKER

HK110AL.002
AU PROG:
SOLIDCYC.AU
DATE 2-2-95
TIME 9:31
SF 78.209
0.1 38301.338
SI 4096
TD 700
SW 50000.000
HZ/PT 24.414

AO 0.007
RG 640
TE 289
02 19741.000
DP 3L P0
LB 0.0
GB 0.0
MI 0.21
H2/CW 1.563E3
SR 38093.80
D1 1.0000000
P4 40.00
P1 4.00
RD 0.0
PW 0.0
DE 15.00
NS 41697
DS 0



Appendix VII. Conversion versus W/F Plots for VAW sample 1.

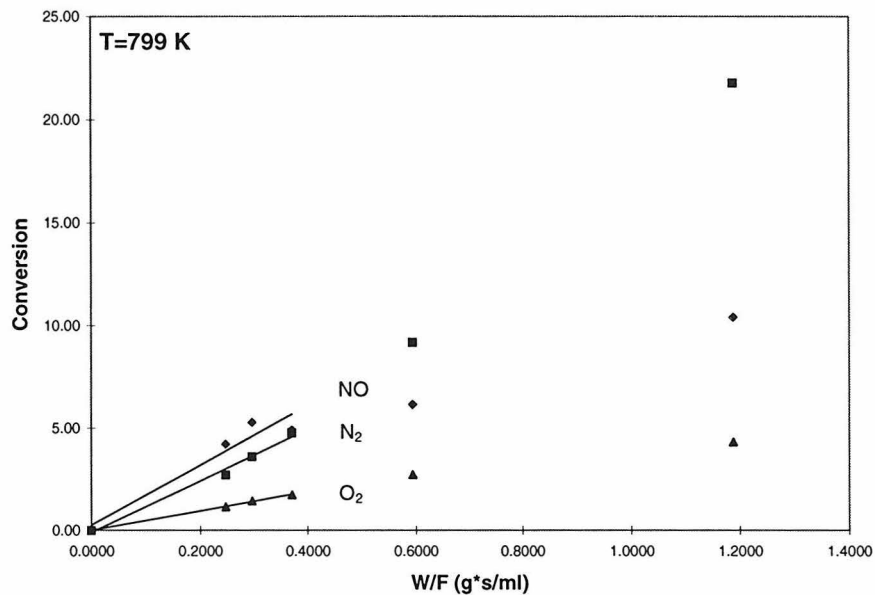


Figure VII-1 Sample 1 ion-exchanged with copper acetate, $T=526$ °C.

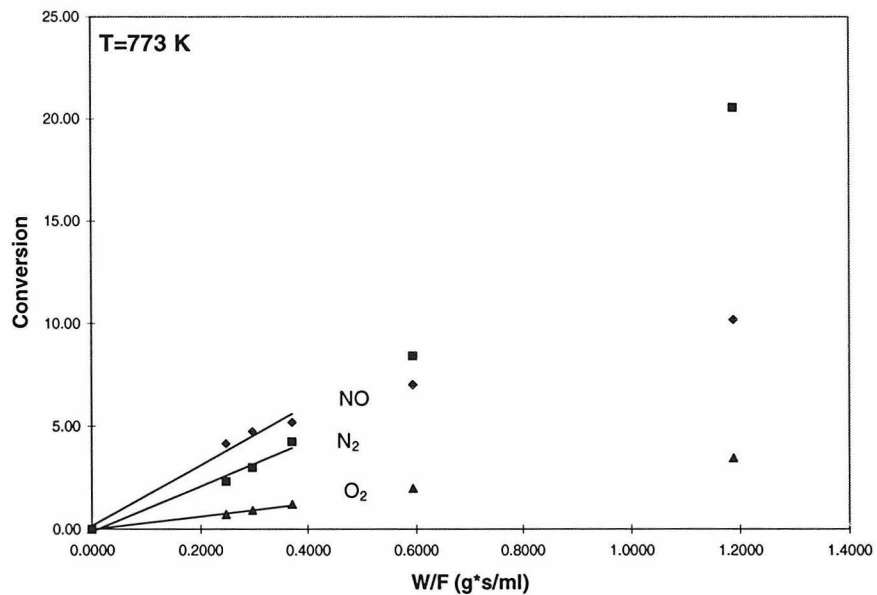


Figure VII-2 Sample 1 ion-exchanged with copper acetate, $T=500$ °C.

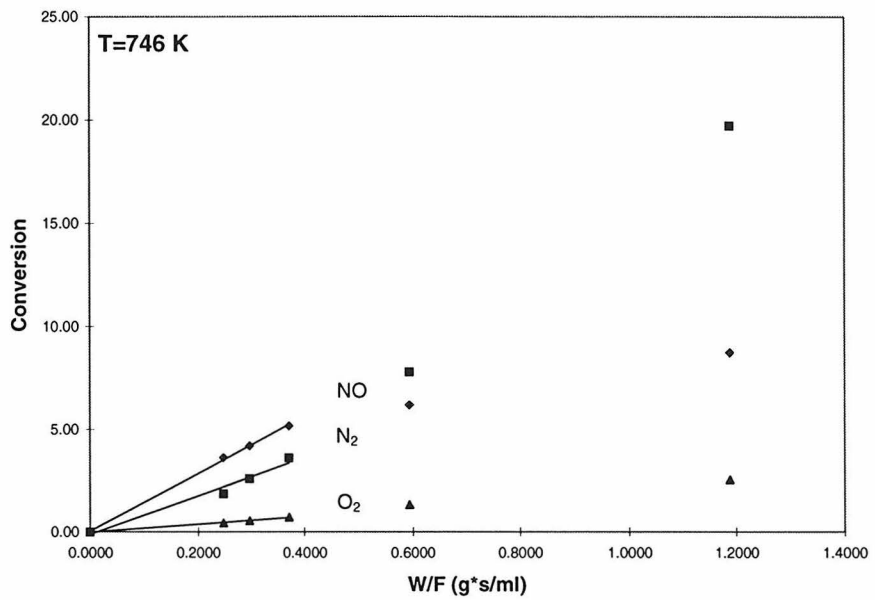


Figure VII-3 Sample 1 ion-exchanged with copper acetate, T=473 °C.

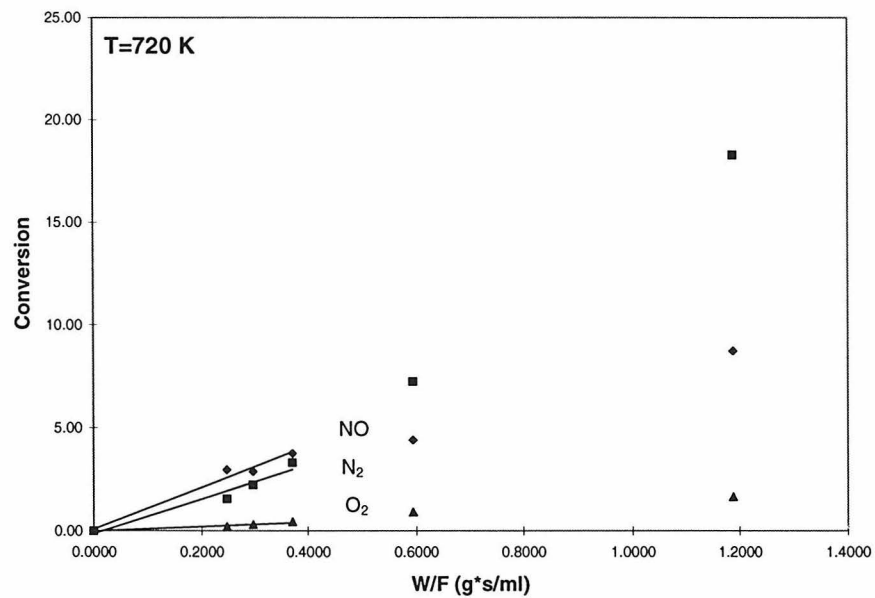


Figure VII-4 Sample 1 ion-exchanged with copper acetate, T=447 °C.

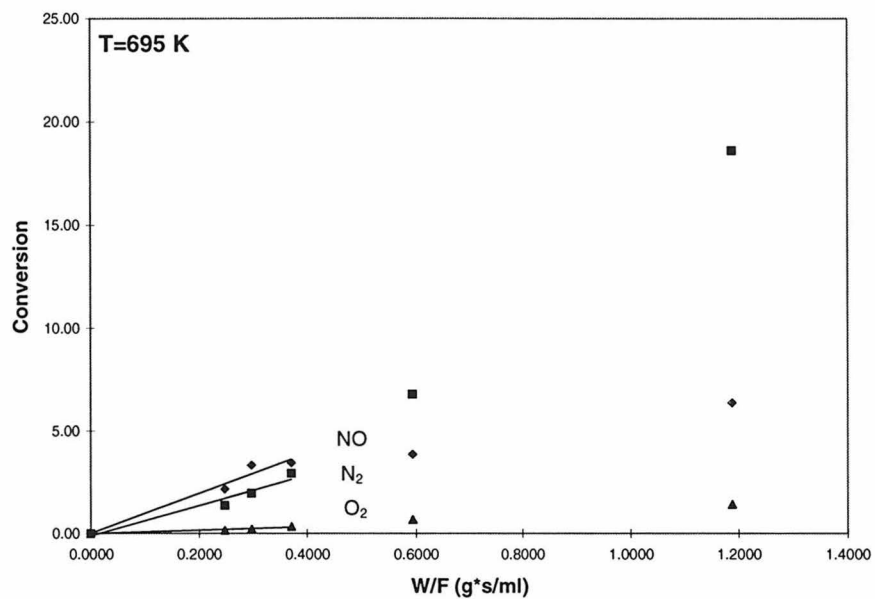


Figure VII-5 Sample 1 ion-exchanged with copper acetate, T=422 °C.

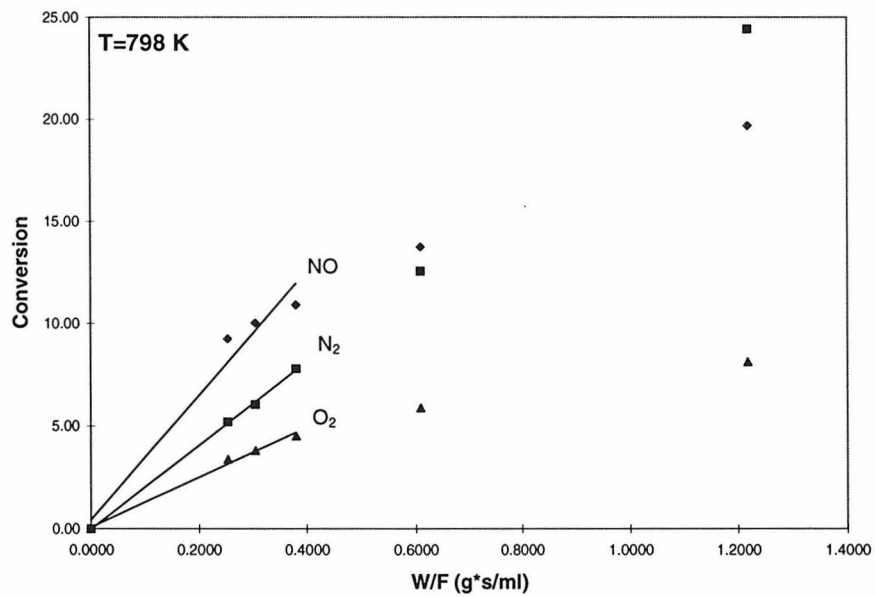


Figure VII-6 Sample 1 ion-exchanged with copper ethylene complex, T=525 °C.

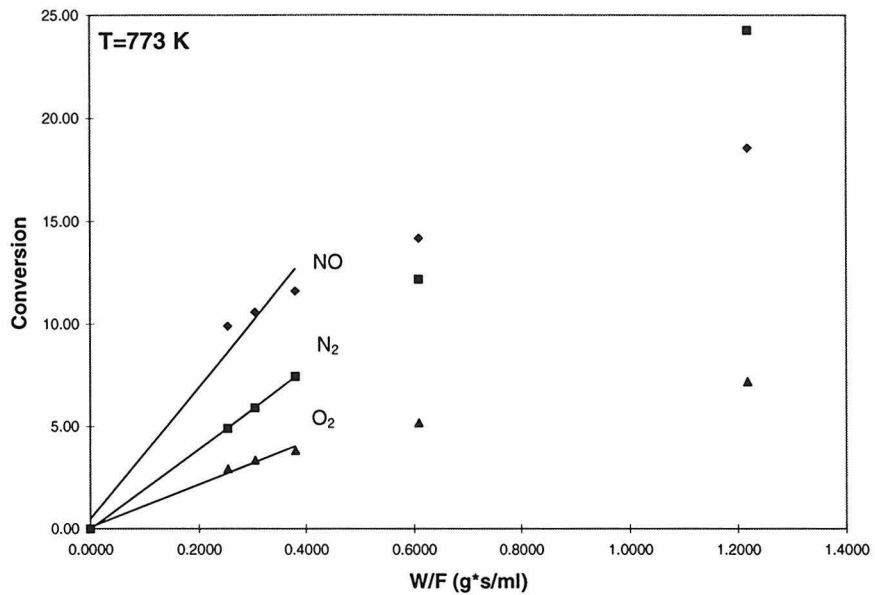


Figure VII-7 Sample 1 ion-exchanged with copper ethylene complex, $T=500\text{ }^{\circ}\text{C}$.

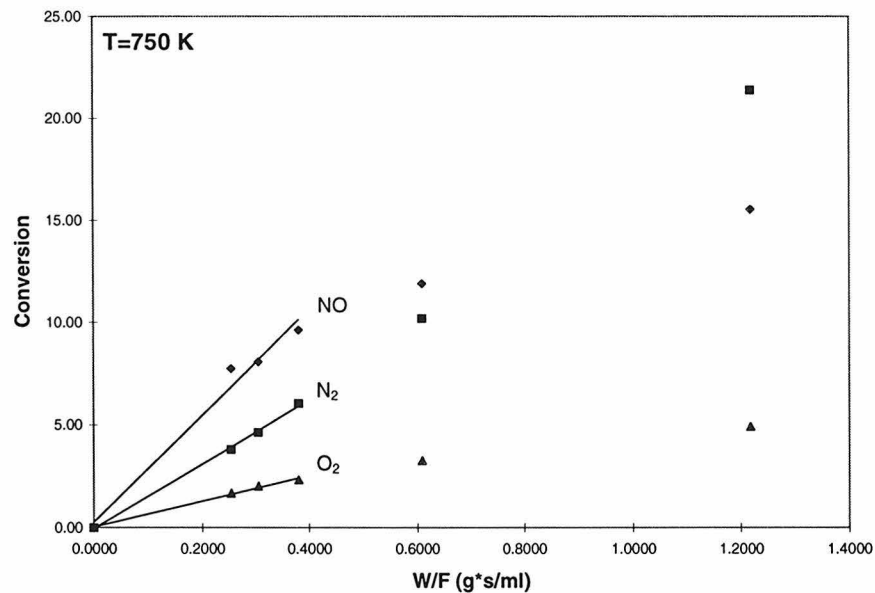


Figure VII-8 Sample 1 ion-exchanged with copper ethylene complex, $T=477\text{ }^{\circ}\text{C}$.

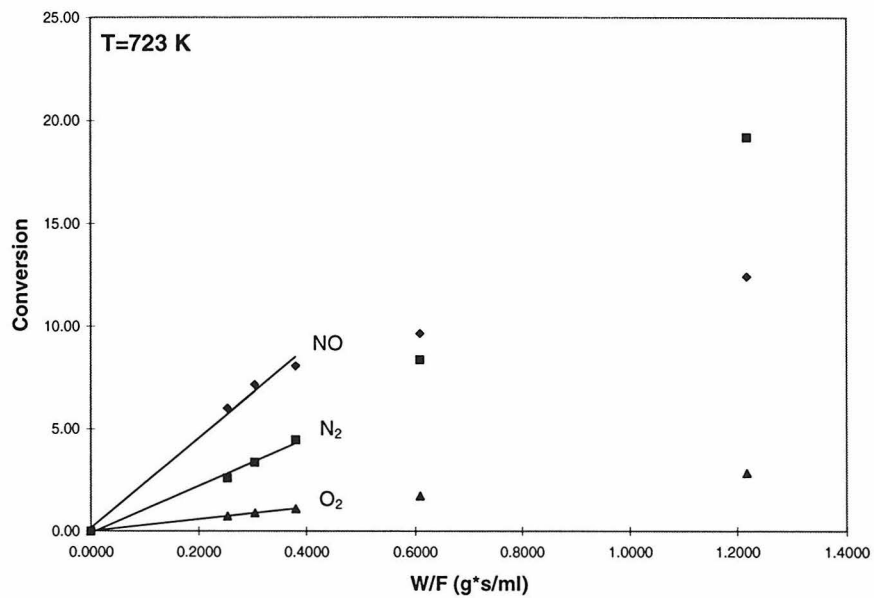


Figure VII-9 Sample 1 ion-exchanged with copper ethylene complex, T=450 °C.

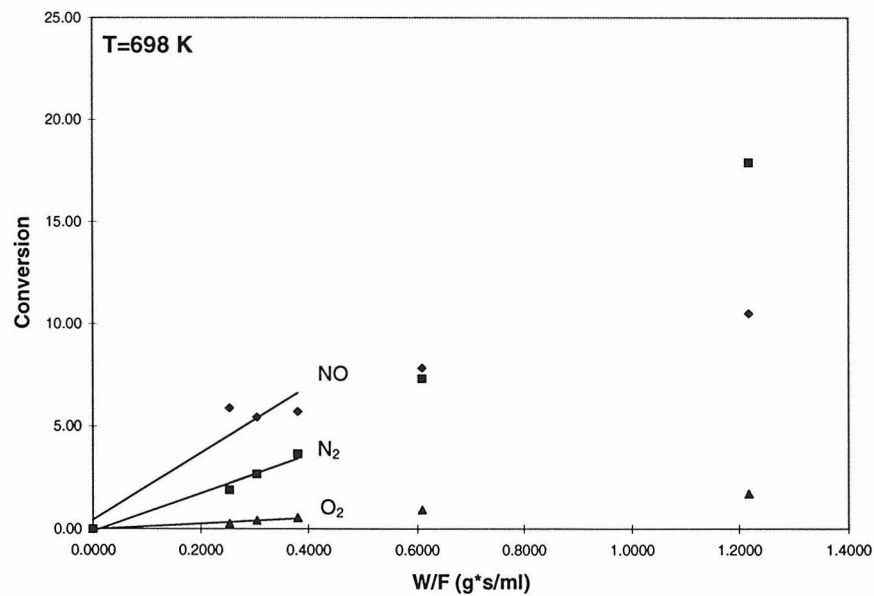


Figure VII-10 Sample 1 ion-exchanged with copper ethylene complex, T=425 °C.